Research Center Borstel
Leibniz-Center for Medicine and Biosciences
Department of Molecular Infection Biology
Director: Professor Dr. U. Schaible

Division of Medical and Biochemical Microbiology
PD Dr. Sven Müller-Loennies

Interactions of Pathogen-Associated Carbohydrates with Integral Components of the Innate and Adaptive Immune System

Dissertation
to
Obtain the Doctoral Degree
at the University of Lübeck
- from the Department of Natural Sciences -

Submitted by
Lena Heinbockel
of Hamburg
Lübeck, April 2011

Doctoral dissertation approved by the Faculty of Technology and Sciences of the University of Lübeck

Date of doctoral examination:	10.11.2011
Chairman of the examination committee:	Prof. Dr. Ulrich Schaible
First reviewer:	PD Dr. Sven Müller-Loennies
Second reviewer:	Prof. Dr. Thomas Peters

Table of Contents

List of Figures and Tables

List of Abbreviations

Ab	Antibody
Ag	Antigen
ATCC	American tissue culture collection
BBS	Barbital-buffered saline
BSA	Bovine serum albumin
CD	Cluster of differentiation
cDNA	Complementary DNA
CFA	Complete Freund's adjuvant
cfu	Colony forming units
Col	Colicin
CRD	Carbohydrate recognition domain
ddH_2O	Double-distilled water
dNTP	Deoxyribonucleotide
E. coli	*Escherichia coli*
EDTA	Ethylenediaminetetraacetic acid
ELISA	Enzyme-linked immunosorbent assay
$F(ab)_2$	Fragment antigen binding with two binding sites
Fab	Fragment antigen binding
FP	Forward primer
FucNAc	*N*-acetyl-L-fucosamine
GA	Glutaraldehyde
Gal	D-Galactose
gIII	*geneIII* of the M13 phage
Glc	D-Glucose
GlcN	D-Glucosamine
HA	Hemagglutinin
HC	Heavy chain
Hep	L-*glycero*-D-*manno*-Heptose
His	Histidine
HKB	Heat-killed bacteria
hMBL	Human mannose binding lectin
HRP	Horseradish peroxidase
IFA	Incomplete Freund's adjuvant
Ig	Immunoglobuline
Kdo	3-deoxy-D-*manno*-oct-2-ulosonic acid
L-Fuc	L-fucose
LC	Light chain
LL	Long linker
LPS	Lipopolysaccharide
mAb	Monoclonal antibody
Man	D-Mannose
ManN	Mannosamine
ManNAc	*N*-acetyl-D-mannosamine
MASP	MBL-associated serine protease
MBL-A	Mannose binding lectin A (1) from mouse
MBL-C	Mannose binding lectin C (2) from mouse
MHC	Major histocompatibility complex
NZB	New Zealand Black

OD	Optical density
P	Phosphate
PBS	Phosphate buffered saline
PCR	Polymerase chain reaction
pfu	Plaque forming units
pIII	Minor coat protein III of the M13 phage
PVDF	Polyvinylidene fluoride
RC	Research center
Rha	Rhamnose
rMBL	Recombinant mannose binding lectin
RNA	Ribonucleic acid
RP	Reverse primer
scFv	Single chain variable region fragment
SDS-PAGE	Sodium dodecyl sulfate polyacrylamide gel electrophoresis
SL	Short linker
TBS	Tris buffered saline
TLR	Toll-like receptor
V_H	Variable heavy chain
V_L	Variable light chain
Wt	Wild type
αMeGlc	α-methyl-D-glucose
αMeMan	α-methyl-D-mannose

1. Introduction

1.1. General Overview

Carbohydrate-protein interactions play a major role in immunological processes, as in cell-cell interactions or infection processes. Hence it is of considerable interest to elucidate the mechanisms of carbohydrate interaction with their binding partners. The generally rather weak molecular interaction of proteins and carbohydrates is explained in the amphiphilic character of most carbohydrates. Both the hydrophobic C-H regions and the hydrophilic hydroxyl groups can be involved in the binding process [1]. Regarding the apolar regions of the carbohydrate, aromatic amino acids are commonly involved in affinity enhancement, whereas, in the polar regions, hydrogen bonds are the primary binding force.
The valency and display of both binding partners exert an enormous influence on the interactions of carbohydrates with proteins [2]. Weak binding can be compensated through an increase in interacting molecules, oligomerised molecules thus playing a major role in such interactions.
Two prominent proteins of the immune system, which recognise surface carbohydrates of pathogens, the antibodies and mannose-binding lectins (MBLs), will be discussed in greater detail. The focus of the first part of this study was on the isolation of neutralising antibodies against the toxic effects of enterobacterial LPS, while the second part was about the interaction of the C-type lectin mannose binding lectin with different *E. coli* and mycobacteria.

Therapeutic antibodies have achieved considerable success in recent decades reviewed in Beck 2010 [3]. In the 1880s von Behring detected that the serum of animals immunised with a toxin can be an effective therapeutic. Since then, the antibody treatment has developed tremendously, and although polyclonal antibody serum is still applied owing to its ability to bind various epitopes on antigens, the focus lies increasingly on monoclonal Antibodies (mAbs). The advantage of mAbs is the increased definability of the application, such as in terms of allergic reactions, certain dosing and specificity. There are currently 26 therapeutic mAbs in clinical use approved by the United States Food and Drug Administration (FDA) as well as thousands undergoing clinical trials (www.clinicaltrials.gov)[4-6]. Even so, anti-carbohydrate antibodies are exceedingly rare, explained by their commonly low affinity [7].

This low affinity is often compensated for through avidity effects, with several anti-carbohydrate Abs being of the IgM class. An exception here is the mAb WN1 222-5 discussed below.

The MBL, however, makes an important contribution to the innate immune response against cell-wall-derived carbohydrates [8]. It is part of the first line defense against many organisms, where binding of MBL can lead to activation of complement and phagocytosis. MBL deficiency is correlated with an increase in susceptibility to various infections [9]. On the contrary intracellular pathogens can benefit from high MBL levels. Furthermore, great differences are described for the recognition of various bacteria. The discrimination between bacteria will be discussed more closely.

1.2. Lipopolysaccharide (LPS)

1.2.1. Structure and Function

Lipopolysaccharides (LPSs) are phosphorylated glycolipids localized in the outer membrane of gram-negative bacteria. They are the major component of the outer leaflet and serve as a permeability barrier of the bacteria. Furthermore they are playing an important role in the interaction of commensals and pathogenic bacteria with their host organisms. In the bacterial kingdom there is an amazing diversity of different LPS structures. Additionally, the environmental conditions can influence the structure of the molecule [10].

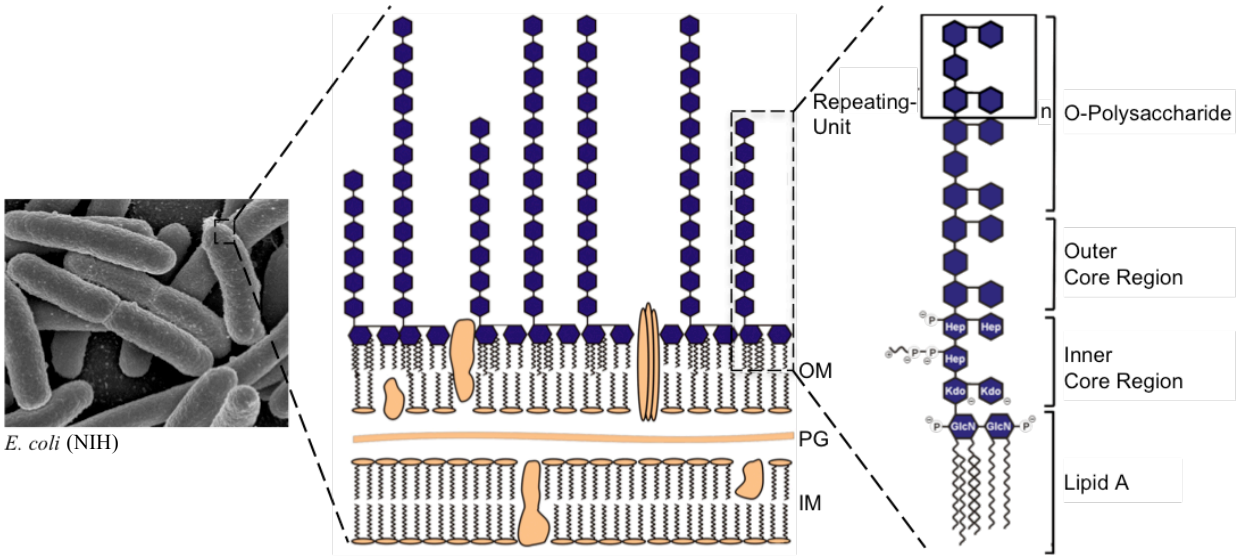

Fig. 1: Localisation of LPS in the gram-negative cell wall.
The gram-negative cell wall consists of two bilayers which form the inner and outer membrane of the bacteria. The inner membrane is mainly composed of phospholipids, while the outer membrane composition is asymmetric. The inner layer of the outer membrane, adjacent to the periplasmic space containing the peptidoglycan, is also composed of phospholipids. The outer layer is constructed mainly of the lipid A part of LPS molecules. In addition both membranes contain integral membrane proteins. The basic chemical structure of enterobacterial LPS is shown. Depicted are the membrane-anchoring lipid A region, the subsequent oligosaccharide core region and the terminal O-polysaccharide, consisting mostly of variable numbers of oligosaccharide repeating units. For clarity other surface associated structures like capsules have been omitted. IM: inner membrane, OM: outer membrane, PG: peptidoglycan.

In many bacteria, in particular from *Enterobacteriaceae*, the LPS molecule is composed of three structural regions: the hydrophobic lipid A, the hydrophilic core region and the long hydrophilic O-polysaccharide (Fig.1, reviewed by Rietschel and Brade [11]). The lipid A portion anchors the amphiphilic molecule to the bacterial membrane and is the most conserved part among different LPS structures. It was identified as the toxic portion of LPS [12], with enormous differences in activity, depending on the degree of acylation and phosphorylation influencing the shape of the molecule [13, 14].

A non-conserved, highly variable region of the LPS is, by contrast, the O-polysaccharide, responsible for the smooth appearance of bacterial colonies. It consists in most cases of a varying number of repeating units, consisting of two to eight monosaccharides. The good accessibility of the O-polysaccharide makes it a common epitope (O-antigen) of antibodies. Different O-antigens are used to differentiate various pathogenic bacteria, termed serotypes. The compositions of *E. coli* serotypes have been collected in a database [15, 16]. Structural examples of the three O-types, which have been used in this study, are depicted in Fig. 2.

O4

->2)αLRha(1->6)αDGlc(1->3)αLFucNAc(1->3)βDGlcNAc(1->

O8

->3)βDMan(1->2)αDMan(1->2)αDMan(1->

O111

αCol(1->6)
|
->4)αDGlc(1->4)αDGal(1->3)βDGlcNAc(1->
|
αCol(1->3)

Fig. 2: The O-polysaccharide structures of the *E. coli* serotypes used in this study.
The repeating units of the serotype O4 [17], O8 [18] and O111 [19].

The third portion of the LPS, the core region, is also composed of carbohydrates like the O-polysaccharide, but is far more conserved regarding structural variability. It includes the LPS characteristic carbohydrate 3-deoxy-D-*manno*-oct-2-ulosonic acid (KDO) and often phosphorylated or phosphoethanolamine carrying heptoses [10, 20]. In *E. coli* five different core-types are distinguished (Fig. 3). A comprehensive overview of the core-structures from *E. coli* and other enterobacteria is given by Holst and Müller-Loennies [21].

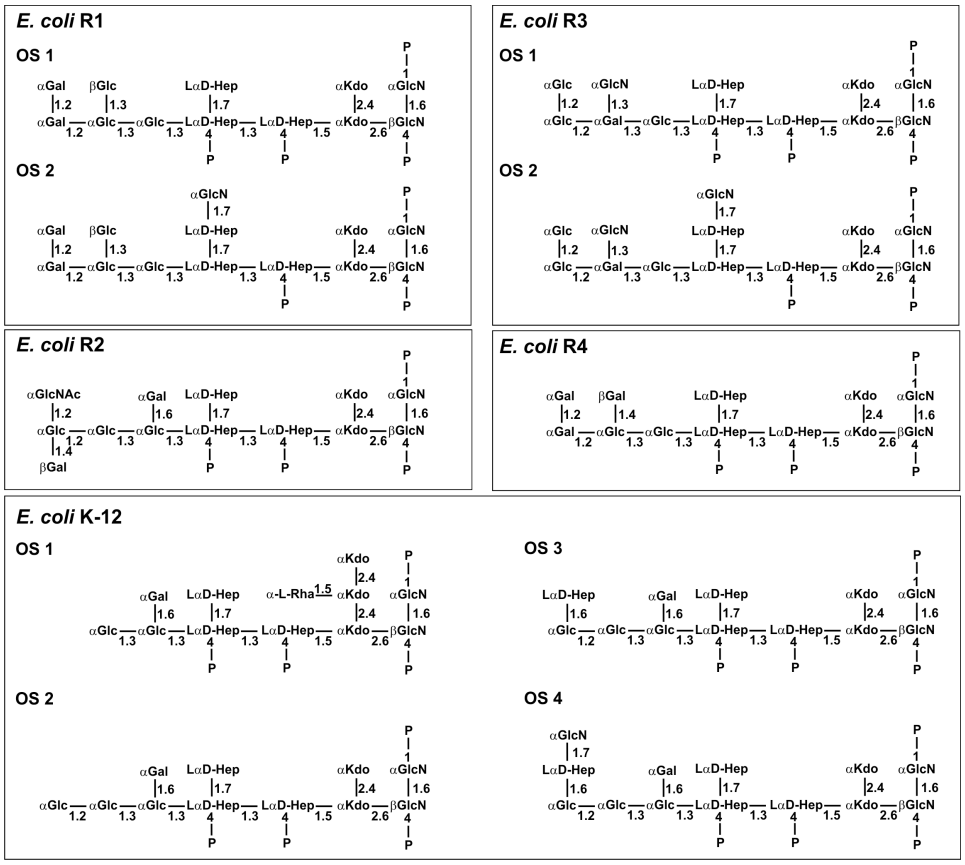

Fig. 3: Chemical structure of *E. coli* LPS core-types [21].

Five core-types of *E. coli* are distinguished due to differences in the outer-core region. For the R2 and R4 one glycoform is reported. The R1 and R3 core-types are further subdivided into two glycoforms, the OS1 and OS2. For the K-12 four glycoforms have been described.

LPS molecules can be extremely strong stimulators of the innate immunity in diverse eukaryotic species ranging from insects to humans (reviewed by Alexander and Rietschel [22]). Since LPS is one of the most potent stimulators of the immune system, it is also known as endotoxin extensively discussed by Beutler and Rietschel [23].

1.2.2. The Role of LPS in Sepsis

Sepsis is defined as an invasion of microorganisms and/or their toxins into the bloodstream, accompanied by the organism's reaction to this invasion [24]. This definition has been developed further over the years, but it condenses the two main points of the disease: the microorganisms as the initiators and the dysregulated immune response as the life-threatening condition.

The body reacts to septic infections with a systemic inflammatory response syndrome (SIRS), an abnormal regulation of cytokines, characterised by an unusual high or low body temperature, a high heart and respiratory rate and an elevated or depressed number of white blood cells. These are non-specific criteria, and thus an early diagnosis of sepsis is difficult. Sepsis can be caused by viral, bacterial, fungal or parasitic pathogens, generally the infection is due to common bacterial organisms such as *Staphylococcus aureus*, streptococci, *Enterobacteriaceae* and *Pseudomonas aeroginosa* [25]. They can invade through open wounds, but more frequently the pathogens enter the blood stream as a consequence of diseases such as pneumonia or urinary-tract infections.

The mortality rate in patients with sepsis lies in a range of 35% and increases to 60% if patients develop septic shock [25]. With that it is a leading cause of death among hospitalised patients, despite of advances in supportive care and the availability of potent antimicrobials. The German Sepsis Society estimates that after cardiovascular disease and cancer, it is the third most common cause of death in Germany [26].

The current treatment of septic patients begins with the rapid administration of appropriate antibiotics [27], followed by other measures such as source control at the site of infection or a relatively new medication with recombinant human-activated protein C (rhAPC). Although antibiotics are the primary aspect of the treatment, they are not sufficient by themselves, and in some cases they can have adverse effects for the patient. This is mainly because of their ability to release highly immunologically active bacterial compounds from the cell-wall should the bacterial cell be destroyed [28]. When used in systemic gram-negative infection, e.g. some classes of ß-lactam antibiotics lead to increased levels of free LPSs [29]. No longer anchored in the bacterial membrane, the lipid A part of the LPS becomes more accessible to the immune system and thereby more toxic.

Like all mammals, humans have a specific cellular recognition of LPS, initialised by the combined actions of LPS binding protein (LBP), CD14 and the Toll-like receptor 4 (TLR4)-myeloid differentiation-2 (MD-2) complex, activating an intracellular signalling network. Strong activation of this immune cascade can cause severe reactions in the host leading to sepsis and septic shock [30].

Since LPS is found in the circulation of many patients with septic shock [25], various approaches have been considered to control the toxic effects of LPS. Examples of such are intravenous immunoglobulins, endotoxin core-specific antibodies, treatment with cytokines or cytokine receptor antagonists. On the whole these approaches have yielded disappointing outcomes for various reasons.

Nevertheless, there are some promising results regarding the neutralisation of the toxic effects of LPS by antibodies. One opportunity is the administration of neutralising antibodies to already infected patients. In animal experiments several of these antibodies have been shown to protect against harmful effects of LPS [31-34]. With the rapidly advancing knowledge about therapeutic antibodies, the approach of LPS neutralising antibodies is again becoming attractive.

Another opportunity to obtain protecting antibodies is to actively immunise with a molecule inducing such antibodies. However, an essential prerequisite for this is the induction of cross-reactive antibodies. Otherwise the protection comprises only distinct serotypes and would be insufficient. A promising candidate for vaccination is the J-5 rough type mutant of the *E. coli* O111:B4, because the conserved, clearly defined core region in this bacteria is not shielded by the O-PS and is thus accessible for antibody binding [35]. Several groups have used this approach with varying results, with some promising outcomes recently being determined [36-38]. Nevertheless, the poor quality of the antibody response to carbohydrates remains one of the main tasks here [39].

The possibility to induce protective immune responses by the use of anti-idiotype antibodies is discussed in the following.

1.3. The Concept of Anti-Idiotype Antibodies

The vaccination with carbohydrate antigens often leads to poor antibody responses and does not induce adequate protection. It is mainly attributed to a T-cell-independent immune response. B-cells are activated by B-cell-receptor crosslinking of carbohydrates, independently of $CD4^+$ helper T-cells. This response consists primarily of IgM antibodies and reveals a shorter half-life compared to the typical immune response to protein antigens. The protein antigens leading to a $CD4^+$ helper T-cell activation allowing the generation of high affinity antibodies and a subsequent memory response. T-cell activation is enabled through binding to MHC class II presented molecules, which are almost exclusively proteins. One exception is zwitterionic capsular polysaccharide from some bacteria, also processed and presented by MHC II. The majority of carbohydrates are dependent on T-cell antigens like immunogenic carrier proteins for the activation of the T-cell dependent immune response [39]. Furthermore, proteins can be used to induce carbohydrate-specific antibodies, on the basis of molecular mimicry. The concept of molecular mimicry of antigens originated in 1974 when

N. K. Jerne published the network theory of the immune system [40], for which he was awarded with the Nobel Price in 1984. The immune network theory describes the immune system as a network of interacting antibodies and lymphocytes, a theory reviewed and extended by others [41-43]. One consequence of this theory is that an antibody is not only thought to bind antigens, but is also an antigen for other antibodies (Fig. 4).

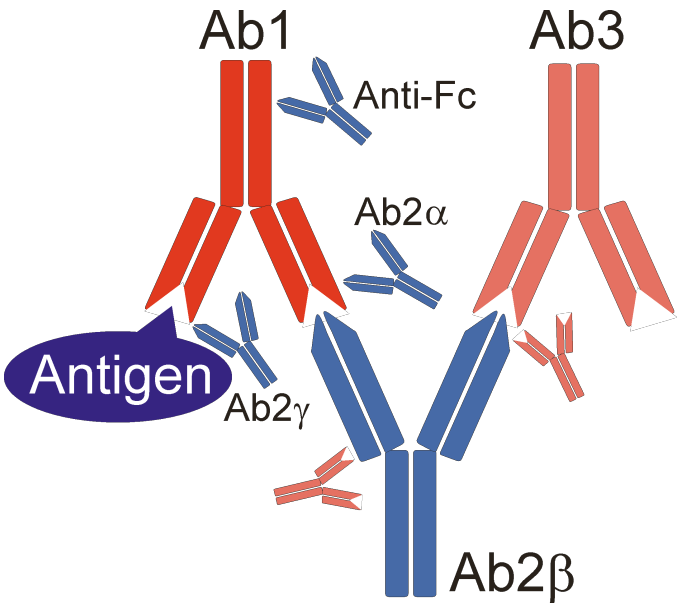

Fig. 4: The concept of anti-idiotype antibodies.
The antigen triggers an immune response leading to the production of antibodies specific for the antigen. These antibodies are called idiotypic antibodies (Ab1), because they carry various epitopes for other antibodies called idiotopes. Antibodies binding to an idiotype antibody are consequently anti-idiotype antibodies (Ab2). Dependent on their epitope, different anti-idiotype antibodies can be distinguished. Ab2β bind to the paratope of the antibody and mimic the internal image of the original antigen. Only Ab2β anti-idiotypes provoke an antibody reaction leading to anti-anti-idiotype antibodies (Ab3), binding the original antigen similar to the idiotype antibody. Several anti-idiotype antibodies were characterised as functional mimics of the original antigen, some being proven also to be structural mimics [44].
Other anti-idiotype antibodies are induced by an idiotype immunisation. Ab2α binds to the variable regions of the antibody without influencing the antigen binding. Ab2γ binds like the Ab2β to the paratope of the idiotype without mimicking the antigen, but by steric hindrance inhibits binding to the antigen. Anti-Fc antibodies bind to the constant region. Figure modified after [6].

Different epitopes on the antibody can be recognised by other antibodies (Ab2). If the corresponding epitope is located at the antigen-binding site, the Ab2 is potentially an internal image of the antigen and is termed anti-idiotype antibody (Ab2β). These anti-idiotypes mimicking the original antigen are potential vaccine candidates able to induce an antibody response surrogated for carbohydrates or harmful substances. There are auspicious attempts

for antigen mimicry [45, 46], in particular for carbohydrate mimicking anti-idiotypes [47-54], one of them is the mAb S81-19 described below.

1.4. The Monoclonal Antibody WN1 222-5

WN1 222-5 is a mouse IgG2aκ with an extraordinary K_D value in nanomolar range [56], an exceptionally high affinity for a carbohydrate-binding antibody, comparable values are usually observed for antibody-protein interactions.
It was isolated from NZB mice immunised with mixtures of heat-killed rough-form enterobacteria [31]. WN1 222-5 exhibits a remarkable cross-reactivity to different members of the *Enterobacteriaceae*. This cross-reactivity is due to a common epitope, the structurally conserved LPS core region (Fig. 5). This distinguishes WN1 222-5 from antibodies usually generated against LPS, which likely bind to O-polysaccharides and thus to only one particular serotype. The *E. coli* R2 core-type (Fig. 3) was elucidated as the structure with the highest binding affinity [56]. As the main determinants of the core-type epitope the side-chain heptose and the 4-phosphate of the inner core region could be discovered [56], available for binding both rough-form and smooth-form LPS. Binding was also shown when LPS was complexed to high-density lipoprotein either anchored in the bacterial membrane or coated to erythrocytes [57]. Furthermore *in vitro* and *in vivo* assays showed neutralising activity on the toxic effects of LPS from WN1 222-5 and its chimerized version SDZ 219-800 [31, 58-60].

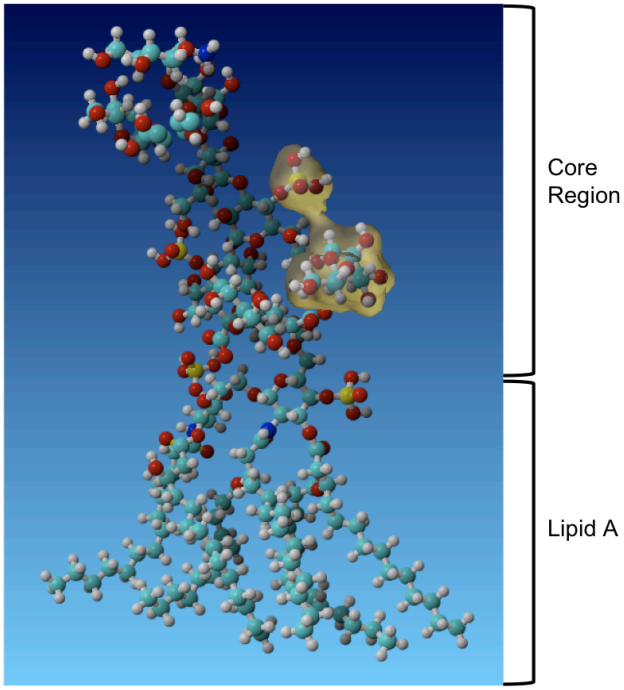

Fig. 5: Epitope of the antibody WN1 222-5.

Displayed is the *E. coli* R3 core-type (chemical structure R3 OS1 in Fig. 3). The antibody WN1 222-5 binds the structurally conserved inner core region of enterobacterial LPS. As main components of its epitope the side-chain heptose and the 4-phosphate on the second heptose were determined [31] (highlighted in yellow). Binding studies with various oligosaccharides also revealed the outer core and the lipid A backbone as relevant for binding. Although the acyl chains could be determined as irrelevant for WN1 222-5 binding, the binding of the antibody to the core region can neutralise the toxic effects caused by the lipid A. The image was created by use of the sweet model construction program [61] and the Yasara simulation program [62].

1.5. The Anti-Idiotype Antibody S81-19

The S81-19 is a mouse IgG isolated subsequently to an immunisation with the mAb WN1 222-5 by Dr. L. Brade (Research Center Borstel) [63]. Anti-idiotype qualities are tested and the ability to mimic functionally in an immunisation the LPS core region, resulting in the induction of LPS binding antibodies.

Four chinchilla bastard rabbits were immunised with the mAb S81-19, and the sera were tested intermittently for their binding activity to defined LPS structures known to be bound by the idiotype WN1 222-5. The rabbit sera exhibit an increased binding activity to various LPSs over time, indicating the presence of anti-anti-idiotype antibodies. The antibody response in the anti-anti-idiotype serum was compared with the binding specificities known for the

WN1 222-5 idiotype. Some similarities in epitope detection were described, like the binding to the R3 core-type, while others could not be confirmed.
In order to further characterise the anti-anti-idiotype antibodies, they should be isolated using the phage display method. A method already proven to be a valid tool for anti-idiotype isolations, too [64, 65].

1.6. Phage Display

1.6.1. The Principle of Phage Display

Phage display is a method widely used as an *in vitro* selection system for specific antigen-binding domains from large peptide or protein libraries. Recombinant libraries found application especially in the search for therapeutic antibodies, reviewed by Hoogenboom 2005 [66]. In principle, the peptides of interest are displayed on the surface of a filamentous phage by inserting the coding gene into the phage genome [67]. As a consequence the phenotype and genotype are linked and traceable together.

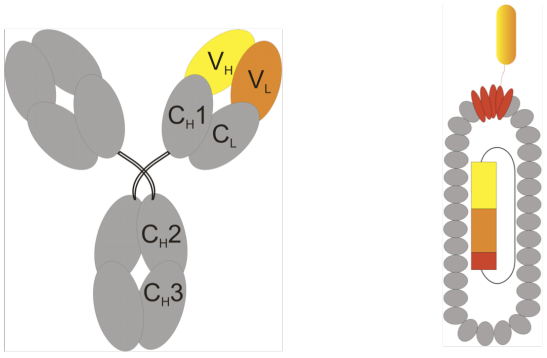

Fig. 6: Display of antibody variable regions on the surface of a filamentous phage.
The antibody variable regions responsible for antigen recognition are cloned into a phagemid vector. The variable region fragments are expressed on the phage surface. By selecting the phages based on the specificity of their presented protein fragment the corresponding DNA is obtainable.

The selection of desired peptides is termed panning, in reference to the sorting process employed by of gold washers using a pan [68]. While panning, the antigen is always immobilised to a solid surface, such as a column matrix, beads or plastic surfaces on polystyrole tubes [69]. The mixture of phages bearing various different polypeptides is

incubated with the immobilised antigen, and non-binders are removed by a number of washing steps. Subsequently the bound phages are eluated and amplified by infection of *E. coli*.

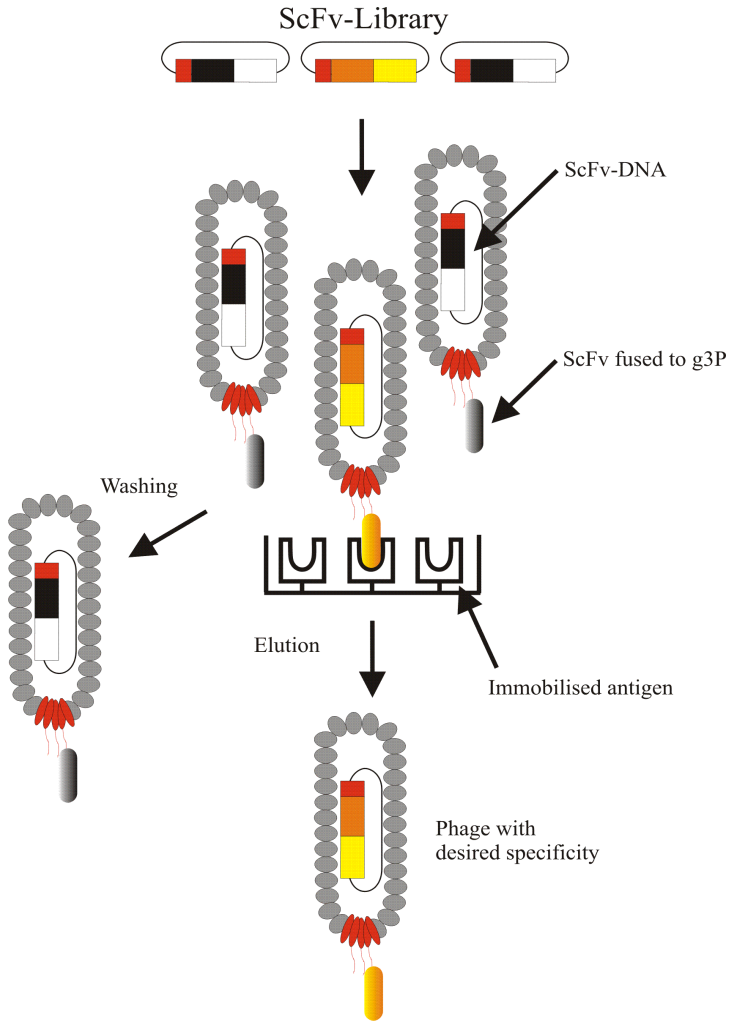

Fig. 7: Principle of phage display.
Phage display is used to select scFvs (single chain variable region fragments) with specific binding properties. Libraries with several different scFv genes were constructed. They were packed into phage particles presenting the scFvs on their surface. The scFv displaying phages are then applied for the panning procedure. Basically, four steps were continuously repeated during panning: binding, washing, eluting and amplifying. In this way, the phages bound to the antigen were multiplied and non-binders removed.

The M13 phage used in this work belongs to the filamentous phages [70]. They are viruses containing a circular single-stranded DNA genome encased in a long protein capsid cylinder. Eleven genes are encoded in the M13 genome, three being involved in the DNA replication, three in the assembly of phage particles, and five are part of the phage capsid. The pVIII is the major coat protein, occasionally used for the fusion and display of relatively small peptides.

For the display of polypeptides, pIII, in the phage life cycle responsible for infection of *E. coli* through the F conjugative pilus, is more suitable. During an infection the capsid proteins are integrated into the bacterial inner membrane and the phage DNA is translocated into the cytosol. There it replicates via a double-stranded replicative form, usable for cloning and sequencing during the phage display. Newly synthesised viral DNA is packed into phage particles at the bacterial membrane until the end of the around 6700 bp ssDNA is reached. The M13 phages do not kill their host during this process but the bacteria continue growing with an approximately 50% slower generation time, observable in plaque formation. Uncoupling of the gene replication and phage assembly by locating the corresponding genes on separate plasmids greatly improves the genetic stability and screening of recombinant polypeptide libraries [71]. If the fusion gene is encoded on a separate genome lacking several genes of the wild type phage, the vector is termed phagemid and a helper phage is necessary for phage packing in order to complement the genes not encoded on the phagemid genome. As is typical of plasmids, the phagemid bears an antibiotic resistance. Another plasmid advantage is the opportunity to isolate abundant double-stranded plasmid DNA for cloning. The pIII fusion proteins applicable for antigen binding range from small peptides to quite large antibody F(ab) fragments. In this study single-chain fragments of the variable regions (scFv) of antibodies are used. During the assembly of the phage display library, the variable regions of the antibodies' light and heavy chain are fused together by a linker, leading to a single-chain fragment. The length of the inserted linker is critical for the display of the scFv (Fig. 8). Long linkers (18 amino acids) lead to the expression of monomer scFvs on the phage surface, while short linkers (7 amino acids) can lead to dimer formation, consequently resulting in further antigen-binding sites [72].

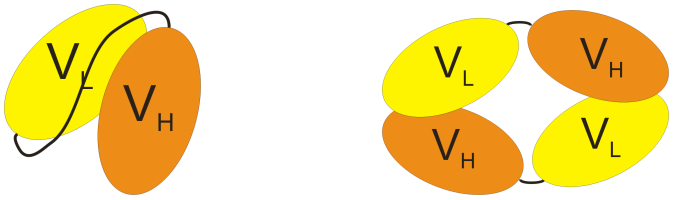

Fig. 8: The scFv valency is decisively influenced by the linker length.
The 18 amino acid long linker is pictured on the left. The two variable regions can interact as they prefer through the flexibility enabled by the long linker. The 7 amino acid short linker is pictured on the right. The linker length is too short to allow for flexibility and the preferred assembly of the variable regions. This promotes an attachment of two scFvs together, leading to dimer formation.

Furthermore, the choice of the vector system influences the quantity of scFv-derived binding sites and, as a consequence, the valency of the phage considerably [73]. Therefore the two phagemids, used in this study, are described in more detail.

1.6.2. The Phagemid pComb3XSS

The pComb3 phagemid vectors were developed for the monovalent display of large peptides on the surface of the filamentous phage M13 [74]. In this study the pComb3XSS vector was used for phage display [75]. This vector was developed for displaying antibody fragments as fusion proteins to the minor coat protein pIII. The pComb3XSS pIII is amino-terminal truncated (aa 230-406). This permits fusion protein display without diminished superinfection by helper phages caused by the pIII amino-terminus.
Since the phagemid has no complete *gIII* it relies on the incorporation of helper phage pIII into phage particles for subsequent infections. During the helper phage driven phage assembly, the scFv-pIII fusion protein and the helper phage wt pIII compete for incorporation into the phage particle. Thus 0-5 scFv-pIII fusion proteins are presented on the phage.
The expression of soluble scFv is possible due to an amber stop codon upstream to the 5'-terminus of the *gIII*. In *E. coli* nonsupressor strains the translation is terminated at the amber stop codon leading to soluble scFvs.
Soluble scFv can be detected or isolated by the use of two different tags. The 6 x histidine tag (His-Tag) at the 3'-end of the scFv and the decapeptide hemagglutinine tag (HA-tag) at the 3'-end of the His-tag.
SfiI restriction sites are used for scFv cloning into pComb3XSS, because the SfiI restriction site is uncommon in genes. It cleaves two copies of its recognition site in one molecule. The cleavage site is in a degenerated region, GGCCNNNN^NGGCC, enabling the ligation in the correct orientation by the use of two different cleavage sequences.
5'-upstream to the SfiI cleavage site the sequence of an ompA leader is located (leader of the *E. coli* outer membrane protein ompA). ScFvs are expressed as ompA fusion proteins, transported to the periplasm, where the leader is removed and the scFv-pIII is incorporated into the phage particle [76]. The protein secretion from the cytoplasm into the periplasm promotes the correct folding of scFvs due to the more oxidising environment and the availability of proteins that catalyse disulfide bond formation [77].

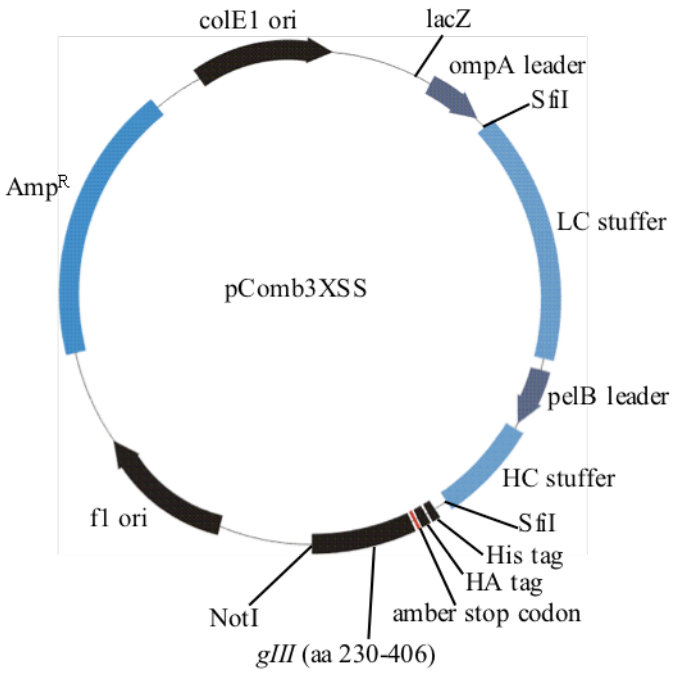

Fig. 9: Phagemid vector pComb3XSS.
The pComb3XSS vector has phagemid-typical features such as two origins of replications (ori), one for the plasmid replication (colE1) and one for the phage replication of ssDNA (f1) supplying material for the phage particles. It carries an ampicillin resistance, used for the selection of infected bacteria. The multiple cloning site is under the control of the lacZ promoter and provides different restriction sites, enabling cloning of both scFvs and Fabs. For scFv cloning the double cleavage enzyme SfiI is beneficial. 5'- upstream to the SfiI site an ompA leader is located. 3'- downstream two tags are placed, followed by an amber stop codon. The minor coat protein pIII is N-terminal truncated and used for presentation of the scFvs.

1.6.3. The Phagemid pHen1

The pHen1 phagemid is, like the pComb phagemid, a vector for displaying peptides fused to the minor coat protein pIII [78]. The pHen1 has a pelB leader sequence 5'-upstream to a SfiI cleavage site. For cloning at the 3'-end of the scFvs, a NotI restriction site is integrated, followed by a c-myc tag and an amber stop codon. In contrast to the pComb vectors, the pHen1 bears a complete *gIII*.
The use of the complete pIII, instead of the truncated one, leads to the difference that wt pIII derived from the helper phage is no longer necessary for subsequent infections of bacteria with phages. To allow superinfection of already infected bacteria, glucose must be present in the culture medium.
The independence from helper phage pIII enables the use of hyperphage for phage packaging. The hyperphage is a helper phage developed for the increase of presented scFv on the phage

surface [79]. It has the pIII phenotype of the helper phage M13K07 but lacks a functional *gIII*. Consequently, it infects bacteria cells and packs phage particles like the helper phage but produces no pIII on its own. Thus, all pIII incorporated into the phage originates from the vectors scFv-pIII fusion genes. This increases the scFv valency considerably. It is assumed that a high valency is preferred to monomeric or dimeric display concerning the isolation of low affinity binders [80].

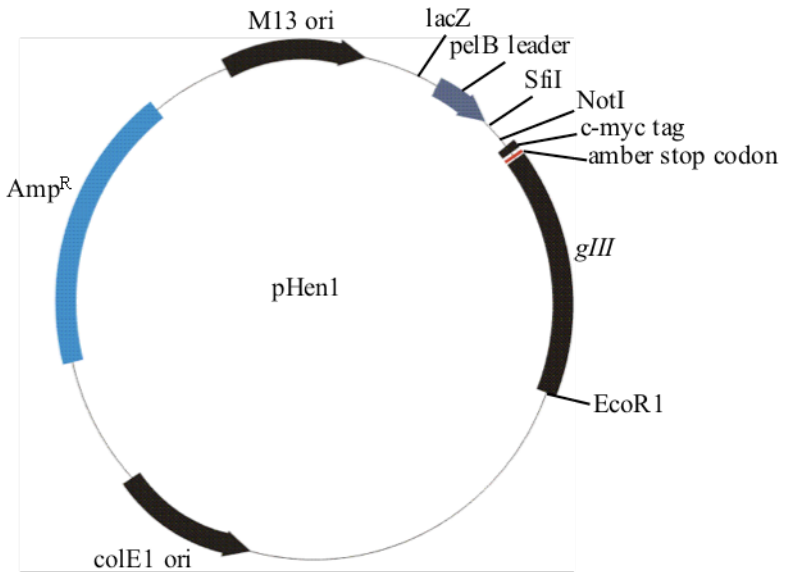

Fig. 10: Phagemid vector pHen1
The pHen1 vector has the phagemid-typical features like the pComb3XSS. In contrast to the pComb3XSS, it carries a pelB leader sequence 5'- upstream to the SfiI site. 3'- downstream the scFv can be cloned through a NotI restriction site, which is followed by a c-myc tag and an amber stop codon. The complete pIII is used for presentation of the scFvs.

1.7. Mannose Binding Lectin

1.7.1. Structure and Function

Lectins are carbohydrate-binding proteins, excluding enzymes and Igs, which are involved in the recognition of carbohydrates during innate immune response. They occur in plants, animals, fungi, microbes and viruses.
In mammalian sera, Mannose-binding lectin (MBL) is found [81] belonging to the family of collectins, which are calcium-dependent lectins (C-type lectins). MBL opsonises a wide range of microorganisms and also interacts directly with phagocytes. Furthermore, it is involved in complement activation via the MBL-associated serin protease (MASP), which shows

proteolytic activity against the complement component C4, inducing the further complement cascade.

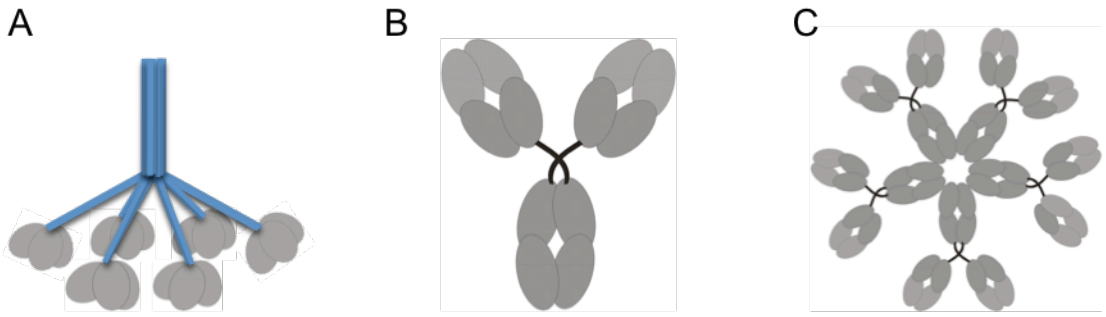

Fig. 11: Valency differences of the carbohydrate recognition molecules from the innate and adaptive immune system.
MBL of the innate immune system binds ligands through their trimeric CRDs (carbohydrate recognition domains), which are further organised to higher oligomers (A). IgGs of the adaptive immune system bind through two identical antigen-binding sites to their ligands (B). IgMs form mainly pentameric polymers each unit composed of two identical binding sites (C). The single binding site of MBLs and IgMs reveals commonly a low affinity for their ligands, which is compensated though high oligomerisations of the molecules. Thus, the increase of avidity leads to significant binding and therefore immunologically active compounds.

In general the soluble pattern-recognition receptors of the innate immune system like MBLs are functionally similar to the antibodies of the adaptive immune system. Collectins are discussed as broad-spectrum anti-carbohydrate antibodies [82].
MBL especially has a much broader specificity then the name implies. Besides mannose, other pathogen-associated carbohydrates are recognised, e.g. N-acetylglucosamine, glucose and fucose. The binding of a single carbohydrate-recognition domain (CRD) to carbohydrates as mannose and β-D-*N*-Acetylgalactosamin is determined by the 3-OH and 4-OH of the sugar ring. Equatorial 3- and 4-OH are bound by the CRDs and the Ca^{2+} directly participates in the bond formations [83].

Structurally, MBL is composed of sub-units formed by three identical polypeptide chains. Each chain contains four regions, the cystein-rich N-terminal region, the collagenous domain, the short α-helical neck region and the C-terminal CRD. The sub-units of MBL form higher oligomers, varying in the degree of oligomerisation from dimers to hexamers (reviewed by Hansen [84]).
The oligomerisation is a crucial feature for binding. Concerning the rather weak binding of a single CRD to a single ligand, it enables an affinity increase due to avidity effects. Thus the

presentation of the multivalent ligands for the multiple CRDs of an MBL molecule plays an important role [85].

Two different MBLs are described for mice, MBL-A and –C, whereas only one MBL is found in humans. Studies of the genes encoding for MBL-A and –C as well as hMBL have revealed that the hMBL sequence is more closely related to the MBL-C [86], supported by analysis of the carbohydrate specificity [87]. The difference between the two mouse MBLs is also emphasised, where the MBL-A reveals a higher affinity for monosaccharides than does the MBL-C.

Serum MBL	Monosaccharide
hMBL	αMeMan, Man > GlcNAc > L-Fuc > ManNAc >> αMeGlc > Glc
MBL-A	L-Fuc > αMeMan, Man, GlcNAc > αMeGlc > Glc > ManNAc >>> Fuc > Gal, GlcN > ManN
MBL-C	αMeMan > Man > L-Fuc > ManNAc > GlcNAc >>> Glc > αMeGlc >>> ManN > Fuc

Tab. 1: Monosaccharide specificities of different MBLs [87].
The 50% inhibition (IC_{50}) values of the monosaccharides specificities are differentiated, whereby > denotes more than 10%, >> more than 50% and >>> more than 100% higher IC_{50}.

1.7.2. Interaction with Bacteria

The considerable difference in monosaccharide binding introduces the issue of potential distinctions in pathogen recognition and further effects on the innate immune response. However, it is necessary to consider the conformational effect and varieties induced by oligosaccharides. Monosaccharides are not the natural binding partner of the MBL and it is not possible to predict the binding from the identity of the terminal carbohydrates from bacterial oligosaccharides alone [88]. Therefore an examination of the recognition of pathogenic and non-pathogenic bacteria is reasonable. The repeating, branched carbohydrates of bacteria match the regular spacing between the MBL CRDs and are consequently recognised [89].

Furthermore, hMBL occurs in variant allels, which changes both the promotor and structural region and influences the stability and serum concentration of the protein [90]. Different serum concentrations of hMBL alter the susceptibility to infections [91]. MBL deficiencies seem to increase susceptibility to some infections [92, 93], while tuberculosis yields contrary results [94]. For tuberculosis, a better uptake into macrophages is assumed where the Mycobacteria are

able to survive. Crucial for the recognition of the bacteria are their cell-wall components (reviewed by Brennan and Nikaido [95]), in particular lipoarabinomannan (LAM) and mannose-capped lipoarabinomannan (ManLAM) seem to play a major role in phagocytosis [96, 97]. Contrary to assumptions the mannose-cap is not exclusively present in pathogenic mycobacteria, but also confirmed in *M. bovis* BCG [98, 99]. Nevertheless, different tuberculosis strains vary in their pathogenicity [100]. In particular strains of the *M. africanum* 2 line are assumed to differ significant in MBL recognition from *M. tuberculosis* strains (personal communication with Dr. K. Walter).

To examine the role of MBL during the recognition of mycobacterial strains, a valid tool for the MBL mycobacterial interaction was investigated in this study. The interaction of MBL with the highly mannosylated mycobacterial cell-wall of various strains was studied, as were the differences between the human and the two murine MBLs.

2. Objectives

The aim of the first part of the thesis was to isolate anti-anti-idiotype scFvs by using the phage display method. Therefore RNA material from four different anti-idiotype antibody S81-19 immunised rabbits was used to construct scFv libraries. The scFv libraries were screened for scFv binding to the anti-idiotype antibody, R3 core-type rough mutant *E. coli* heat-killed bacteria and R3 oligosaccharide conjugated to BSA in order to receive anti-anti-idiotype scFvs. The anti-anti-idiotype scFv should reveal the binding pattern characteristics of the idiotype antibody WN1 222-5. The isolation and characterisation contribute to the understanding of the application from the anti-idiotype approach to induce cross-reactive and core-specific LPS-neutralising antibodies.

The aim of the second part of the thesis was to introduce a method in order to compare the interaction of several bacteria with a relevant representative of the innate immune system, the mannose-binding lectin (MBL). A method should be developed to compare various bacterial strains as well as different forms of MBL. It ought to be examined whether the rather weak binding of MBL molecules differ in binding to various mycobacterial strains. The result of this investigation could provide new insights to the question as to whether cell-wall composition differences recognised by MBL participate in an increased internalisation of the bacteria into host cells.
For further MBL-studies an assay should be established to investigate in addition the capability of MBL for complement activation.

3. Materials

Aqueous solutions were prepared with double deionized (Milli Q) water.

3.1. Bacteria Strains and LPS Conjugate

E. coli ER2537	[F′ *lacI*^{q} Δ(*lacZ*)*M15 proA*$^{+}$*B*$^{+}$/*fhuA2 supE thi* Δ(*lac-proAB*)Δ(*hsdMS-mcrB*)*5*], NEB (Frankfurt)
E. coli O111 oligosaccharide	Conjugated via glutaraldehyde to BSA, kindly provided by Prof. Dr. H. Brade (RC Borstel)
E. coli R3 core oligosaccharide	Conjugated via glutaraldehyde to BSA (139 nmol ligand/ml), kindly provided by Prof. Dr. H. Brade (RC Borstel)
E. coli R3 rough type mutant bacteria	Heat-killed bacteria, kindly provided by Prof. Dr. H. Brade (RC Borstel)
E. coli TG1	F'traD36 lacI^{q} Δ(lacZ) M15 proA^{+}B^{+} /supE Δ(hsdM-mcrB)5 (r_k- m_k- McrB^{-}) thi Δ(lac-proAB), kindly provided by Dr. U. Mamat (RC Borstel)
E. coli TOP10F’	F′*lac*Iq Tn*10* (TetR) *mcr*A Δ(*mrr hsd*RMS-*mcr*BC) Φ80*lac*ZΔM15 Δ*lac*X74 *rec*A1 *ara*D139 Δ(*ara-leu*)7697 *gal*U *gal*K *rps*L *end*A1 *nup*G. Invitrogen (Karlsruhe)
M. africanum West African2 10476/01	Heat-killed and living bacteria are kindly provided by Dr. S. Niemann (RC Borstel)
M. bovis Bovis 4258/00	Heat-killed and living bacteria are kindly provided by Dr. S. Niemann (RC Borstel)
M. tuberculosis Beijing 1934/03	Heat-killed and living bacteria are kindly provided by Dr. S. Niemann (RC Borstel)
M. tuberculosis Beijing 17919	Heat-killed bacteria kindly provided by Prof. Dr. U. Schaible (RC Borstel)
M. tuberculosis Cameroon 1417/02	Heat-killed and living bacteria are kindly provided by Dr. S. Niemann (RC Borstel)

M. tuberculosis H37Rv ATCC 27294	Heat-killed and living bacteria are kindly provided by Dr. S. Niemann (RC Borstel)
M. tuberculosis Haarlem 9532/02	Heat-killed and living bacteria are kindly provided by Dr. S. Niemann (RC Borstel)
M. tuberculosis X-type 4412/04	Heat-killed and living bacteria are kindly provided by Dr. S. Niemann (RC Borstel)

3.2. Bacteriophages and Phagemids

M13K07	Helper phage M13K07 is a derivative of M13, which carries the mutation Met40Ile in *geneII*, leading to a decreased DNA replication. The p15A origin of replication and the Kan^R gene from Tn903 were inserted within the M13 origin of replication [101]. Invitrogen (Karlsruhe)
M13K07ΔpIII	Hyperphage M13K07ΔpIII with a wild-type pIII phenotype provides helper phage function in packaging a common phage display phagemid, but has no functional *gIII* [79]. Progen (Heidelberg)
pComb3XSS	Phagemid vector for the presentation of scFv-pIII (aa230-406) fusion proteins on M13-Phages and the expression of soluble scFv. Carrier of an Amp^R [76].
pHen1	Phagemid vector for the presentation of scFv-pIII fusion proteins on M13-Phages and the expression of soluble scFv. Carrier of an Amp^R. MRC, Cambridge University

3.3. Oligonucleotide Primer

The rabbit scFv library primers used in this study were generated after Barbas III et al. 2001[76].

Name	Sequence
Amplification of LC	
Vκ5' RSCVK1	5'-gggcccaggcggccgagctcgtgmtgacccagactcca-3'
Vκ5' RSCVK2	5'-gggcccaggcggccgagctcgatmtgacccagactcca-3'
Vκ5' RSCVK3	5'-gggcccaggcggccgagctcgtgatgacccagactgaa-3'
Vκ3' RKB9Jlo-B (short linker)	5'-ggaagatctagaggaaccacctttgatttccacattggtgcc-3'
Vκ3' RKB9Jo-B (short linker)	5'-ggaagatctagaggaaccacctaggatctccagctcggtccc-3'
Vκ3' RKB42Jo-B (short linker)	5'-ggaagatctagaggaaccacctttgacsaccacctcggtccc-3'
Vκ3' RKB9Jlo-BL (long linker)	5'-ggaagatctagaggaaccacccccaccaccgcccgagccaccgc caccagaggataggatctccagctcggtccc-3'
Vκ3' RKB9Jo-BL (long linker)	5'-ggaagatctagaggaaccacccccaccaccgcccgagccaccgc caccagaggataggatctccagctcggtccc-3'
Vκ3' RKB42Jo-BL (long linker)	5'-ggaagatctagaggaaccacccccaccaccgcccgagccaccgc caccagaggatttgacsaccacctcggtccc-3'
Vλ5' RSCλl	5´-gggcccaggcggccgagctcgtgctgactcagtcgccctc-3'
Vλ3' RJλo-B (short linker)	5´-ggaagatctagaggaaccaccgcctgtgacggtcagctgggtccc-3'
Vλ3' RJλo-BL (long linker)	5´-ggaagatctagaggaaccacccccaccaccgcccgagccaccgc caccagaggagcctgtgacggtcagctgggtccc-3'
Amplification of HC	
V_H5' RSCVH1	5´-ggtggttcctctagatcttcccagtcggtggaggagtccrgg-3'
V_H5' RSCVH2	5´-ggtggttcctctagatcttcccagtcggtgaaggagtccgag-3'
V_H5' RSCVH3	5´-ggtggttcctctagatcttcccagtcgytggaggagtccggg-3'
V_H5' RSCVH4	5´-ggtggttcctctagatcttcccagsagcagctgrtggagtccgg-3'
V_H3' RSCG-B	5´-cctggccggcctggccactagtgactgayggagccttaggttgccc-3'

Overlap Extension	
RSC-F (sense)	5’-gaggaggaggaggaggaggcggggcccaggcggccgag ctc-3’
RSC-B (reverse)	5’-gaggaggaggaggaggagcctggccggcctggccactagtg-3’

Further Primers	**Sequence**
LH301-FP (scFv WN1 222-5 from pSJF8 into pComb3XSS)	5’- gggcccaggcggccgagctcgacatccagatgaaccagtc -3’
LH301-RP (scFv WN1 222-5 from pSJF8 into pComb3XSS)	5’- cctggccggcctggcctgaggagacggtgactgagg -3’
LH383-RP (scFv from pComb3XSS into pSJF8)	5’- gggggatccagaagcgtagtccggaacgtcgtacgggtatgcacta gtgactgacggagcctt -3’
NH1704-02 FP (pComb3XSS primer for colony PCR/sequencing)	5’- gctatcgcgattgcagtggc -3’
NH1765-02 RP (pComb3XSS primer for colony PCR/sequencing)	5’-gccccttattagcgtttgccatc -3’
LH566-RP_NotI (scFv from pComb3XSS into pHen1)	5’- gggggcggccgctgagaggacggtgaccag -3’

All oligonucleotide primers were obtained from Eurofins MWG (Ebersberg).

3.4. Primary and Secondary Antibodies

Anti-C4	Rabbit IgG, polyclonal, directed against complement factor C4, Abcam (Cambridge, UK)
Anti-c-myc	Mouse IgG1, monoclonal (9E10), directed against cmyc (NEQKLISEEDLC), kindly provided by R. MacKenzie (National Research Council Canada, Ottawa)
Anti-HA	Rat IgG1, monoclonal, HRP-conjugated, directed against hemagglutinin (YPYDVPDYA), Roche Diagnostics (Mannheim)
Anti-HisG	Mouse IgG2a, monoclonal, directed against 6xHis + Gly, Invitrogen (Karlsruhe)
Anti-Mouse	Goat IgG, polyclonal, AP-conjugated, Dianova (Hamburg)
Anti- Mouse	Goat IgG, HRP-conjugated, Jackson (West Grove, USA)
Anti- Mouse	Goat IgG, polyclonal, Alexa680-conjugated, Invitrogen (Karlsruhe)
Anti- Mouse	Goat IgG, polyclonal, IRDye800-conjugated, Rockland/Biomol (Hamburg)
Anti-hMBL	Mouse IgG1, monoclonal, Cl. D8.18, HRP-conjugated, Hycult biotech (Uden)
Anti-MBL-A	Rat IgG, monoclonal, Cl. 8G6, HRP-conjugated, Hycult biotech (Uden)
Anti-MBL-C	Rat IgG2a, monoclonal, Cl. 16A8, HRP-conjugated, Hycult biotech (Uden)
Anti-p3	Mouse IgG2a, monoclonal, HRP-conjugated, directed against M13 p3, NEB (Frankfurt)
Anti-p8	Mouse Ab, monoclonal, HRP-conjugated,Directed against M13 p8, GE Healthcare (Freiburg)
Anti-rat	Goat IgG, HRP-conjugated, Jackson (West Grove, USA)
S81-19	Mouse IgG, monoclonal, directed against WN1 222-5 mAb, kindly provided by L. Brade (RC Borstel)
WN1 222-5	Mouse IgG2a, monoclonal, originated in an immunisation of NZB-mize with heat-killed *S. minnesota* and *E. coli* strains [31]. Kindly provided by L. Brade (RC Borstel).

3.5. Mannose Binding Lectins

rMBL-A	2077-MB R&D systems (Wiesbaden-Nordenstadt)
rMBL-C	2208-MB R&D systems (Wiesbaden-Nordenstadt)
rhMBL	2307-MB R&D systems (Wiesbaden-Nordenstadt)
hMBL	Human complement serum, 51764, Sigma-Aldrich (Munich)

3.6. Antibiotics

Ampicillin	β-lactam antibiotic, Roth (Karlsruhe)
Carbenicillin	β-lactam antibiotic, Roth (Karlsruhe)
Kanamycinsulphate	Aminoglycoside, Roth (Karlsruhe)
Polymyxin B sulphate	Polypeptide, Sigma-Aldrich (Fluka) (Munich)
Tetracyclin	Tetracycline, Serva (Heidelberg)

3.7. Enzymes, Polymerase Chain Reaction and Reverse Transcription Reagents

E. coli RNaseH 2 U/µl	Invitrogen (Karlsruhe)
Super Script II 200 U/µl	Invitrogen (Karlsruhe)
6 x DNA loading dye	Fermentas (St. Leon-Rot)
DEPC-H_2O	Roth (Karlsruhe)
DNA ladder 1kb and 100 bp	Fermentas (St. Leon-Rot)
dNTP mix, 0,1 M	Analytic Jena (Jena)
Glycogen 20 mg/ml	Roche Diagnostics (Mannheim)
Master Mix hot start Y	Peqlab (Erlangen)
NotI	Fermentas (St. Leon-Rot)
Oligo(dT) primer	Invitrogen (Karlsruhe)
RNA purification system, peqGOLD TriFast	Peqlab (Erlangen)
SfiI	Fermentas (St. Leon-Rot)
T4 DNA Ligase	Fermentas (St. Leon-Rot)

3.8. Kits

AP conjugate substrate kit	Biorad (Munich)
Gel extraction, innuPREP	Analytic Jena (Jena)
PCR Purification, QIAquick	Qiagen (Hilden)
Plasmid Miniprep, QIAprep Spin	Qiagen (Hilden)

3.9. Buffer, Staining and Developing Solutions

Agarose gel 1%	1 g agarose/100 ml TAE buffer.
Alkaline phosphatase (AP) buffer	0.1 M $NaHCO_3$, 1 mM $MgCl_2$ x 6 H_2O in ddH_2O. pH adjustment with NaOH to 9.8.
BBS/Ca^{2+}	10 mM Diethylbarbituric acid sodium salt, 145 mM $NaCl_2$, 10 mM $CaCl_2$.
Blocking buffer – blots and ELISA	5% dry milk powder in TBS.
Blocking buffer – ELISA BSA	3% BSA in TBS.
Blocking buffer – ELISA BSA in BBS/Ca^{2+}	2% BSA in BBS/Ca^{2+}.
Blocking buffer – ELISA casein	2.5% casein, 0.01% thimerosal in PBS.
Blocking buffer – ELISA casein - Tween	2.5% casein, 0.01% thimerosal, 0.05% Tween 20 in PBS
Citrate buffer	0.1 M Na-citrate. pH adjustment with 2.5 M citric acid to 4.5.
Conservation solution	22% methanol, 5% glycine in ddH_2O.
Coomassie Brillant Blue staining solution	0.2% coomassie, 40% methanol, 10% acetic acid (glacial) in ddH_2O.
Coomassie destaining solution	20% methanol, 10% acetic acid (glacial) in ddH_2O.

EDTA solution	0.5 M $Na_2EDTA \cdot 2H_2O$ in ddH_2O. pH adjustment to 8.0 with NaOH.
ELISA coating buffer	0.05 M $NaHCO_3$. pH adjustment with 0.05 M Na_2CO_3 to 9.2. 0.01% thimerosal. Sterile through 0.2 µm filter.
Ethanol, 70% (v/v)	700 ml of technical grade ethanol dissolved in ddH_2O to 1 l.
Isopropyl-β,D-thiogalactoside (IPTG)	1 M IPTG in ddH_2O. Stored at -20°C.
PBS	0.0027 M KCl, 0.137 M NaCl, 0.0081 M Na_2HPO_4, 0.0015 M KH_2PO_4 in ddH_2O. pH adjustment with HCl to 7.2.
Phage precipitation solution	20% PEG 8000, 2.5 M NaCl in ddH_2O.
SDS-PAGE running buffer, 5 x	125 mM Tris, 960 mM glycine, 0.5% SDS in ddH_2O.
Substrate solution - AP	10 ml AP buffer, 0.1 ml solution A, 0.1 ml solution B (AP conjugate kit).
Substrate solution - HRP	1 mg ABTS/ml 0.1 M citrate buffer pH 4.5, 25 µl 0.1% H_2O_2.
Syto24	Invitrogen (Karlsruhe)
TAE buffer	40 mM Tris, 0.1% acetic acid (glacial), 1 mM EDTA (pH 8.0) in ddH_2O.
TBS (Tris-buffered saline)	50 mM Tris, 150 mM NaCl in ddH_2O. pH adjustment to 7.5 with HCl.
TBST	500 mM NaCl, 20 mM Tris, 0.05% Tween20 in ddH_2O.

Transfer buffer	25 mM Tris, 192 mM glycine, 4% methanol in ddH_2O. pH adjustment to 8.2 with HCl.

3.10. Culture Media

All media for bacterial cultivation were sterilised by autoclaving for 20 min. at 121°C and 1,2 bar. The heat-labile components were filtered sterile by passing them through a 0.2 µm filter.

LB (Luria Bertani)	Ready to use, Roth (Karlsruhe)
M9 (minimal) medium	1 l 1 x M9 salts, autoclaved. Added sterile 0.5 ml 2 M $MgCl_2$, 0.1 ml 1 M $CaCl_2$, 0.5 ml 10 mg/ml vitamin B_1, 10 ml 20% glucose, 20 ml 20% peptone 5.
M9 salt solution 10 x	60 g Na_2HPO_4, 30 g KH_2PO_4, 10 g NH_4Cl, 5 g NaCl, ddH_2O to 1 l.
SB (super broth)	10 g MOPS (3(*N*-morpholino)propanesulfonic acid), 30 g tryptone, 20 g yeast extract. pH 7, ddH_2O to 1 l.
SOC	20 g tryptone, 5 g yeast extract, 0.5 g NaCl. pH 7, ddH_2O to 1 l, autoclaved.

	Added sterile 10 mM $MgCl_2$,
	20 mM glucose.
TB (Terrific Broth) 10 x	24 g yeast extract,
	12 g tryptone,
	4% glycerine in 100 ml ddH_2O.
TOP Agar	1 l 1 x LB medium,
	6 g agar-agar.
YT 2 x	16 g tryptone,
	10 g yeast extract,
	5 g NaCl.
	Adjusted pH to 7 with NaOH, ddH_2O to 1 l.

3.11. Reagents

2-mercaptoethanol	Biorad (Munich)
2,2'-azino-bis(3-ethylbenzthiazoline-6-sulphonic acid) (ABTS)	Sigma-Adrich (Munich)
3(*N*-morpholino)propanesulfonic acid (MOPS)	Sigma-Aldrich (Fluka) (Munich)
Acrylamide/Bisacrylamide	30% Biorad (Munich)
Agar-agar	Roth (Karlsruhe)
Agarose	Eurogentec (Cologne)
Ammonium persulfate (APS), 10%	Merck (Darmstadt)
Bovine serum albumin (BSA)	PAA (Pasching, AT)
Bromophenol blue	Serva (Heidelberg)
Casein	Sigma-Adrich (Munich)
Chloroform	Merck (Darmstadt)
Disodium hydrogen phosphate	Sigma-Aldrich (Fluka) (Munich)
Dithiothreitol (DTT)	Invitrogen (Karlsruhe)
Ethanol	
Ficoll-Paque	GE Healthcare (Amersham) (Munich)
Glycerol	Merck (Darmstadt)

Glycine	Serva (Heidelberg)
Glycogen	Roche (Mannheim)
Hydrochloric acid	Merck (Darmstadt)
Hydrogen peroxide	Merck (Darmstadt)
Isopropanol	
MAPSII elution buffer, pH 6.8	Biorad (Munich)
Methanol	Merck (Darmstadt)
N,N,N`,N`-Tetramethylethylendiamine (TEMED)	Biorad (Munich)
Non fat dry milk	Biorad (Munich)
Polyethylene glycol 8000	Roth (Karlsruhe)
Potassium chloride	Merck (Darmstadt)
Protein loading dye 6 x	Fermentas (St. Leon-Rot)
Protein prestained ladder	Fermentas (St. Leon-Rot)
PVDF membrane	Millipore (Billerica, USA)
SDS	Biorad (Munich)
Sodium azide	Merck (Darmstadt)
Sodium chloride	Roth (Karlsruhe)
Sodium citrate dihydrate	Merck (Darmstadt)
Sodium hydrogen carbonate	Merck (Darmstadt)
Sodium hydroxide	Merck (Darmstadt)
Stripping solution	Thermo Scientific (Rockford, IL, USA)
Sulfuric acid, 95-97%	Merck (Darmstadt)
Thimerosal	Roth (Karlsruhe)
TMB	USB (Staufen)
Tris	Roth (Karlsruhe)
Tryptone	Roth (Karlsruhe)
Tryptone no. 5	Roth (Karlsruhe)
Tween 20	Biorad (Munich)
Western blot filter paper	Schleicher and Schuell (Dassel)
Yeast extract	Roth (Karlsruhe)

3.12. Laboratory Equipment

96-well plate	NUNC Maxisorp™, Thermo Scientific (Rockford, IL, USA)
Blot cell Mini-Trans	Biorad (Munich)
Centrifuge bottles, 0.02 l	Herolab (Wiesloch)
Centrifuge bottles, 0.25 l	Herolab (Wiesloch)
Centrifuge bottles, 0.5 l	Herolab (Wiesloch)
Centrifuge bottles, 1 l	Polypropylene, Beckman Coulter (Krefeld)
Centrifuge Tabletop	Rotanta 460R, Hettich (Tuttlingen)
Centrifuge tube, 50 ml	CentriStar, Corning (Amsterdam, NL)
Centrifuge, Avanti J-26 XP Rotor: JLA 8100, JA-10, JA-14 and JA-20	Beckman Coulter (Krefeld)
Centrifuge, Biofuge pico	Heraeus
DNA gel electrophoresis apparatus	Biorad (Munich)
Electrophoresis power supply	Biorad (Munich)
Electroporation apparatus, Micro Pulser (0.2 cm cuvettes)	Biorad (Munich)
ELISA reader	Tecan
Gel documentation system	Biorad transilluminator, software Quantity One 4.6.1 (Munich)
Heat block	Duotherm, Biometra (Göttingen)
Micro tubes, 1.5 ml and 2 ml	Sarstedt (Nümbrecht)
Microscope Eclipse TS100	Nicon (Melville, USA)
Mini-Trans Blot cell	Biorad (Munich)
Needles 0.9 x 40 mm	Becton Dickinson (Heidelberg)
Odyssey detection system	Li-cor, (Lincoln, NE, USA)
PCR reaction tubes 0.2 ml, lid chain	Sarstedt (Nümbrecht)
Pipette aid	Pipetboy, Integra Bioscience (Fernwald)
Pippette tips	Sarstedt (Nümbrecht)
SDS-PAGE electophoresis chamber	Miniprotean II, Biorad (Munich)
Shake incubator	Certomat BS-1, B. Braun biotech international (Sartorius) (Göttingen)

Spectrophotometer	NanoDrop, ND-1000, Peqlab (Erlangen)
Syringe Filter, 0.2 µm	Thermo Scientific (Nalgene) (Rockford, IL, USA)
Syringe, 2 ml	Becton Dickinson (Heidelberg)
Thermocycler	Biometra (Göttingen)
Ultrasonic bath	Sonorex, Bandelin (Berlin)
Waterbath	UC, Julabo (Seelbach)

4. Methods

4.1. Phage Display

The phage display procedures were performed according to Barbas III, Burton et al. 2001. They comprise as main steps the construction of a scFv library from immunised rabbits and the selection of distinct binding scFv-phages from this library.

4.1.1. Construction of ScFv Libraries from Immunised Rabbits

The immunisation was performed by Dr. L. Brade. Four chinchilla bastard rabbits (charles river) were immunised as described in Tab. 2 [63].

Rabbit/Material collection	**Day**	**Amount [µg]**	**Immunogen**
436	1	100	S81-19 IgG (+CFA) into lymphnotes
	42, 326	150	S81-19 $F(ab)_2$ (+IFA) subcutaneous
Blood, spleen, bone marrow	632		
438	1	100	S81-19 IgG (+CFA) into lymph nodes
	42, 487	150	S81-19 $F(ab)_2$ (+IFA) subcutaneous
	720	130	S81-19 $F(ab)_2$ (+IFA) intravenous
Blood, spleen, bone marrow	728		
437	1	100	S81-19 $F(ab)_2$ (+CFA) into lymph nodes
	42, 326	150	S81-19 $F(ab)_2$ (+IFA) subcutaneous
Blood, spleen, bone marrow	636		
439	1	100	S81-19 $F(ab)_2$ (+CFA) into lymph nodes
	42, 487	150	S81-19 $F(ab)_2$ (+IFA) subcutaneous
	720	130	S81-19 $F(ab)_2$ (+IFA) intravenous
Blood, spleen, bone marrow	728		

Tab. 2: Immunisation pattern of four rabbits immunised with mAb S81-19 anti-idiotype.

4.1.1.1. RNA Isolation

Total RNA of the anit-idiotype immunised rabbits was isolated from spleen, bone marrow and peripheral blood lymphocytes.
Spleen and bone marrow of the rabbits were homogenised separately in a glass homogenisator, to lyse the cells, and inactivate RNAses 10 ml peqGOLD TriFast were added. The mixture was divided in 1.5 ml portions in 2 ml tubes. Afterwards 300 µl chloroform were added to each resuspension, mixed and incubated for 10 min. at room temperature. It was centrifuged with 16200 x g for 10 min. at room temperature, that 3 phases were formed, a red phenol chloroform phase, an interphase with DNA and proteins and a colourless hydrous phase on the top bearing the RNA. The colourless phase was collected and transferred into a 1.5 ml reaction tube. 750 µl isopropanol were added, mixed and incubated for 15 min. at room temperature. The tubes were centrifuged with 16200 x g for 10 min. at 4°C and the isopropanol supernatant was discarded with a pipette. Followed by 2 washing steps, the pellets were resuspended in 500 µl 70% ethanol in DEPC-ddH_2O and centrifuged with 16200 x g for 10 min. at 4°C. The pellets were air dried for 10 min. at room temperature and afterwards resuspended in 100 µl DEPC-ddH_2O in total for each sample.

The isolation of the RNA from rabbit peripheral blood lymphocytes was made using 9 ml whole blood, collected from the rabbit ear vein. 1 ml 3.8% Na-citrate was provided in the collection tube. The citrate anticoagulated whole-blood cells were carefully given above 10 ml Ficoll and centrifuged at 1500 x g for 1 h at room temperature. The mononuclear cell layer was collected from between the Ficoll red blood cells and the plasma. 20 ml PBS was added to wash the cells and centrifuged with 1500 x g at 4°C for 10 min. The resulting pellet was resuspended in 5 ml PBS and the cells were counted using CASY cell counter program 1 for human mononuclear cells.
The cell suspension was divided in 1200 µl portions and centrifuged with 2100 x g for 10 min. at 4°C. To resuspend the pellets 1 ml peqGOLD TriFast was used. Subsequently a phenol-chloroform extraction was performed as described above.

4.1.1.2. Reverse Transcription

The isolated RNA was reverse transcribed to single- stranded cDNA. 20 µg RNA were incubated with 4 µg Oligo(dT)$_{12-18}$ primer and DEPC-ddH_2O was added to a total volume of 100 µl. It was incubated for 10 min. at 70°C, cooled down 1 min. on ice and centrifuged to the bottom of the tube. As a reaction mix 32 µl 5 x first strand buffer, 8 µl 10 mM dNTP mix (each 10 mM) and 16 µl 100 mM dithiothreitol (DTT) were added and incubated for 5 min. at 42°C. 8 µl of 200 U/µl Super Script II were added and incubated for 1 h at 42°C, then heated for 15 min. to 70°C, cooled down for 1 min. on ice and centrifuged to the bottom of the tube. Afterwards 8 µl of 2 U/µl *E. coli* RNaseH were added and incubated for 20 min. at 37°C. The library cDNA was stored at -20°C.

4.1.1.3. Construction of ScFvs

In a first round of polymerase chain reaction (PCR) rabbit variable light and heavy chain genes were amplified from cDNA by using V_L and V_H primers described by Barbas et al. [76]. The V_L primers are provided with a sense primer extension, including a SfiI restriction site and a reverse primer containing a short or long linker sequence tail. Whereas V_H primers have sense primers containing a linker sequence, corresponding to the V_L reverse primer sequence tail, used for linking both in a second PCR to one fragment together. The V_H reverse primers contain a sequence tail with a SfiI restriction site.

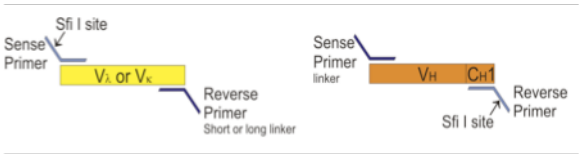

Fig. 12: Amplification of the antibody variable region genes.
$V_κ$, $V_λ$ and V_H were amplified using various primer combinations. Simultaneously the linkers were attached to one site and to the other a SfiI restriction site was introduced.

The following conditions were used for the different primer combinations:

PCR Mixture	
~ 0.5 µg	cDNA
60 pmol	sense primer
60 pmol	reverse primer
50 µl	master mix hot start Y
100 µl	total volume with sterile ddH_2O

Cycle Step	**Temperature**	**Time**	**No. of Cycles**
Initial Denaturation	95°C	5 min.	1
Denaturation	94°C	15 sec.	
Annealing	56°C	30 sec.	30
Extension	72°C	90 sec.	
Final Extension	72°C	10 min.	1

The amplified genes were purified using a PCR purification kit according to the manufacturers protocol and quantified by measuring the absorbance at a wavelength of 260 nm in the NanoDrop photometer.

In a second round of PCR, called overlap extension PCR, the V_L and V_H PCR products were mixed in a 1:1 ratio, to join them randomly via their adhered linkers (Fig. 13). They were amplified with primers recognising the sequence ends that were generated during the first PCR round.

Fig. 13: Overlap extension PCR.

The sequence tails generated in the first round of PCR were used to amplify the combined variable region gene fragments.

PCR Mixture	
~ 0.1 µg	amplified V_L DNA
~ 0.1 µg	amplified V_H DNA
60 pmol	sense primer
60 pmol	reverse primer
50 µl	master mix hot start Y
100 µl	total volume with sterile ddH_2O

Cycle Step	Temperature	Time	No. of Cycles
Initial Denaturation	95°C	5 min.	1
Denaturation	94°C	15 sec.	
Annealing	56°C	30 sec.	25
Extension	72°C	120 sec.	
Final Extension	72°C	10 min.	1

The resulting short and long linker scFv PCR products were combined in 2 separated pools and ethanol precipitated. Followed by purification of the DNA fragment using a 1% agarose gel for the separation of different sized fragments. The band with the expected size of 700 bp was sliced from the gel and regained with the use of a gel extraction kit according to the manufacturers protocol.

4.1.1.4. Restriction Digest

The purified overlap extension product and the phagemid vector pComb3XSS were prepared for cloning by a restriction digest with the enzyme SfiI.

Mixture for Insert Digest	
10 µg	PCR product
360 U	SfiI enzyme
20 µl	10 x NEB2 buffer
100 µl	total volume with sterile ddH_2O

Mixture for Vector Digest	
20 µg	pComb3XSS vector
120 U	SfiI enzyme
20 µl	10 x NEB2 buffer
100 µl	total volume with sterile ddH_2O

Both digests were incubated for 16 h at 50°C. The digested DNA fragments were separated by agarose gel electrophoresis. The PCR product (~700 bp), vector (~3400 bp) and stuffer (~1600 bp) fragment were retrieved using a gel extraction kit.
The obtained DNA fragments were quantified by measuring the OD at 600 nm in a spectrophotometer.

4.1.1.5. Ligation

In ligation reactions the T4-DNA-ligase of the *E. coli* phage T4 was used to combine, under ATP consumption, covalently the ends of DNA fragments.
Firstly small scale ligations were performed to verify the suitability of the DNA fragments for the library ligation.
In one reaction the ligation efficacy of the vector was tested by ligating the stuffer fragment as a control insert back into the sliced vector.

Ligation Mixture	
0.14 µg	pComb3XSS vector
0.14 µg	pComb3XSS stuffer
2 µl	10 x T4 ligase buffer
1 µl	T4 ligase
20 µl	total volume with sterile ddH_2O

In another reaction the vector was tested for self ligation properties.

Ligation Mixture	
0.14 µg	pComb3XSS vector
2 µl	10 x T4 ligase buffer
1 µl	T4 ligase
20 µl	total volume with sterile ddH_2O

In a third reaction the PCR product was joined to the vector in a small scale test.

Ligation Mixture	
0.14 µg	pComb3XSS vector
0.07 µg	PCR product
2 µl	10 x T4 ligase buffer
1 µl	T4 ligase
20 µl	total volume with sterile ddH_2O

The reactions were incubated for 16 h at room temperature. 1 µl of each reaction was added to 50 µl electrocompetent *E. coli* ER2537 and transformed by electroporation (program Ec2) into the cells. The transformed cells were internalised in 1 ml prewarmed (37°C) SOC medium and incubated for 1 h at 37°C with 220 rpm. Afterwards the culture was diluted 10-fold and 100-fold and plated on LB plates with carbenicillin (0.1 mg/ml). The plates were incubated for 16 h at 37°C, the colonies counted, and the number of transformants per µg vector DNA was calculated.

The large scale library ligation was performed to get a high yield of different rabbit scFv genes.

Ligation Mixture	
1.4 µg	pComb3XSS vector
0.7 µg	PCR product
20 µl	10 x T4 ligase buffer
10 µl	T4 ligase
200 µl	total volume with sterile ddH_2O

It was incubated for 16 h at room temperature. Afterwards the DNA was ethanol precipitated and the DNA pellet resuspended in 15 µl sterile ddH_2O.

4.1.1.6. Transformation of the Phage Libraries

300 µl electrocompetent *E. coli* ER2537 were melted on ice, the resuspended 15 µl DNA was added and the mixture proportioned to 3 cooled 0.2 mm cuvettes. The DNA was transformed by electroporation (program Ec2), and the cuvette was immediately afterwards flushed with 5 ml prewarmed (37°C) SOC medium. The bacteria culture was incubated for 1 h at 37°C with 220 rpm. Then 10 ml SB medium and 3 µl cabenicillin (100 mg/ml) were added.
2 µl of this culture were diluted in 200 µl SB and 10 µl and 100 µl plated on LB agar containing 0.1 mg/ml carbenicillin, to determine the titer of phage forming units. The agar plates were incubated 16 h at 37°C.
The 15 ml culture was incubated for 1 h at 37°C with 220 rpm, then 4.5 µl carbenicillin (100 mg/ml) were added, and it was incubated for another hour. 2 ml M13K07 helper phages were added, the culture was transferred to a 500 ml polypropylene centrifuge bottle, 183 ml SB medium and 92.5 µl carbenicillin (100 mg/ml) were added and the culture was incubated for 2 h at 37°C with 220 rpm. Then 280 µl of kanamycin were added, and it was further incubated for 16 h.
The culture was centrifuged with 2830 x g for 15 min. at 4°C and the supernatant transferred into a 500 ml centrifuge bottle. For phage precipitation 8 g (4%) of PEG-8000 and 6 g (3%) NaCl were added and dissolved by shaking with 220 rpm for 5 min. at 37°C. For a better precipitation the culture was then cooled for 30 min. on ice.
The phages were precipitated by centrifuging with 14333 x g for 15 min. at 4°C. The supernatant was discarded and the pellet dried for 10 min. in the inverted centrifuge bottle, to remove remaining precipitation liquid. 2 ml of 1% BSA in TBS was used to resuspend the phage pellet. The 2 ml were transferred to a 2 ml tube and centrifuged with 16200 x g for 5 min. at 4°C. Then the supernatant was passed through a 0.2 µm filter into a new 2 ml tube. The phage preparation was stored at 4°C.

4.1.2. Panning on Immobilised Antigens

The constructed rabbit scFv libraries were used for the selection of specific binders. Therefore different variations of the following principle procedure were performed.

Coating: For the first round of panning 2 single wells were coated with 1 of 3 different antigens.

1. 50 pmol/well of *E. coli* R3 core rough type LPS conjugated via glutaraldehyde to BSA
2. 2 µg/well of *E. coli* R3 core rough type heat-killed bacteria
3. 1 pmol/well of S81-19 mAb

As coating buffer 0.05 M carbonate buffer was used, and 50 µl/well antigen solution was incubated 16 h at 4°C. In the first round of panning two wells were used, in the subsequent rounds one.

Blocking: The well was blocked with 150 µl of one of three different blocking buffers: 3% BSA in TBS, 2.5% casein in PBS or 5% milk powder in TBS and incubated for 1 h at 37°C.

Phage binding: The blocking solution was taped on a paper towel, 50 µl of freshly prepared phages were added to the well and incubated for 2 h at 37°C.

Washing: The phage solution was discarded from the well, and 150 µl 0.5% Tween20 in TBS were added. It was resuspended 5 times, then incubated for 5 min., and subsequently the washing solution was taped out on a paper towel. This washing step was repeated in the first round of panning 5 times, in the later rounds 8, 10, 12 and 15 times.

Elution: Afterwards the bound phages were acidic eluted with 50 µl 0.1% BSA in 100 mM glycin-HCl pH 2.2. The acid was incubated for 10 min., then resuspended 10 times, and the eluate was transferred to a 1.5 ml tube containing as neutralisation solution 3 µl 2 M Tris.

Amplification: The eluted phages were added to 2 ml log-phase *E. coli* ER2537 culture and incubated for 15 min. at room temperature. 6 ml SB medium and 1.6 µl carbenicillin (100 mg/ml) were added to the culture.

To determine the phage output titer after each panning round, 2 µl of the 8 ml culture were diluted in 200 µl SB medium, 10 µl and 100 µl of this dilution were plated on LB agar containing 100 µg/ml carbenicillin and incubated overnight at 37°C.

The 8 ml culture was incubated for 1 h at 37°C with 230 rpm, then 2.4 µl carbenicillin (100 mg/ml) were added and incubated again for 1 h. 1 ml of the helper phages M13K07 was added for phage particle packaging, together with 91 ml SB medium and 46 µl carbenicillin (100 mg/ml). It was incubated for 2 h at 37°C with 230 rpm, then 140 µl kanamycin (50 mg/ml) were added and again incubated overnight.
For the preparation of the phages the culture was centrifuged for 15 min. with 2830 x g at 4°C. To the supernatant 4 g PEG 8000 and 3 g NaCl were added, dissolved for 10 min. with 230 rpm at 37°C and cooled then for 30 min. on ice. It was centrifuged for 15 min. with 14333 x g at 4°C and the precipitation solution carefully removed from the phage pellet. The pellet was resuspended in 2 ml 1% BSA in TBS and centrifuged again for 5 min. with 16200 x g at 4°C. The phage supernatant was filtered through a 0.2 µm filter and stored at 4°C.
The phage input titer for the next panning round was determined by using 1 µl of a 10^{-9} dilution of the filtered phage solution in 50 µl log-phase *E. coli* ER2537 culture. It was incubated for 15 min. at room temperature, subsequently plated on LB agar containing 100 µg/ml carbenicillin and incubated overnight at 37°C. The colonies were counted and the phage titer calculated.

4.1.3. Phage Reamplification

To avoid protease cleavage effects of the scFvs on phage selection, it is necessary to use only freshly prepared phages for panning. On the other hand reamplification can lead to a decreased complexity of the library and should not be repeated frequently.
10 µl of the phage preparation were used to inoculate a 50 ml *E. coli* ER2537 culture with an OD_{600} of ~1 grown in a 500 ml centrifuge bottle. The culture was incubated for 15 min. at room temperature, then 10 µl of 100 mg/ml carbenicillin were added and incubated for 1 h at 37°C with 220 rpm. To determine the amount of phage infected bacteria, 10 µl of a 10^{-4} dilution were plated on LB agar plates, containing 0.1 mg/ml carbenicillin. They were incubated overnight at 37°C, and the amount of colony forming units were counted.
To the 50 ml culture 15 µl 100 mg/ml carbenicillin were added and incubated for an additional hour. Then 2 ml M13K07 helper phages, 148 ml SB medium and 75 µl 100 mg/ml carbenicillin were added and incubated for 2 h at 37°C with 220 rpm. 280 µl 50 mg/ml kanamycin were added and incubated for additional 16 h.
The phage rescue was performed as described for the library transformation.

4.1.4. Subcloning into the pHen1 Phagemid

The scFv library, derived from S81-19 (anti-idiotype) immunised rabbit 437, was subcloned into the pHen1 phagemid vector.

4.1.4.1. Plasmid Preparation

Therefore 10 ml *E. coli* ER2537 log-phase culture in SB medium were infected with 10 µl of the phage preparation from the 437 library in the pComb3XSS vector. They were allowed to infect the cells for 15 min. at room temperature and afterwards they were incubated for 30 min. at 37°C with shaking at 230 rpm. Then 5 µl 100 mg/ml carbenicillin were added, and it was incubated under the same conditions for 1 h. Again 5 µl 100 mg/ml carbenicillin were added and it was incubated under the same conditions overnight. The plasmid preparation was performed using a plasmid miniprep kit according to the manufacturers protocol.

4.1.4.2. Appending of a NotI Site

For the appending of a NotI restriction site on the 3'- end of the scFv, a PCR master mix was prepared.

PCR Mixture	
~ 4 µg	plasmid DNA
60 pmol	NH1704-02_FP primer
60 pmol	LH566-RP_NotI primer
800 µl	master mix hot start Y
1600 µl	total volume with sterile ddH_2O

The mixture was given in 0.1 ml portions to 0.2 ml PCR tubes. The thermocycle conditions were as described for scFv construction.
A PCR purification kit was used, according to the manufacturer protocol, to concentrate the PCR samples to a volume of 80 µl. Then an agarose gel electrophoresis was performed, and the expected scFv of around 750 bp was sliced from the gel. For the gel extraction a gel extraction kit was used according to the manufacturers protocol.

4.1.4.3. Restriction Digest

The PCR product and the pHen1 plasmid were first digested with SfiI at 50°C for 4 h.

Mixture for Insert Digest	
15 µg	PCR product
30 U	SfiI enzyme
10 µl	10 x buffer G
100 µl	total volume with sterile ddH_2O

Mixture for Vector Digest	
10 µg	pHen1 plasmid
30 U	SfiI enzyme
10 µl	10 x buffer G
100 µl	total volume with sterile ddH_2O

The digestion mixtures were cooled down to room temperature and were then incubated with the second enzyme NotI at 37°C for 2 h.

Additives for Both Mixtures	
3 µl	NotI (fast digest)
12 µl	fast digest buffer green
5 µl	sterile ddH_2O

The digested DNA was separated from digestion products by agarose gel electrophoresis and extracted from the gel using a gel extraction kit according to the manufacturers protocol.

4.1.4.4. Ligation and Transformation

The ligation mixture was incubated for 4 h at room temperature.

Ligation Mixture	
1 µg	pHen1 vector
1 µg	PCR product
10 µl	10 x T4 ligase buffer
5 µl	T4 ligase
100 µl	total volume with sterile ddH_2O

Afterwards the DNA was precipitated with ethanol and transformed into electrocompetent *E. coli* TG1 cells via electroporation, as described in detail for the pComb3XSS library transformation.

4.1.5. Amplification of Single Phages

Single phages, amplified from infected *E. coli* colonies from the titer determination plates, were tested for their antigen binding in ELISA. Therefore single colonies were used to inoculate 5 ml SB medium containing 50 µg/ml carbenicillin and incubated for 5 h at 37°C with shaking at 250 rpm. 50 µl M13K07 helper phage was added and incubated for another 2 h. Then 7 µl kanamycin (50 mg/ml) were added and the cultures incubated overnight at 37°C with shaking at 250 rpm.
Phage harvesting was implemented by centrifugation with 10916 x g for 15 min. at 4°C. The supernatant was mixed in a 5:1 ratio with 20 % PEG and 2.5 M NaCl, and the phages were precipitated while cooling them for 30 min. on ice. Afterwards it was centrifuged for 10 min. with 16200 x g at 4°C and the supernatant was carefully removed with a pipette. The pellet was resuspended in 50 µl TBS.

4.1.6. Soluble Expression of ScFvs

For the infection with single phages 10 ml SB medium, containing 10 µg/ml tetracycline, were inoculated with 10 µl of a TOP10F' bacterial stock. It was incubated for 2 h at 37°C with 230 rpm. Then 10 µl of the single phage preparation were added and allowed to infect during 20 min. without shaking at room temperature. 10 µl carbenicillin (100 mg/ml) were added, and it was incubated for 1 h at 37°C with 230 rpm. 100 ml SB medium, 45 µl carbenicillin (100 mg/ml) and 100 µl 1 M IPTG for the induction of the scFv expression were added. It was incubated overnight at 37°C with 230 rpm. The culture was centrifuged for 15 min. at 4°C with 2830 x g and the supernatant stored at 4°C.
The cell pellet was weighed and twice the volume MAPSII elution buffer, and 1/100 volume polymyxin B were added. It was incubated during gently mixing for 4 h at 4°C. Then it was centrifuged for 15 min. at 4°C with 16200 x g and the scFv containing supernatent stored at 4°C.

4.1.7. Preparation of Helper Phages

Packaging of pComb3 phages requires the support of helper phages, providing the proteins for replication and assembly, which are lacking in the pComb3 phagemids. To receive an appropriate amount of helper phages for the library panning, they were amplified and concentrated by precipitation.
Single M13K07 helper phages were obtained by inoculating 2 ml of SB medium with 2 µl electrocompetent *E. coli* ER2537 (stored at -70°C) and incubated for 90 min. at 37°C with 230 rpm. 1 µl of a 10^{-6}, 10^{-7} and 10^{-8} dilution of a 1 x 10^{11} pfu/ml M13K07 preparation was used to inoculate 50 µl of *E. coli* culture. They were incubated for 15 min. at room temperature, then 3 ml melted top agar (~ 40°C) were added and spread over a LB agar plate. The plates were incubated overnight at 37°C.
M13K07 infected cells growing slower than non-infected cells lead to a plaque formation. A single plaque was picked with a pipette tip and used for infection of a 10 ml *E. coli* ER2537 log-phase culture. It was incubated for 2 h at 37°C with 230 rpm. 5 ml of the culture were used to inoculate 250 ml SB medium, 350 µl kanamycin (50 mg/ml) were added and it was incubated for 16 h at 37°C with 230 rpm. Afterwards the culture was centrifuged for 15 min.

with 2830 x g at 4°C and the supernatant was transferred to 50 ml tubes. The tubes were incubated for 20 min. in a 70°C water bath and then centrifuged like before.
240 ml phage supernatant were precipitated by adding 9.6 g PEG 8000 and 7.2 g NaCl, the components were solved for 10 min. at 37°C with 220 rpm and cooled for 30 min. on ice. It was centrifuged for 15 min. with 14333 x g at 4°C and the supernatant carefully removed from the pellet, to avoid precipitating residues. The pellet was resuspended in 20 ml SB medium and centrifuged for 10 min. with 16200 x g at 4°C. The phage supernatant was filtered through a 0.2 µm filter and stored at 4°C.
The phage titer was determined by the same procedure as described to get single phage plaques.

4.1.8. Preparation of Electrocompetent *E. coli*

For the generation of electrocompetent *E. coli* it is necessary to prepare high resistance media with a low ionic strength. Therefore 5 ml of SB medium were inoculated with a single colony grown on M9 agar plate for 16 h. This preculture was incubated for 16 h at 37°C with 220 rpm. 2.5 ml of the culture were used to inoculate 500 ml SB in a 2 l flask supplemented with 10 ml 20% glucose and 2.5 ml 2 M $MgCl_2$. It was incubated at 37°C with 200 rpm until an OD_{600} of ~0.8 was reached. All following steps were performed on ice.
The bacteria culture was proportioned on 500 ml centrifuge bottles. It was centrifuged for 20 min. with 2830 x g at 4°C, and the supernatant was discarded. Each pellet was resuspended in 25 ml precooled 10% glycerol combined with another pellet, and 10% glycerol was added to a total volume of 200 ml. It was centrifuged as before and the pellet was resuspended again in 200 ml 10% glycerol. After another centrifugation the pellet was resuspended in 13 ml 10% glycerol and centrifuged for 15 min. with 11000 x g at 4°C. The pellet was resuspended in 2.5 ml 10% glycerol and afterwards in 100 µl volumes proportioned in 1.5 ml screw-cap tubes. The bacterial suspension was frozen with liquid nitrogen and stored at -70°C.

4.2. Binding Assays

4.2.1. ELISA

Bacteria were immobilised on Nunc PolySorb plates with U bottom shaped wells by incubation overnight at 4°C with 50 µl/well bacteria solution. The plates were blocked with 200 µl 2% BSA in BBS/Ca^{2+} for 1 h at 37°C at 110 rpm. The wells were washed 2 times with BBS/Ca^{2+}.
50 µl rMBL dilution was added and titrated through the following wells. The plate was incubated for 1 h at 37°C with 110 rpm. The wells were washed 2 times with BBS/Ca^{2+}. 50 µl of 1 µg/ml anti-hMBL, anti-MBL-A or anti-MBL-C antibodies in blocking buffer were added and incubated for 1 h at 37°C with 110 rpm. The wells were washed 2 times with BBS/Ca^{2+}. 50 µl of 1 µg/ ml of horseradish peroxidase conjugated anti-mouse antibody or anti-rat antibody in blocking buffer were added and incubated for 1 h at 37°C with 110 rpm. The wells were washed 3 times with BBS/Ca^{2+}. 50 µl of ABTS substrate solution were added to the wells and incubated for 30 min at 37°C with 110 rpm. The optical density was measured in an ELISA reader at 405 nm.

4.2.2. Phage ELISA

To monitor whether the amount of phages carrying a scFv of interest increases during the panning rounds, it is possible to perform ELISAs directly with the phages using an anti-M13 antibody. The following ELISA procedure was also used for the detection of amplified single phages.
In general, the same concentration of antigen in 50 µl/well coating buffer was used to coat a 96-well MaxiSorp plate, as it was used in the previous panning. It was incubated overnight at 4°C.
The antigen solution was discarded by tapping the plate on a paper towel. To block remaining binding sites on the polystyrene wells, 200 µl/well 2.5% casein in PBS were added and incubated for 1 h at 37°C. Phages in different concentrations were diluted in blocking buffer, and 50 µl/well were incubated for at least 1 h at 37°C. The phage solution was removed and the wells washed with either PBST or PBS between 3 and 10 times, adjusted for the respective test.

Phages were detected with an anti-M13 antibody specific for the major coat protein pVIII of M13 derived phages. 50 µl/well of the recommended 1:5000 dilution of the Ab were incubated for 1 h at 37°C, and the wells were washed 3 times with PBS.
Quantification of the bound horseradish peroxidase conjugated anti-M13 antibody was achieved by adding ABTS as substrate, which can be determined after deprotonation at it is colour change to green. The development solution was incubated for 30 min. at 37°C, and the optical density measured in an ELISA reader at 405 nm.

4.2.3. Inhibition ELISA

Nunc MaxiSorb plates with U bottom shaped wells were coated overnight at 4°C with 50 µl/well of 10 µg/ml mannan. The plates were blocked with 200 µl 2% BSA in BBS/Ca^{2+} for 1 h at 37°C at 110 rpm.
50 µl rMBL were preincubated with various inhibitor concentrations in a nunc V bottom micro well plate. The inhibitors were titrated by resuspending 50 µl of the previous well 10 times in 50 µl blocking buffer. The titrated inhibitors were incubated with 50 µl rMBL for 1 h at 37°C with 110 rpm.
The blocking buffer was removed from the mannan coated well by tapping the plate on paper towel and the wells were washed 1 x with BBS/Ca^{2+}. Then the inhibitor rMBL mixture was resuspended 3 times and 50 µl were transferred to the mannan coated plate. It was incubated for 30 min. at 37°C with 110 rpm. The wells were washed 2 times with BBS/Ca^{2+}. 50 µl of 1 µg/ml anti-hMBL, anti-MBL-A or anti-MBL-C antibodies in blocking buffer were added and incubated for 1 h at 37°C with 110 rpm. The wells were washed 2 times with BBS/Ca^{2+}. 50 µl of 1 µg/ ml of horseradish peroxidase conjugated anti-mouse antibody or anti-rat antibody in blocking buffer were added and incubated for 1 h at 37°C with 110 rpm. The wells were washed 3 times with BBS/Ca^{2+}. 50 µl of ABTS substrate solution were added to the wells and incubated for 30 min. at 37°C with 110 rpm. The optical density was measured in an ELISA reader at 405 nm.

4.2.4. Complement Activation Assay

Nunc MaxiSorb plates with U bottom shaped wells were coated overnight at 4°C with 50 µl/well of 1 µg/ml mannan or 50 pmol/well Gal-BSA. The plates were blocked with 200 µl 2% BSA in BBS/Ca^{2+} for 1 h at 37°C at 110 rpm. The blocking buffer was removed from the mannan coated well by tapping the plate on paper towel and the wells were washed 1 x with BBS/Ca^{2+}. Human complement serum was diluted 1:40 and 50 µl/well were added to the wells. It was incubated for 1 h at 37°C with 110 rpm. The wells were washed 2 times with BBS/Ca^{2+}. 50 µl of 1 µg/ml anti-hMBL antibody in blocking buffer were added and incubated for 1 h at 37°C with 110 rpm. The wells were washed 2 times with BBS/Ca^{2+}. 50 µl of 1 µg/ml of horseradish peroxidase conjugated anti-mouse antibody or anti-rat antibody in blocking buffer were added and incubated for 1 h at 37°C with 110 rpm. The wells were washed 3 times with BBS/Ca^{2+}. 50 µl of ABTS substrate solution were added to the wells and incubated for 30 min. at 37°C with 110 rpm. The optical density was measured in an ELISA reader at 405 nm.

4.3. General Methods

The methods were modified after Molecular Cloning: A Laboratory Manual [102].

4.3.1. Storage of Bacteria

Individual colonies of all strains were obtained by separating the cells on agar plates. Strains carrying the F' factor were plated on M9 agar and other strains were plated on LB, containing the suitable antibiotic. Incubations were performed at 37°C, and the plates were stored up to 2 weeks at 4°C.
For long time storage 0.5 ml of a fresh 16 h culture was mixed with 0.5 ml sterile glycerol (87%). The bacterial suspension was frozen with liquid nitrogen and stored at -70°C.

4.3.2. DNA Staining

Bacteria were stained with syto24. 1 µl syto24 was diluted in 100 µl PBS and transferred to the bacteria-coated polysorb well. It was incubated for 20 min. at 37°C. The bacterial load was estimated by fluorescence microscopy.

4.3.3. Sodium Dodecyl Sulfate-Polyacrylamide Gel Electrophoresis (SDS-PAGE)

The SDS-PAGE was used for the separation of proteins according to their size.
Firstly the gels were prepared as followed.

12.5% polyacrylamide resolving gel	
4.12 ml	30% acrylamide
2.5 ml	1.5 M Tris
100 µl	10% SDS
5 µl	TEMED
50 µl	10% APS
3.23 ml	ddH_2O

The solution was mixed, immediately poured between two glass plates of the SDS-PAGE apparatus and overlayed with ethanol to prevent bubbles from polymerising. After 45 min. the ethanol was removed and the gel surface rinsed with ddH_2O. A broader linked stacking gel was provided above the resolving gel to focus the proteins before separation.
The 4% stacking gel was prepared from the following solution:

4% polyacrylamide stacking gel	
1 ml	30% acrylamide
1.9 ml	0.5 M Tris
80 µl	10% SDS
8 µl	TEMED
40 µl	10% APS
4.5 ml	ddH_2O

The solution was thoroughly mixed, poured on the top of the resolving gel and a comb was inserted. After 45 min. the polymerised gel was assembled into the SDS-PAGE apparatus and running buffer was poured above.
Protein samples were mixed with the appropriate amount of loading dye and, if desired, with DTT or ß-mercaptoethanol. They were heated for 5 min. to 90°C and loaded on the gel. The gel was run with 100 V until the dye front reached the end of the gel.
The gel was incubated in coomassie brilliant blue staining solution for 30 min. and afterwards in coomassie destaing solution until the protein bands were visible. The gel was rinsed with ddH_2O and placed between two in 5% glycerin and 22% ethanol softened cellophane sheets.

4.3.4. Western Blot

The western blot method was used for specific detection of proteins, separated before by SDS-PAGE. Following SDS-PAGE, the stacking gel was removed and the resolving gel was used for the transfer of proteins onto a PVDF membrane.
The PVDF membrane was shortly activated in methanol and rinsed afterwards 4 times with ddH_2O. To avoid air bubbles during blotting, 2 foam pads and 4 sheets of filter paper were wet in transfer buffer before placing them into the gel holder cassette. A foam pad and 2 filter papers were placed on one side of the cassette, the gel was laid above them and the membrane

was laid thoroughly on the gel, to avoid air inclusions. The other 2 filter papers and the foam pad were placed on the membrane, the cassette was closed and placed with the membrane in the direction of the anode into the blotting apparatus. An ice block was placed in the apparatus, and the rest of the tank was filled with blotting buffer. The proteins were blotted from the gel to the membrane for 30 min. at 100 V (0.4 A).
Subsequently the membrane was incubated for 1 h in 5% dry milk powder in TBS to block the free binding sites on the membrane. The primary and, if required, the secondary antibody were diluted in blocking buffer.

4.3.5. Polymerase Chain Reaction (PCR)

PCR is a method for rapid enzymatic amplification of a specific DNA sequence [103]. Therefore oligonucleotides were used flanking the DNA fragment of interest.
In principle the method is based on 3 reaction steps: denaturation of the DNA strand, annealing of the specific oligonucleotides to their complementary strand and elongation of the oligonucleotides by DNA polymerase under usage of free dNTPs. This process is repeated cyclic, resulting in an exponential amplification of the DNA fragment.
The used DNA polymerase was the Taq polymerase of the thermophilic bacterium *Thermus aquaticus*, provided with an inhibitory antibody. The release of the polymerase is caused by a hot start denaturation step for 5 min. at 95°C, this offers the advantage of a decreased amount of side products.
The different applications of the PCR required variations in reaction mixtures, temperatures and times. The tested optimal conditions were described for the respective applications.
As standard 0.1 ml reactions were performed in 0.2 ml tubes in a thermocycler.
PCR products were analysed in agarose gel electrophoresis.

4.3.6. Colony PCR

To verify whether a bacterial colony contains plasmid with an insert of a desired size, single colonies were picked with an inoculation loop and dipped in a PCR tube containing 20 µl reaction mixture. Each reaction mixture was composed of 10 µl hot start master mix, 6 pmol forward primer, 6 pmol reverse primer and water to the total volume of 20 µl.

The PCR conditions were the hot start conditions described for the common PCR.

4.3.7. Agarose Gel Electrophoresis

Plasmid DNA, DNA fragments and PCR products were separated on horizontal agarose gels. Therefore 1% agarose in TAE buffer was heated in a microwave until the agarose was dissolved completely, cooled down to approximately 60°C and poured in a gel chamber. The cooled and hardened gel was used with TAE as running buffer.
Generally 10 µl sample were mixed with 2 µl 6 x loading dye and loaded in the wells, next to 5 µl 1 kb or 100 bp DNA ladder for subsequent analysis of the bands' sizes. Migration was performed with supply of 90 V. Afterwards the gel was exposed to a 0.5 µg/ml ethidiumbromide water bath for 15 min., rinsed once with water and recorded by a UV transilluminator.

4.3.8. Ethanol Precipitation

To concentrate DNA samples and change buffer solutions, DNA was either ethanol precipitated or isolated via a PCR purification kit column.
It was precipitated by adding to the DNA sample 1 µl glycogen (20 mg/ml), 1/10 volume of 3 M sodium acetate (pH 4.8) and 2 volumes of 100% ethanol. Then the solution was extensively mixed and cooled for 1 h at -70°C. The cool sample was centrifuged for 45 min. with 16200 x g at 4°C, and the supernatant was carefully removed with a pipette.
The DNA pellet was washed by adding carefully 1 ml 70% ethanol, without destroying the pellet. It was centrifuged again for 5 min., and the supernatant was removed. The pellet was enabled to dry on air completely and then resuspended in an appropriate volume of the desired buffer.

4.3.9. DNA Sequencing

The DNA sequences of the scFvs were determined by using a plasmid preparation of a single colony as template. Therefore 5 ml SB medium, containing 0.1 mg/ml ampicillin, were inoculated with a single colony from an overnight grown LB + 0.1 mg/ml Ampicillin agar plate. The liquid culture was incubated overnight at 37°C with 230 rpm.
Subsequently the plasmids were preparated using the plasmid miniprep kit according to the manufacturer's protocol. 50-100 ng/µl plasmid DNA and 2 pmol/µl primer, both in a total volume of 15 µl per sequence analysis were sent to Eurofins MWG operon, Anzinger Str. 7a, 85560 Ebersberg, Germany for sequencing.
The sequencing results were analysed with the either the software 4Peaks (Version 1.7.2) or DNAStar Lasergene (Version 8.0).

5. Results

5.1. Construction of an Idiotype ScFv

For the isolation of antibody fragments with similar binding properties like the idiotype mAb WN1 222-5 a scFv WN1 222-5 was constructed in order to valuate the usability of the approach. The scFv and phage WN1 222-5 should be used as controls for the phage panning procedure and binding assays. Therefore the variable regions of the WN1 222-5 antibody were cloned into the pComb3XSS vector. Determination of the WN1 222-5 scFv was done by colony PCR (Fig. 14) and subsequent sequencing (Fig. 15).

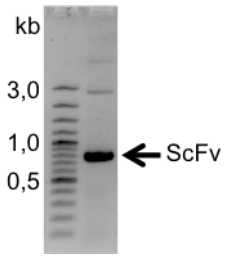

Fig. 14: Colony PCR of the scFv WN1 222-5 after transformation.
The correct insert size was determined subsequent to transformation by bacterial colony PCR.

Fig. 15: Amino acid sequence of scFv WN1 222-5 in one letter code.
The sequence of scFv WN1 222-5 subsequent to cloning into the pComb3XSS vector. Figured with ompA leader sequence (grey), 18 aa linker (blue), His6 tag (grey), haemagglutinin tag (grey), amber stop codon and the beginning of the truncated N-terminus of pIII from the M13 phage. Complementarity determining regions (CDRs) determined after sequence analysis with IMGT database [104].

5.2. Anti-Anti-Idiotype ScFvs

5.2.1. Construction of Rabbit ScFv Libraries

ScFv libraries were constructed to obtain the rabbit antibody gene pool for subsequent high throughput screening for specific binding antibody fragments.

5.2.1.1. Isolation of total RNA

The construction of a scFv library of an immunised rabbit requires the isolation of total antibody mRNA. Hence, the complete spleen, bone marrow material of the femurs and the harvested peripheral blood lymphocytes were used from four rabbits immunised with S81-19 mAb as described in methods. The RNA was extracted and reverse transcribed to first-strand cDNA (Fig. 16).

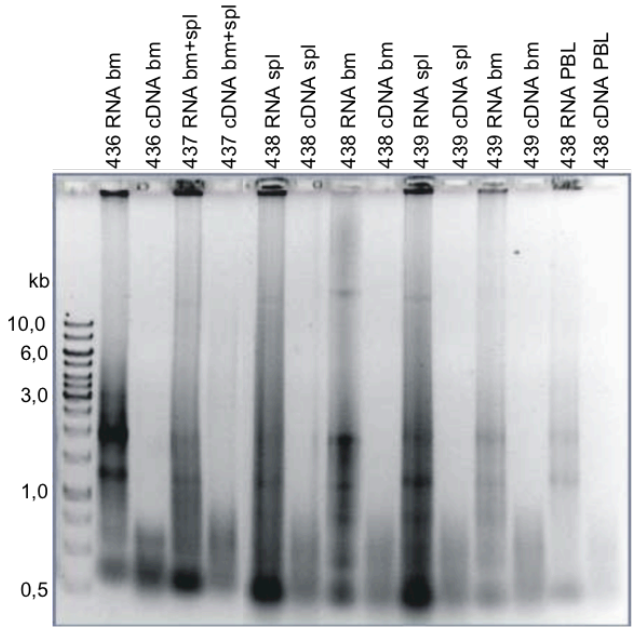

Fig. 16. Total RNA and reverse transcribed cDNA.
RNA and cDNA samples separated on a 1% agarose gel. Isolated total RNA indicates two bands corresponding to the rRNAs and a broad smear of RNAs of different sizes. Reverse transcribed first-strand cDNA was constructed using oligo-(dt) primer, excluding non-polyadenylated rRNA from transcription.

5.2.1.2. Construction of ScFvs

Different scFv libraries were constructed from the RNA of four different rabbits. The four rabbits were diverse in serum reaction to various antigens including the LPSs of the *E. coli* rough type mutants R1, R2, R3 and R4 (Fig. 3). All sera showed in previous dot blot analysis a clear binding to the R3 core type oligosaccharide [63].
Furthermore, the scFv libraries were constructed with linkers of two different length for linking light and heavy chain fragments together to a scFv. A summary of the constructed scFv libraries is given in Tab. 3.

As demonstrated for the rabbit 436 libraries the PCR reaction with the combined primer pairs led to amplification of several of the variable region gene segments (Fig. 17). During this first round of PCR the SfiI restriction site, as well as the linker for the subsequent connection between the V_L and V_H chain was attached.

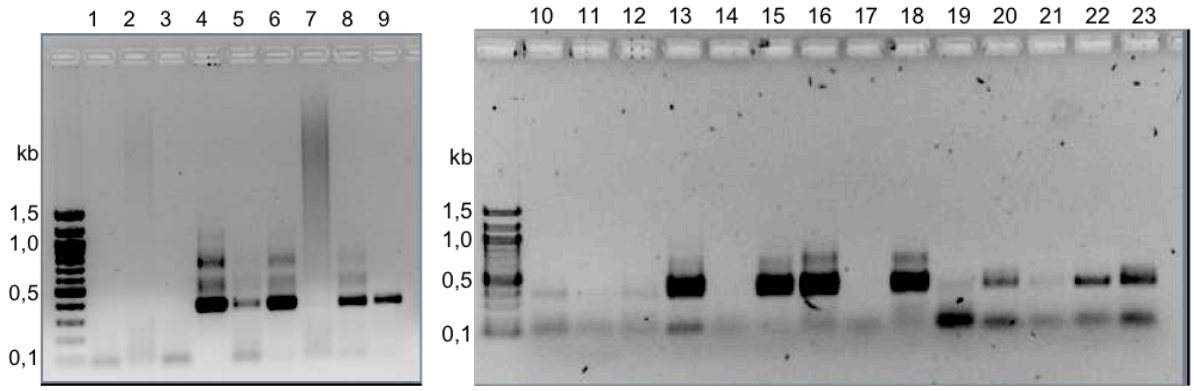

Fig. 17: Amplification of the variable region gene segments from rabbit 436.
1% agarose gel for the size control of the PCR products. Lane and primer combinations: short linker - 1 RSCVK1 and RKB9Jlo-B, 2 RSCVK3 and RKB9Jo-B, 3 RSCVK2 and RKB9Jlo-B, 4 RSCVK1 and RKB42Jo-B, 5 RSCVK2 and RKB42Jo-B, 6 RSCVK1 and RKB9Jo-B, 7 RSCVK3 and RKB42Jo-B, 8 RSCVK2 and RKB9Jo-B, 9 RSCλl and RJλo-BL, long linker -10 RSCVK1 and RKB9Jlo-BL, 11 RSCVK3 and RKB9Jo-BL, 12 RSCVK2 and RKB9Jlo-BL, 13 RSCVK1 and RKB42Jo-BL, 14 RSCVK3 and RKB9Jlo-BL, 15 RSCVK2 and RKB42Jo-BL, 16 RSCVK1 and RKB9Jo-BL, 17 RSCVK3 and RKB42Jo-BL, 18 RSCVK2 and RKB9Jo-BL, 19 RSCλl and RJλo-BL, 20 RSCVH1 and RSCG-B, 21 RSCVH3 and RSCG-B, 22 RSCVH2 and RSCG-B, 23 RSCVH4 and RSCG-B. The desired PCR products were around 400 bp in length.

The first round of PCR was repeated six times and the PCR products with attached V_L short linker, V_L long linker or V_H were collected in separated pools. Purification on a 1.2% agarose gel yielded in 1-2 µg PCR product DNA per variable region gene.

In the second round of PCR the attached overlapping ends of the variable region light and heavy chain were joined together and amplified. This overlap extension PCR resulted several times in low quantities of DNA product, indicated by poorly visible DNA bands in the agarose gel (Fig. 18).

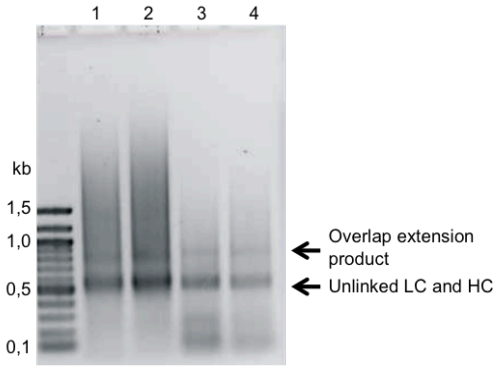

Fig. 18: Overlap extension PCR.

Lane 1: rabbit 436 short linker product, 2: 436 long linker product, 3: 437 short linker product and 4: 437 long linker product. Overlap extension PCR products with a size of around 750 bp. Unjoined variable region fragments at 500 bp.

Therefore the reaction conditions where optimised (Fig. 19). The use of hot start Taq polymerase instead of conventional Taq polymerase led to an increase in scFv PCR product. Even more crucial for the yield of the desired product was the exact 1:1 molar ratio of the applied light chain to heavy chain.

The various PCR reactions were collected and concentrated by ethanol precipitation. The concentrated DNA was separated in an agarose gel, and the desired band at around 750 bp was extracted. Finally a yield of each scFv PCR product of 10 µg was received.

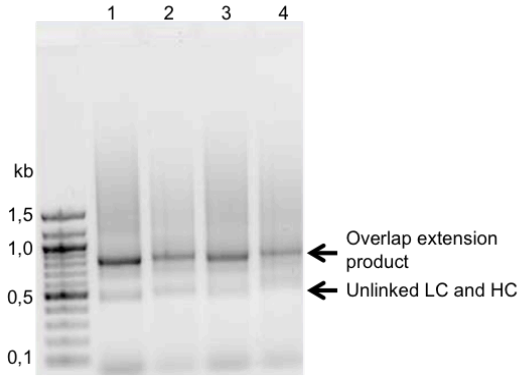

Fig. 19. Product increase of the overlap extension PCR.

Lane 1: rabbit 436 short linker product, 2: 436 long linker product, 3: 437 short linker product and 4: 437 long linker product. Overlap extension PCR products with a size of around 750 bp. Unjoined variable region fragments were still detectable at 500 bp.

5.2.1.3. Cloning of the ScFvs

10 µg of each scFv PCR product and 20 µg of the pComb3XSS vector per library were digested with the restriction enzyme SfiI. The digested DNA was controlled and isolated by agarose gel electrophoresis. In case of the pComb3XSS vector it became apparent that the cleavage was not complete after one hour as described in the manufacturers protocol (Fig. 20). The large size of the 1600 bp large stuffer fragment enables the detection of single cut vector. The enzymatic digestion was considerably enhanced after 16 hours. The digested DNA was isolated from the agarose gel and directly used for the ligation.

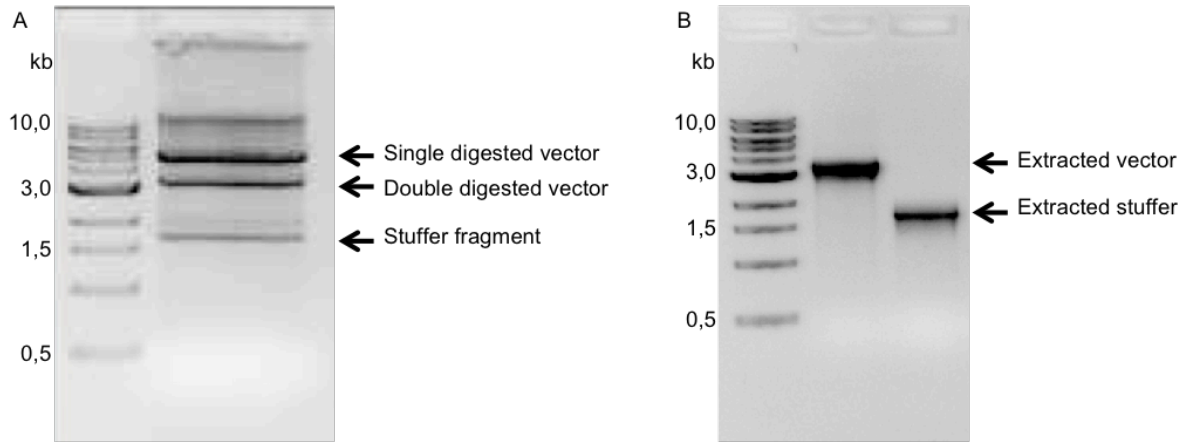

Fig. 20: SfiI restiction enzyme digest of the pComb3XSS phagemid vector.
A: 5 µg of pComb3XSS vector after one hour of restriction digest at 50°C with 60 U SfiI. B: Gel extracted double digested vector and isolated stuffer fragment.

Prior to the library ligation, the quality of the digested vector and inserts were determined by small scale ligations. The insert small scale ligations resulted, depending on the prepared scFv insert, in amounts of 4 to 11 x 10^6 cfu/µg applied vector DNA. Vector plus insert religations resulted in around 5 x 10^6 cfu/µg vector DNA. The vector ligations without insert resulted in amounts between 0.3 to 1.3 x 10^6 cfu/µg vector DNA.
Ligations of library DNA yielded in library sizes summerised in Tab 3. Afterwards the bacteria were infected with helper phages for phage packaging.

	Rabbit 436		Rabbit 437	Rabbit 438	Rabbit 439
Source of RNA	Bone marrow	Bone marrow	Bone marrow and spleen	Peripheral blood lymphocytes	Bone marrow and spleen
Linker Length	7 aa	18 aa	18 aa	18 aa	18 aa
Total No. of	2×10^5	2×10^5	1×10^5	1×10^5	1×10^4
Inserts/Independent Transformants	13/15	14/15	8/8	8/10	4/10

Tab. 3: ScFv libraries assembled in the pComb3XSS vector and library sizes.

The quality of the scFv libraries was examined by a size control (Fig. 21) of the inserted scFv and by sequence analysis of several clones.

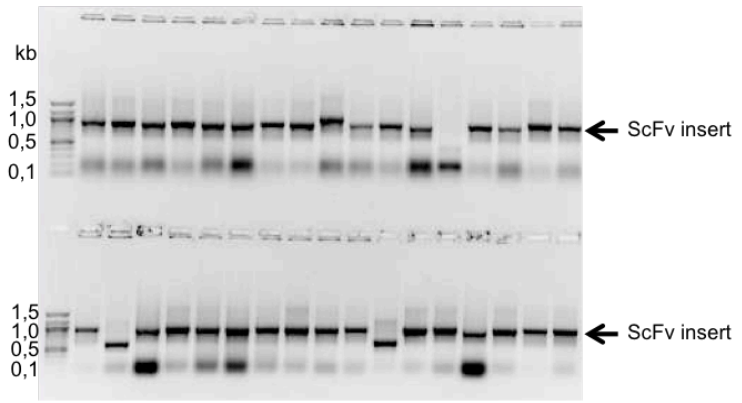

Fig. 21: Colony PCR of the rabbit 436 libraries.
Insert size analysis by direct use of bacterial colonies for PCR. Lane 1-15 rabbit 436 SL library, DNA band in lane 9 is oversized for a scFv, and in the colony tested in lane 13 no insert was detected. Lane 16-31 rabbit 436 LL library, solely lane 19 reveals a DNA band of the wrong size. Lane 32-34 rabbit 437 LL library.

5.2.2. Panning Procedures

5.2.2.1. Phage Binding to Anti-Idiotype Antibodies

As a first step the anti-idiotype antibody S81-19 was used as antigen for phage panning.
It was the immunising antigen and should therefore lead to the isolation of phages, which bind to the protein.
Two different selection procedures were performed. In the first one 100 ng S81-19 mAb per well were applied for three pannings implemented with the scFv libraries 436 (long linker), 437 and 439.

In the second procedure 100 ng S81-19 F(ab)$_2$ per well were used for panning with the libraries 436 (short linker) and 437, to distinguish binding to the Fc and the variable antibody domains.

Both procedures were performed under panning conditions like described. The phage titer and the insert steadiness were monitored and revealed continually stable results. The binding ability was verified after the panning procedure using the reamplified phage mixtures of the respective rounds. All five screened scFv libraries showed unambiguous binding after four rounds of panning against the anti-idiotype S81-19 (Fig. 28). The applied 436 short linker library revealed clear binding after the third round of panning (Fig. 22).

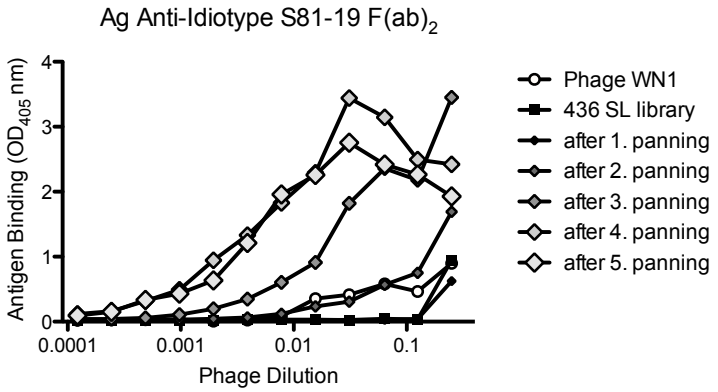

Fig. 22: Phage ELISA against the anti-idiotype S81-19 F(ab)$_2$ as antigen.

The scFv short linker phage library 436 and the phage mixtures subsequent five rounds of panning tested for binding to the anti-idiotype F(ab)$_2$. The isolated phage WN1 222-5 was used as a binding control. After the second round of panning a slight binding is detectable, increasing after the third round and reaching the maximal measured level after the fourth round.

5.2.2.2. Phage Binding to R3-Conjugates

In the next step it was investigated whether a glycoconjugate can be used for phage selection. Therefore the *E. coli* R3 core-type oligosaccharide conjugate was applied, a structure shown to bind to antibodies in the anti-anti-idiotype sera.

The first library used for the selection of antigen binding scFvs against R3-GA-BSA conjugate was the bone marrow and spleen derived long linker library constructed from donor material of rabbit 437. The ligand frequency in the conjugate amounted 341 nmol ligand/ml. The wells for panning were coated with 50 pmol in 50 µl carbonate buffer.

Previous to the first, second and fourth panning step the library phages were reamplified. The panning procedure was performed as described in the method section.

Phage Preparation	Phage Titer (cfu/ml) of Panning Round				
	1	2	3	4	5
Input	3×10^{8}	2×10^{13}	8×10^{12}	$> 4 \times 10^{13}$	5×10^{12}
Output	1×10^{5}	2×10^{4}	n.d.	3×10^{5}	3×10^{4}

Tab. 4: Phage titer monitoring of the first R3 conjugate panning.

The phage titer was controlled previous and past the binding step of each panning round (Tab. 4). To estimate the stability of the insert throughout the panning procedure and amplifications, colonies from titer plates were used straight forward in PCR reactions. The colony PCR revealed a substantial loss of scFv genes containing phages (Fig. 23).

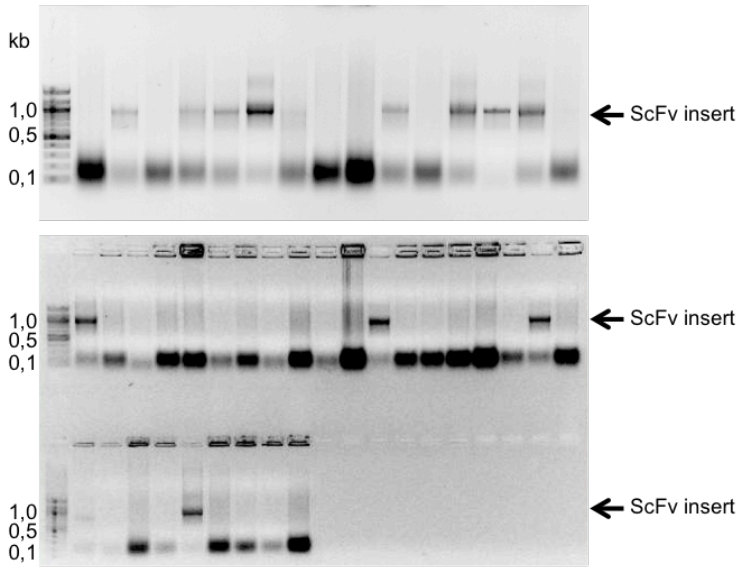

Fig. 23: Insert size analysis by colony PCR of the scFv 437 library panning.
The upper gel shows the colony PCR results subsequent the third panning round. Already indicating a loss of insert bearing phages during panning. The lower gel shows the results after the fifth panning round. Only 4 of 28 tested colonies had an insert of the correct size.

More important, the amplified phage mixtures subsequent panning rounds as well as individually amplified phages possessing scFv inserts of the correct size, were screened for their binding properties in ELISA. No binding phages could be detected.
To investigate whether reduction of the amplifications between the panning rounds would increase the number of clones with insert, two distinct modifications of the regular panning procedure have been implemented. The 437 scFv library was reamplified before the initial

panning step. Afterwards no further reamplifications of the phages have been included in the panning procedure.

Additionally the washing steps were decreased. The wash buffer was not resuspended and subsequent incubated during the washing steps. Instead the wash buffer was given briefly to the well after phage incubation and immediately removed with care.

Phage Preparation	**Phage Titer (cfu/ml) of Panning Round**			
	1	2	3	4
Input	1×10^{8}	4×10^{12}	3×10^{12}	1×10^{13}
Output	1×10^{5}	2×10^{4}	6×10^{4}	7×10^{3}

Tab. 5: Phage titer monitoring of the second R3 conjugate panning.

The phage titer was monitored and revealed no significant loss of phages during the panning (Tab. 5). Furthermore, under these conditions the colony PCR indicated no loss of scFv inserts over time.

The phage mixtures of the amplified phages after the panning rounds and several amplified single phages were analysed in ELISA for their binding activity (Fig. 24). The phage mixtures revealed a minor signal for binding against the anti-idiotype mAb. Two of the screened single phages, gained after the fourth panning round, suggested a slight binding. The binding was repeatedly determined using R3 conjugate as well as the anti-idiotype immunogen and casein as immobilised antigens. There was a low comparable optical density measurable for the three antigens, including the casein control antigen.

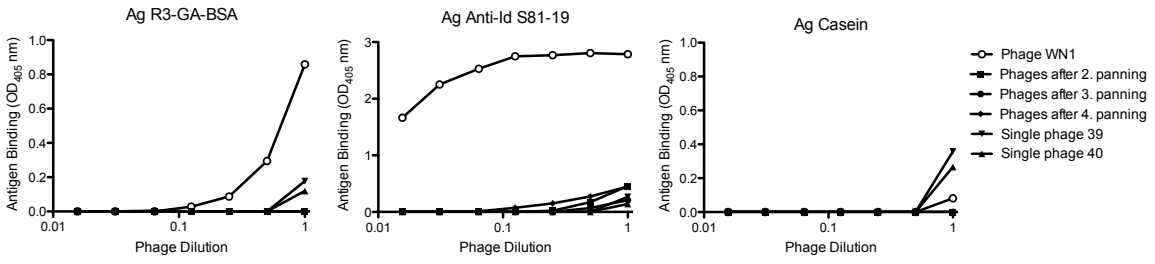

Fig. 24: Phage ELISA with three different antigens.

The phage mixtures after the second, third and fourth panning round and two amplified single phages were determined for their binding activity against the R3 conjugate, the anti-idiotype mAb S81-19 and casein as a control. Phage WN1 222-5 was applied as a positive control for the phage binding ability.

To verify whether there are some specific binding scFvs presented on the phages, the scFvs were expressed without pIII in an *E. coli* TOP10F' nonsuppressor strain (Fig. 25). The scFv supernatant from the polymyxin B treated bacteria cells was used straight forward for two ELISA variants in parallel. The first was implemented using 2.5% casein and 0.05% Tween20 in PBS, and in the second 5% skim milk powder in TBS was used as blocking solution and as a negative binding control. The former reconfirmed the results of the two single phages for the anti-idiotype and casein binding activity. R3 conjugate binding was not observed. The second revealed no binding activity of the single phages. Interestingly the control scFv WN1 222-5 binding was increased using the Tween20 free buffer.

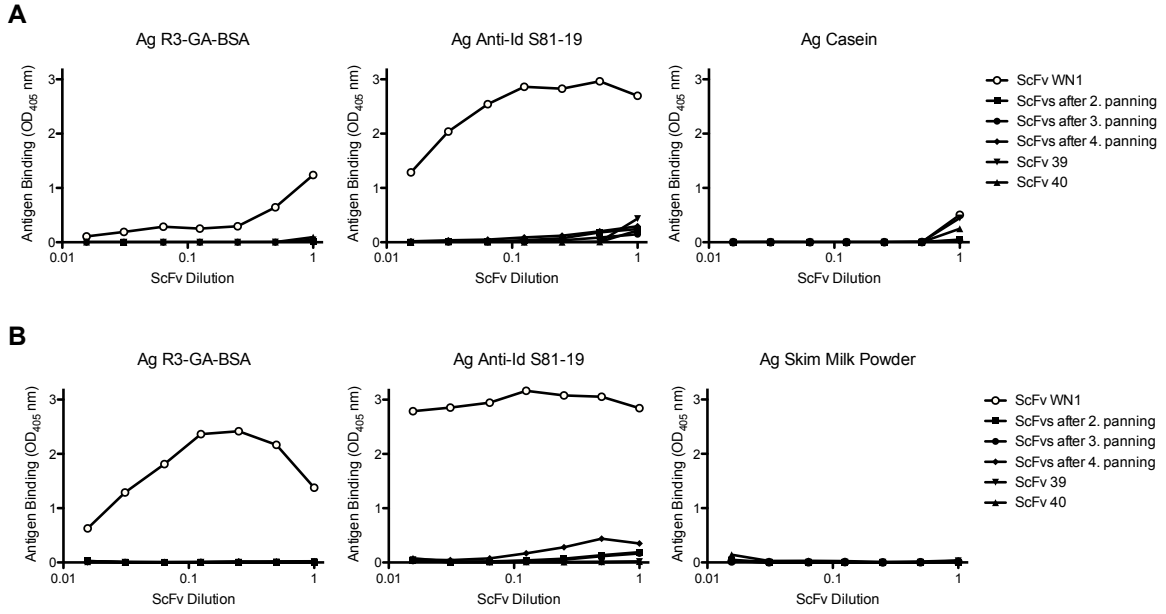

Fig. 25: ScFv ELISA with three different antigens and two varied buffer conditions.
The first ELISA row (A) shows scFv mixtures and two isolated scFvs determined for their binding to R3 conjugate, anti-idiotype antibody and casein, using casein buffer as blocking and dilution buffer. Only binding of the scFv WN1 222-5 control was detectable to the R3 conjugate, a minor binding of the other scFvs to the anti-idiotype and casein is visible.
In the second ELISA row (B) 5% skim milk powder in TBS was used as blocking and diluting buffer. The overall measured binding of the scFv WN1 222-5 control was slightly higher than for the PBS buffer. No binding of the isolated scFvs could be detected.

5.2.2.3. Phage Binding to Heat-killed Bacteria

One reason for the lack of binding to the R3 conjugate could have been that the antigen concentration immobilised on the ELISA plate was too low. Therefore the form of antigen presentation was altered from R3 conjugate to R3 heat-killed bacteria. 2 µg of the bacteria per well were used to provide a high density of immobilised antigen.

The scFv library 437 was used again for the first panning procedure according to the described standard protocol. Stable phage titers were observed in the range of 1 x 10^{13} cfu/ml phages for the input titer and 1 x 10^{5} cfu/ml phages for the output titer. Also the insert control via colony PCR revealed no loss of scFv inserts. Nevertheless no binding phages to R3 bacteria could be detected in the phage mixtures subsequent the panning rounds.
To investigate whether the source of DNA was responsible for the lack of binding phages, the scFv library 438, derived from peripheral blood lymphocytes, was applied for an additional panning. The procedure was performed according to the described standard protocol, except one further reamplification step subsequent the third panning round. No deviations from the phage titers compared with the previous panning were observed and no loss of inserts was detected. No phages binding to R3 bacteria could be detected in the phage mixtures subsequent the panning rounds.

As a next step an increase in avidity was applied by using the scFv library 436 with a short linker between the antibodies variable region light and heavy chain for a further panning against R3 heat-killed bacteria as immobilised antigens. A reamplification step was performed subsequent the second panning.
The phage titer monitoring during the panning was constant (Tab. 6), with a slight decrease of phages after the reamplification previous to the third panning round. The insert control of some individual clones indicated a slight loss of scFv insert carrying phages compared to the initial library where 87% of the tested colonies had an insert of the correct size (Fig. 26).

Phage Preparation	**Phage Titer (cfu/ml) of Panning Round**			
	1	2	3	4
Input	4 x 10^{13}	4 x 10^{13}	2 x 10^{11}	5 x 10^{13}
Output	n.d.	2 x 10^{5}	2 x 10^{5}	2 x 10^{5}

Tab. 6: Phage titer monitoring of the scFv 436 short linker library .

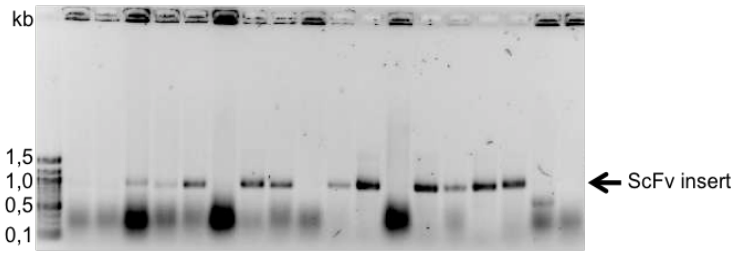

Fig. 26: Insert size analysis by colony PCR of the scFv 436 short linker library panning.
In well 1-6 PCR results from colonies of the output titer determination plate subsequent panning round three. 50% of the colonies revealed a distinct insert of the correct size. In well 7-12 the results of colonies from the output titer plate subsequent panning round four. 67% of the colonies revealed a distinct insert of the correct size. In well 13-18 the results of colonies from the output titer plate subsequent panning round five. 67% of the colonies with a distinct insert of the correct size and one insert revealing the size of only one variable region fragment.

Three further library pannings were performed using the R3 heat killed bacteria as antigen. The phage ELISA results of the libraries 437 (bone marrow and spleen derived with a long linker), 438 (PBL derived with a long linker) and 436 (bone marrow derived with a short linker) were summarised in Fig. 27 and Fig. 28 with no detectable binding activity.

5.2.2.4. Comparison of the Phage Binding Results of the pComb3XSS Libraries

The phage ELISA results of the complete phages from the various pannings after five rounds were summarised (Fig. 27 and Fig. 28). In Fig. 27 the various phages after panning against R3 conjugate, R3 heat-killed bacteria and against anti-idiotype S81-19 were screened for binding to R3 core type O111 LPS conjugate. It was no binding of phages detectable.
In Fig. 28 the equal phages were used to determine the binding against the anti-idiotype S81-18. The five phages derived subsequent panning against the anti-idiotype S81-19 revealed decidedly binding to the anti-idiotype S81-19 antigen. For the phages panned against R3 conjugate or R3 heat-killed bacteria no binding could be detected.

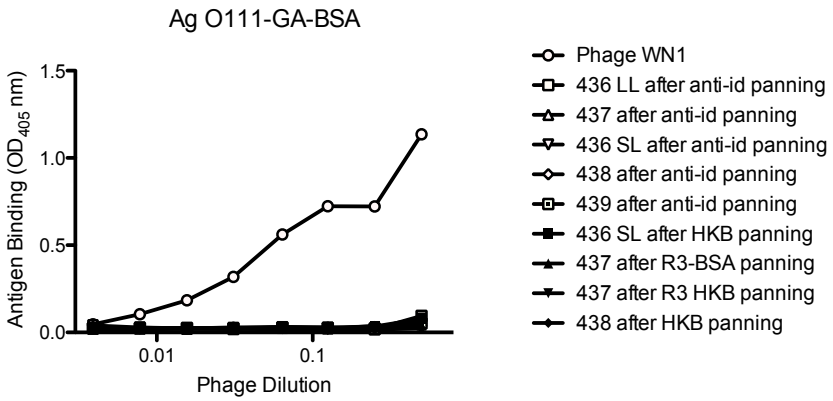

Fig. 27: Phage ELISA against the R3 core type O111 LPS-BSA conjugate as antigen.
The phage mixtures derived from the diverse libraries were used in different panning procedures and subsequent five rounds of panning analysed for binding to the R3 core type O111-GA-BSA conjugate. It was no binding detectable for the various phages. The isolated phage WN1 222-5 was used as a binding control.

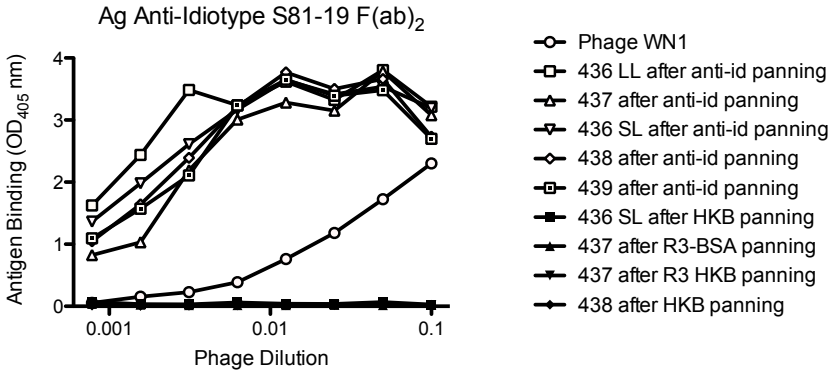

Fig. 28: Phage ELISA against the anti-idiotype S81-19 F(ab)$_2$ as antigen.
The phage mixtures derived from the diverse libraries were used in different panning procedures and subsequent five rounds of panning analysed for binding to the anti-idiotype S81-19 F(ab)$_2$. It was no binding detectable for the phages after the panning procedures with R3 conjugate or R3 heat-killed bacteria as antigen (black symbols). Whereas the phages panned against the S81-19 revealed all a clear binding to it (white symbols). The isolated phage WN1 222-5 was used as a binding control.

5.2.3. Subcloning into pHen1

To increase the number of scFv displayed by the phages, the scFv library 437 was cloned from the pComb3XSS into the pHen1 vector (Fig. 10). The pHen1 phagemid includes in contrast to the pComb3 vectors the complete *gIII* and enables consequently the infection of bacteria by these phages. Therefore the application of a hyperphage, lacking the *gIII* in its

genome, for packaging of the phagemid was possible, which should lead to the expression of up to five copies of the scFv attached to pIII.

The phage library 437 was used for the infection of *E. coli* ER2537. A plasmid preparation was used for scFv amplification in a PCR introducing a NotI restriction site at the 3'-end of the scFv. The scFv genes and the pHen1 vector were digested first with SfiI and subsequent with NotI. Afterwards the DNA was ligated into the pHen1 vector and amplified using helper phage M13K07 for phage packaging.
Preliminary to the first panning the 437 pHen1 library was amplified by infecting an *E. coli* TG1 culture with the phages and using hyperphage M13K07ΔpIII for phage packaging.

The amplified hyperphage packed phages were controlled and quantitative compared to the helper phage packed pHen1 phages, the helper phage packed pComb3XSS phages and the helper phage (Fig. 29). The western blot staining with an anti-cmyc tag antibody reveals the quantitative production of scFv-pIII fusion proteins by hyperphage packaging (Fig. 30).

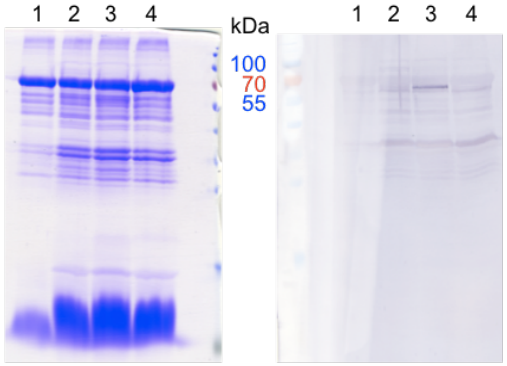

Fig. 29: SDS-PAGE and western blot of phage particles.
Lane 1: Helper phage M13K07; lane 2: scFv library 437 in pHen1 packed with helper phage; lane 3: scFv library 437 in pHen1 packed with hyperphage and lane 4: scFv library 439 in pComb3XSS. The coomassie stained SDS gel on the left side revealed the ß-mercaptoethanol reduced and denaturated phage components in similar quantities. The western blot of the same phages on the right side was stained with the anti-c-myc tag antibody and developed using alkaline phosphatase. In lane 3 the c-myc tag of the scFv-pIII fusion protein is detectable, but further molecules are stained unspecifically.

Two further western blots revealed the scFv-pIII fusion protein as abundantly present on hyperphage packed phage particles (Fig. 30).

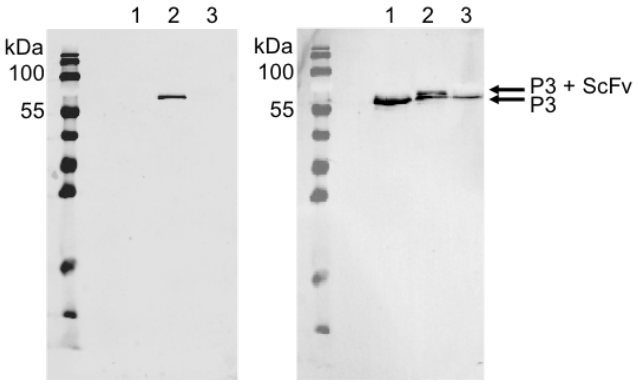

Fig. 30: Western blot of phage particles.
Lane 1: scFv library 437 in pHen1 packed with helper phage; lane 2: scFv library 437 in pHen1 packed with hyperphage and lane 3: helper phage M13K07. The blot on the left side was stained with an anti-c-myc tag antibody and further detected by an Alexa680 conjugated anti-mouse antibody. It presents the scFv-pIII fusion protein in lane 2. In lane 1 the scFv-pIII fusion protein was not detectable. The blot on the left side was stripped using stripping buffer for 20 min. and stained again with the anti-pIII antibody [105] and subsequent with an IR-dye conjugated anti-mouse antibody resulting in the blot on the right side. For the phages in lane 1, packed with the helper phage, the pIII band at around 60 kDa implies high quantities of pIII. In lane 2 the two bands for the scFv-pIII fusion protein (above) and for the pIII (below) are clearly determinable. In lane 3 the helper phage shows the band of its pIII.

Two pannings were performed using the R3-GA-BSA conjugate and the anti-idiotype S81-19 $F(Ab)_2$ as immobilised antigens in parallel. In total four rounds of panning were implemented, whereas the phages previous to the first and second panning were amplified with the hyperphage M13K07ΔpIII for phage packaging and the subsequent phages were packed by the helper phage M13K07.
Minor fluctuations could be recognised in the phage titers, but no substantial loss of phages (Tab. 7).

Phage Preparation	**Phage Titer (cfu/ml) of Panning Round**			
R3-GA-BSA	1	2	3	4
Input	2×10^{13}	1×10^{13}	2×10^{13}	6×10^{11}
Output	2×10^{4}	2×10^{3}	2×10^{6}	3×10^{4}
S81-19				
Input	2×10^{13}	2×10^{12}	5×10^{13}	2×10^{12}
Output	2×10^{4}	6×10^{3}	7×10^{5}	4×10^{6}

Tab. 7: Phage titer monitoring of the scFv 437 library during panning against R3 conjugate and anti-idiotype S81-19 antigens.

The binding of the phage mixtures subsequent panning rounds was determined by phage ELISA (Fig. 31).

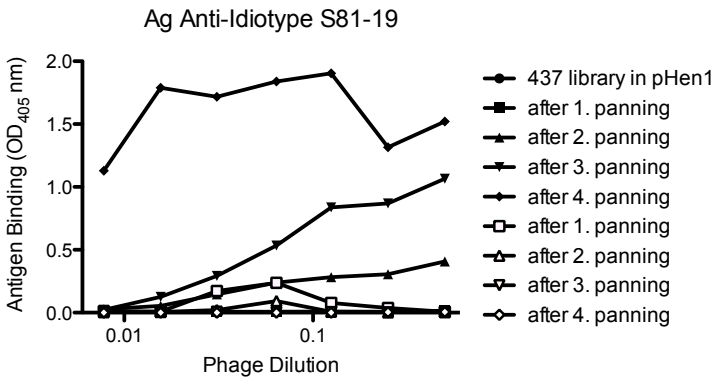

Fig. 31: Phage ELISA of the scFv 437 library subcloned into pHen1 against the anti-idiotype S81-19 as antigen.

The amplified 437 library phages and the phages of the panning procedure against the antigen S81-19 are figured with black symbols. In white symbols the phages of the panning procedure against the antigen R3 conjugate.

In conclusion the phages of the anti-idiotype S81-19 panning showed after three rounds of panning distinct binding, while the phages panned against the R3 conjugate revealed no binding to the anti-idiotype. For the phages of both pannings no binding could be detected against the R3 conjugate.

5.3. Recognition of Bacterial Carbohydrates by MBL

5.3.1. MBL Binding Studies

MBL interacts with various carbohydrates, including different monosaccharides as well as polysaccharides [87]. In humans one form of MBL has been identified, whereas two forms are found in mice. The three MBLs, human MBL (hMBL) and the murine MBL-A and MBL-C were investigated for their binding properties to pathogenic and non-pathogenic bacteria and also to isolated bacterial cell-wall carbohydrates.

At first it was investigated whether the binding to the *E. coli* R3 rough type mutant, the *E. coli* smooth type O8 serotype and *M. tuberculosis* H37Rv ATCC differs between the three rMBLs. Therefore an inhibition ELISA was performed detecting rMBL binding to a ligand, subsequent to preincubation of rMBL with the various heat-killed bacteria. The ELISA revealed extensive differences between the three rMBLs in recognition of the bacteria

(Fig. 32). The rhMBL showed binding to the *M. tuberculosis* H37, but not to the tested *E. coli* preparations. On the contrary the rMBL-A binds to all three heat-killed bacterial preparations in a comparable manner. For the rMBL-C only a slight binding to the *M. tuberculosis* H37 was detected.

Another inhibition ELISA was performed with decreased rhMBL and rMBL-C concentrations and with two different mycobacteria as well as two different *E. coli* strains (Fig. 33). The rMBL-A revealed again an obvious binding to all four heat-killed bacterial preparations. But the inhibition observed was more pronounced for the *E. coli* O4 and O111 than for the *M. tuberculosis* EAI and Beijing. In contrast binding of the rhMBL to the two mycobacterial strains was observed, while no binding to the *E. coli* O111 and only a minor binding to the O4 was detected. The rMBL-C showed only limited binding to the *M. tuberculosis* EAI, but no inhibition was detectable to the other heat-killed bacteria.

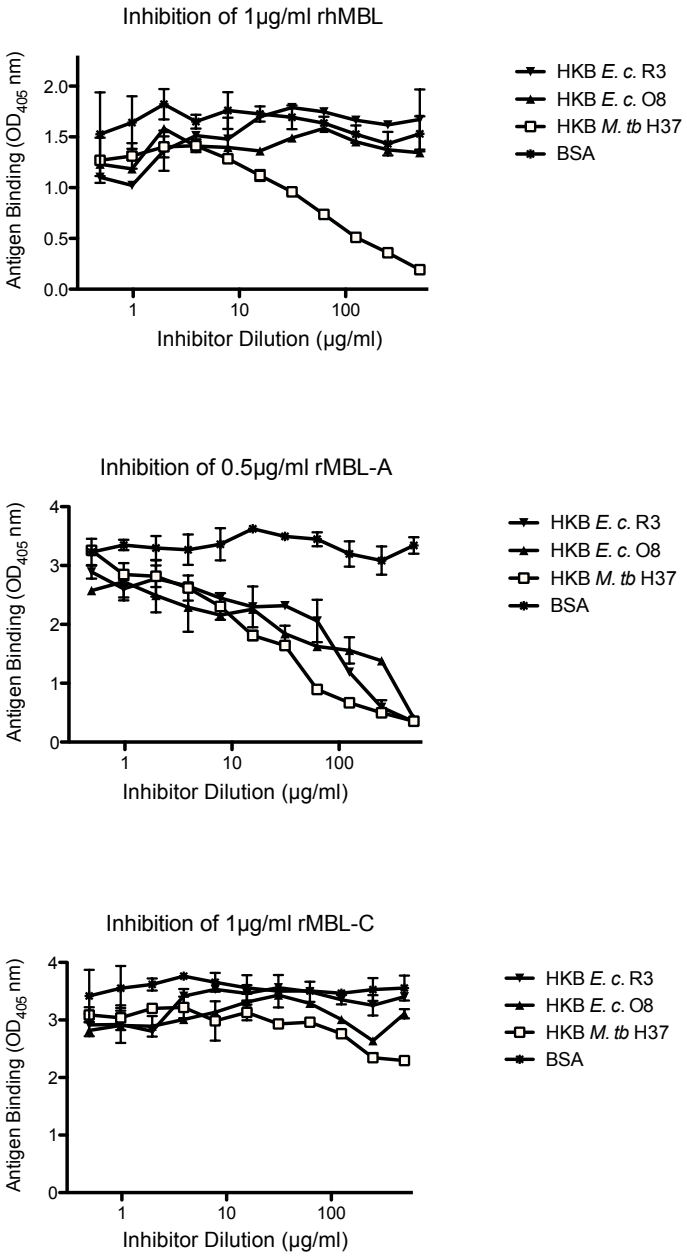

Fig. 32: Inhibition ELISA of MBL with various HKB.

The binding of rhMBL was compared with the two mouse variants of rMBL. As inhibitors three different heat-killed bacterial preparations were used and titrated in 1:2 steps. The *E. coli* rough type mutant R3, the *E. coli* smooth type O8 serotype, *M. tuberculosis* H37Rv ATCC 27294 strain and BSA as a control were tested.

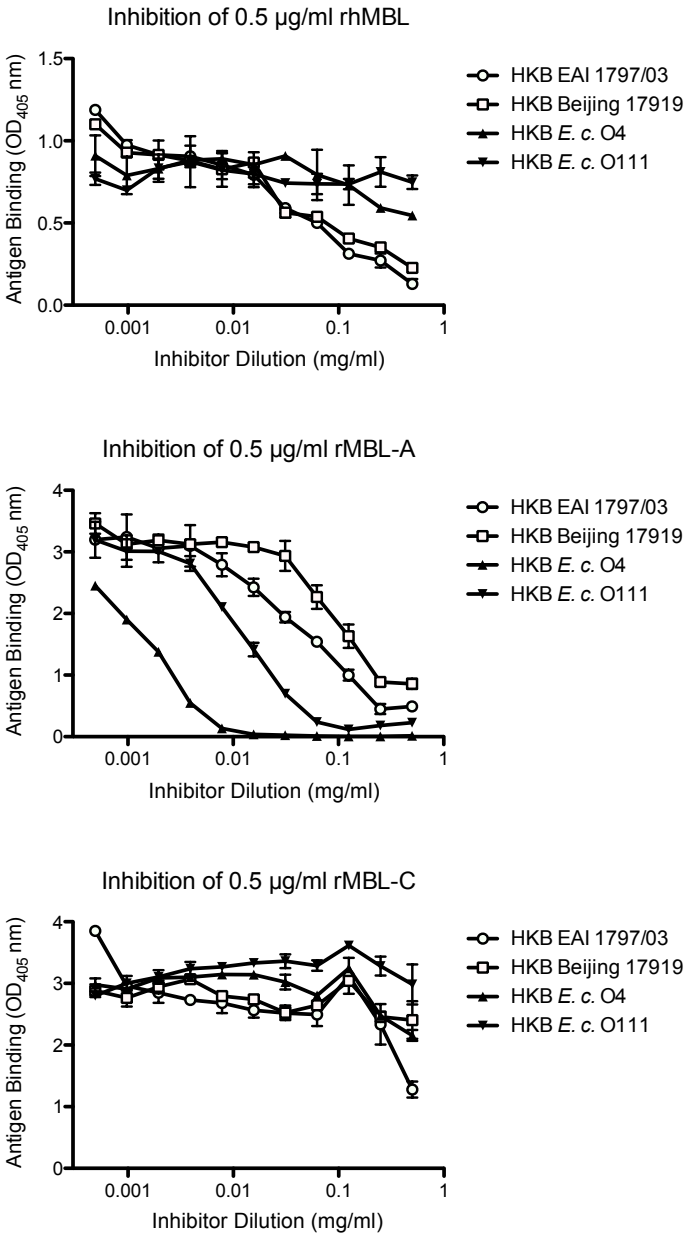

Fig. 33: Inhibition ELISA of MBL with heat-killed mycobacteria and *E. coli*.
Binding of rhMBL, rMBL-A and rMBL-C to *M. tuberculosis* EAI and Beijing as well as *E. coli* O4 and O111 was determined by inhibition ELISA. rhMBL binding to mannan was inhibited by preincubation of the rhMBL with the mycobacteria, but not with *E.coli*. rMBL-A binds to the four heat killed bacteria, while the best binder was the *E.coli* O4 serotype followed by the O111. The mycobacteria revealed as well binding, but to a lower extent. The rMBL-C reveals slight binding to the *M. tuberculosis* EAI, not to the other bacteria.

In a next step four different *E. coli* rough type mutants were tested for their binding potential to rMBL (Fig. 34). Analyzed were preparations from whole heat-killed bacteria and isolated, deacylated oligosaccharides derived from all four mutants. Again the three rMBLs differed in their binding to the bacteria and oligosaccharides. The rhMBL revealed binding to the R2 core type heat-killed bacteria and oligosaccharides, but only moderate binding to the other

core types was detected. The rMBL-A showed distinct binding to the R2 and R3 heat-killed bacteria, moderate binding to the R1 bacteria and no binding to the R4 bacteria. However the binding to the isolated oligosaccharides varied from the binding to the corresponding heat-killed bacteria. The R2 oligosaccharide appeared to be the best binding oligosaccharide, followed by the R1 and further the R4. For the R3 oligosaccharide no binding was detected. The binding of the rMBL-C to mannan was only slightly inhibited by the R2 heat-killed bacteria, but not by the other rough mutants. And also for the oligosaccharides no binding to rMBL-C was detected, except for the R2 oligosaccharide.

In comparison the three tested rMBLs revealed different binding to the bacteria and oligosaccharides, while the most obvious difference was a generally lower binding of rhMBL and rMBL-C compared to rMBL-A.

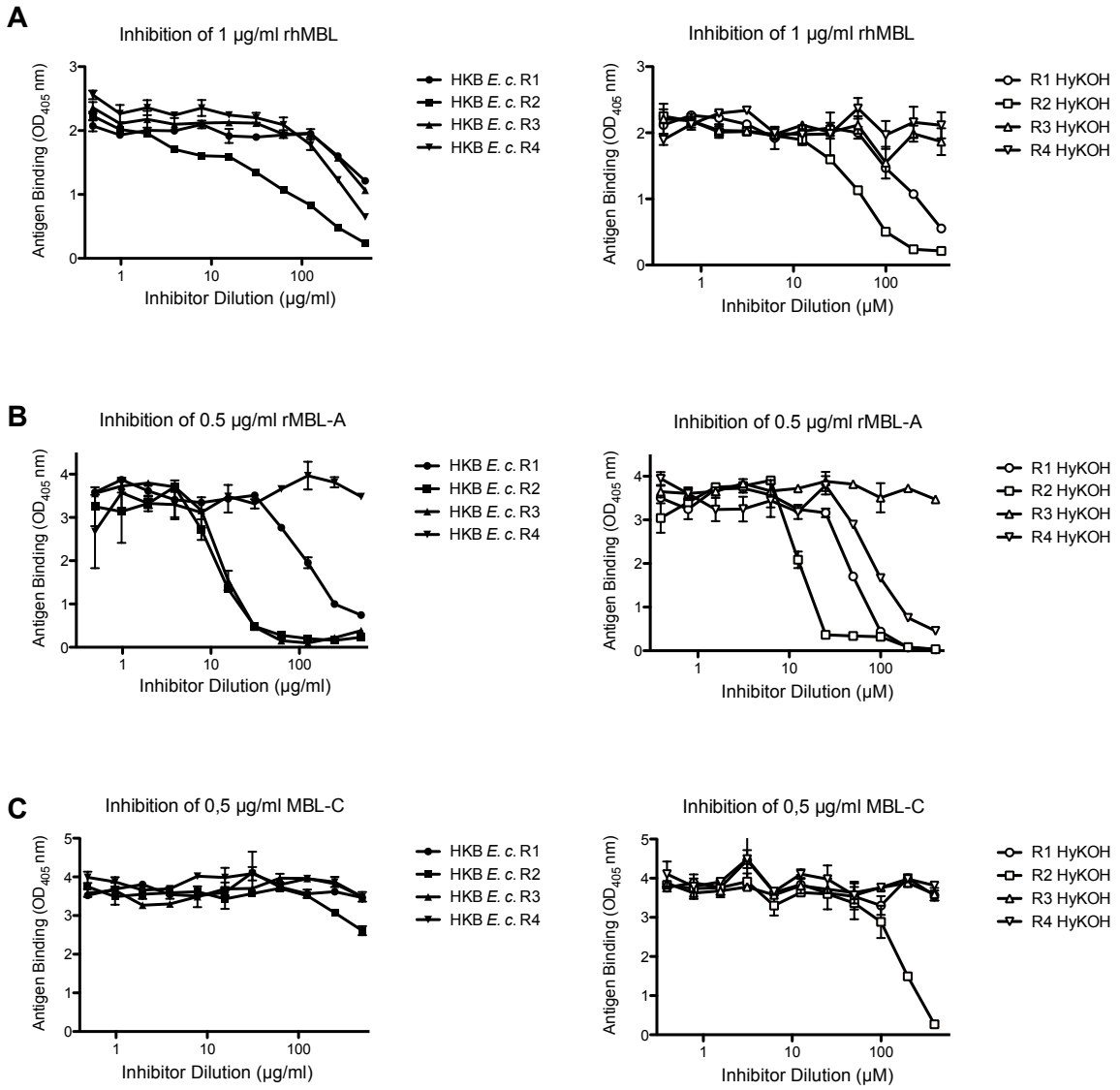

Fig. 34: Inhibition ELISA of MBL with *E. coli* heat-killed bacteria and oligosaccharides.
The binding of rhMBL (A), rMBL-A (B) and rMBL-C (C) to four different *E. coli* rough type mutants and their corresponding oligosaccharides was detected by inhibition ELISA. The inhibition of binding from rMBL to mannan coated wells was determined after preincubation of the rMBL with the bacteria and oligosaccharides. The R2 core type was the best inhibitor as bacterium and as oligosaccharide for the three rMBL. Broad differences are shown in the intensity of the inhibition of the three MBL. The rhMBL showed in addition to the R2 also slight binding to the other rough type bacteria and to the R1 oligosaccharide. The rMBL-A revealed clear binding to the bacteria, except of the R4 rough type and to the oligosaccharides, except of the R3 core type. The rMBL-C revealed only minor binding to the R2 bacteria and oligosaccharides, but no further binding was detected.

The rhMBL revealed in first ELISA studies marginal binding to *E. coli* heat-killed bacteria and *E. coli* core type oligosaccharides. On the contrary there was obvious binding of rhMBL to *M. tuberculosis* H37Rv, EAI and Beijing. Further heat-killed mycobacteria were tested for

their interaction with rhMBL (Fig. 35). All of the heat-killed bacteria showed similar binding to rhMBL.

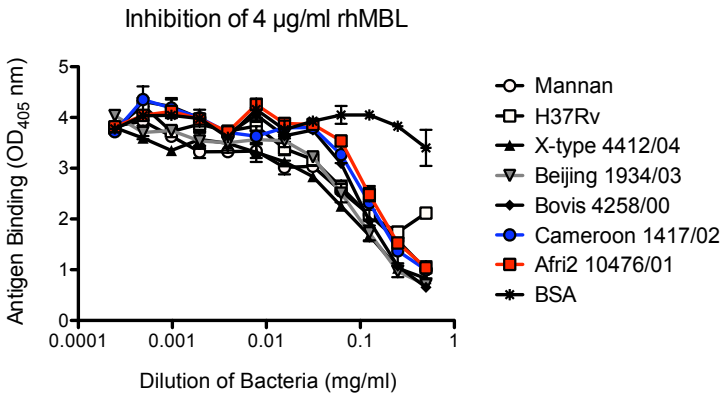

Fig. 35: Inhibition ELISA of rhMBL with mannan and different heat-killed mycobacteria.
The inhibition of binding from rhMBL to mannan-coated wells was determined after preincubation of the rhMBL with various heat-killed mycobacteria. All applied mycobacteria revealed binding to rhMBL with only minor variations in binding strength.

To overcome the potential drawback of the inhibition ELISA, that variations in solubility of the bacteria could lead to fluctuations in the concentration, a direct binding ELISA was applied (Fig. 36). Quantification difficulties should be eliminated by covering the bottom of a 96 well plate complete with bacteria. Since mycobacteria have a rather hydrophobic cell-wall the heat-killed bacteria were coated to a hydrophobic 96 well plate. Subsequently the rMBLs were titrated 1:2 steps starting from 2 µg/ml. Obvious differences in the recognition of the different mycobacteria are determined for the rMBL-A. It bound to the *M. tuberculosis* Beijing and X-type better then to the H37Rv and to *M. bovis* Bovis. The binding to the *M. tuberculosis* Cameroon and the *M. africanum* Afri2 was markedly less than to the other heat-killed bacteria. The rhMBL revealed similar interactions like the rMBL-A, but overall a decreased binding. The rMBL-C showed also rather minor binding compared to the same concentration of rMBL-A.

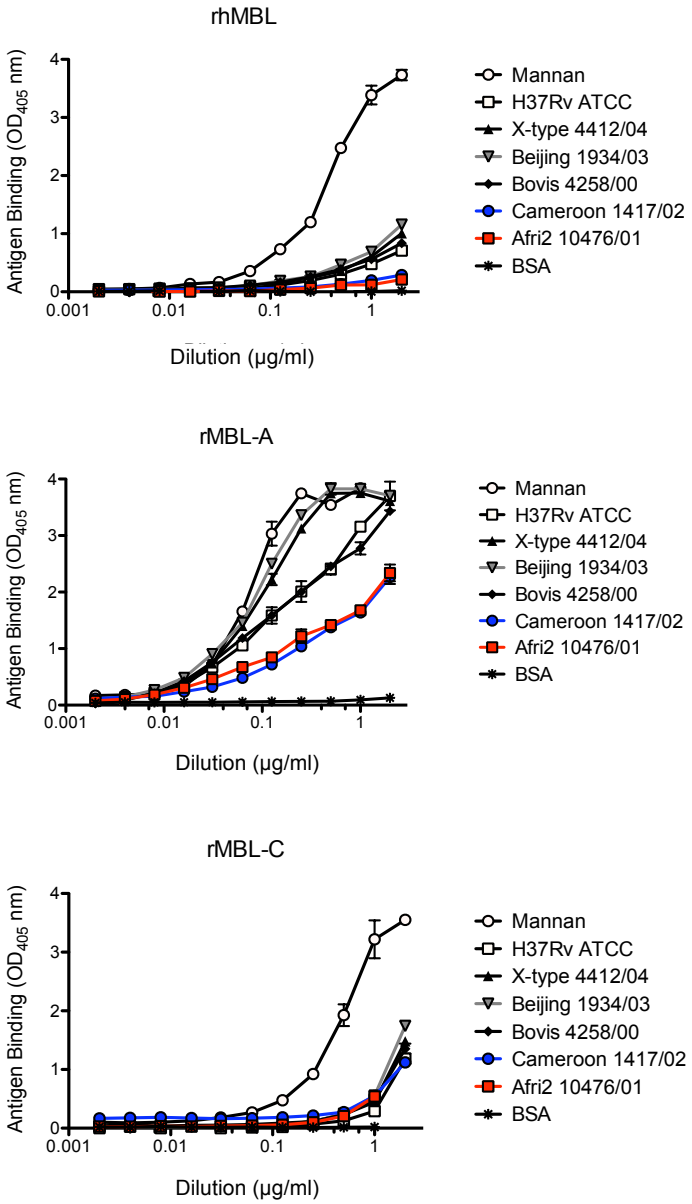

Fig. 36: Hydrophob ELISA of various heat-killed mycobacteria.
The rhMBL, rMBL-A and rMBL-C were determined for their binding potential to several heat-killed mycobacteria immobilised on a hydrophobic plastic surface. Again the binding of the rhMBL and the rMBL-C was in total less then the binding of the rMBL-A. For the rMBL-A obvious differences in the binding to the different heat killed mycobacteria was observed.

It should be clarified if the heat-killed mycobacteria reveal a similar MBL binding pattern, like the corresponding living bacteria with an intact cell envelope. Therefore three different living mycobacteria were titrated and immobilised on a polysorb flat bottom plate and detected with rMBL-A. The titration was feasible despite the clotting and stacking bacteria. The rMBL-A varied in binding to the bacteria (Fig. 37). It revealed slight binding to the

M. africanum Afri2, an increased binding to the *M. tuberculosis* H37 and the *M. tuberculosis* Haarlem was detected slightly better then the other two.

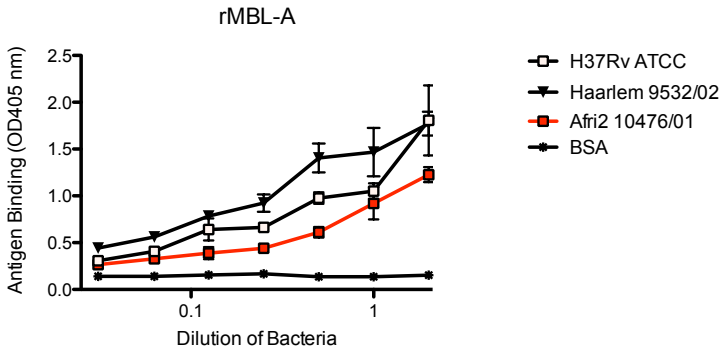

Fig. 37: ELISA with rMBL-A on a polysorb flat bottom plate to enable subsequent fluorescent detection of bacteria.

ELISA to determine the binding of rMBL-A to three different immobilised living mycobacteria. The bacteria were titrated 1:2 along 7 wells.

It should be clarified if there is a coincidence of differences in binding and the bacterial load on the hydrophobic plate. Two wells of each mycobacterium were stained and observed in the fluorescence microscope (Fig. 38). The distribution of the bacteria on the well surface was irregular and the bacteria did not cover the whole well. Thus, the binding differences of the rMBL-A in ELISA can not be exclusively attributed to differences in interaction, because quantities and presentation of the bacteria vary. Therefore an inhibition ELISA with various living mycobacteria was performed.

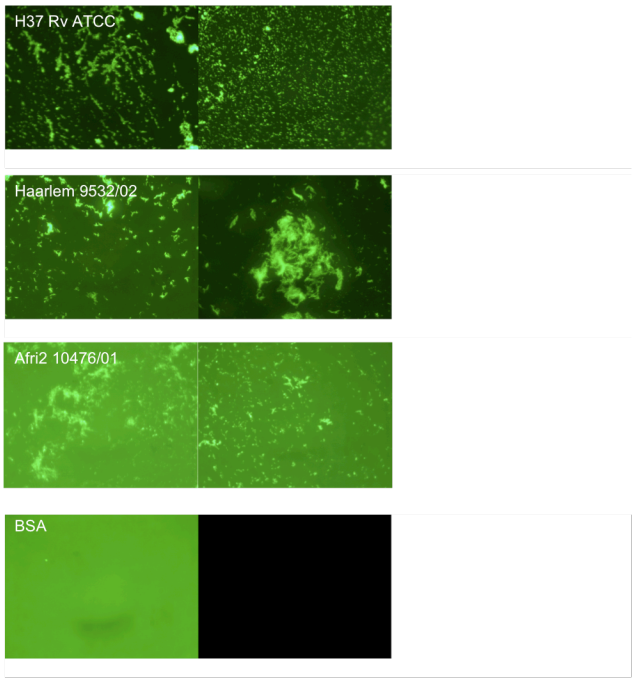

Fig. 38: Syto 24 staining of mycobacteria coated to hydrophobic wells.
The mycobacteria were stained with DNA dye syto24 subsequent the ELISA in Fig. 37. The two equal wells with the highest bacterial load of the three different bacteria were stained and monitored in the fluorescence microscope. The pictures were taken with an exposure time between 0 and 2 seconds. Noticeable is the irregular distribution of the bacteria at the well. Already the two wells of the same mycobacterium revealed strong variations in the distribution. A complete coverage of the well with bacteria was not observed.

It was implemented like the inhibition ELISA with the heat-killed mycobacteria (Fig. 35), except the adjustment of the bacteria proportions. The heat-killed mycobacteria were lyophilised and to the same concentration dissolved in ELISA BBS/Ca^{2+} buffer. While the living bacteria were dissolved in ELISA BBS/Ca^{2+} buffer and the OD_{600} was determined. The inhibition ELISA with the intact mycobacteria revealed for the three rMBLs markedly different results than the ELISA with the heat-killed bacteria and the ELISA with direct plate coated bacteria (Fig. 39). Mannan (start 0.25 mg/ml) in solution is bound by rMBL-C far better than the bacteria, by rhMBL slightly better than the bacteria and by rMBL-A less than the bacteria, except the *M. tuberculosis* H37 and Cameroon. The binding of the rhMBL and the rMBL-A to the *M. tuberculosis* H37 was reduced compared to the other bacteria, which is less pronounced for the rMBL-C. In contrast the strongest inhibition by bacteria was determined for rhMBL and rMBL-C with the *M. tuberculosis* Beijing and X-type and the *M. africanum* Afri2. While the best binding for rMBL-A was detected with the *M. tuberculosis* X-type, *M. africanum* Afri2 and *M. bovis* Bovis.

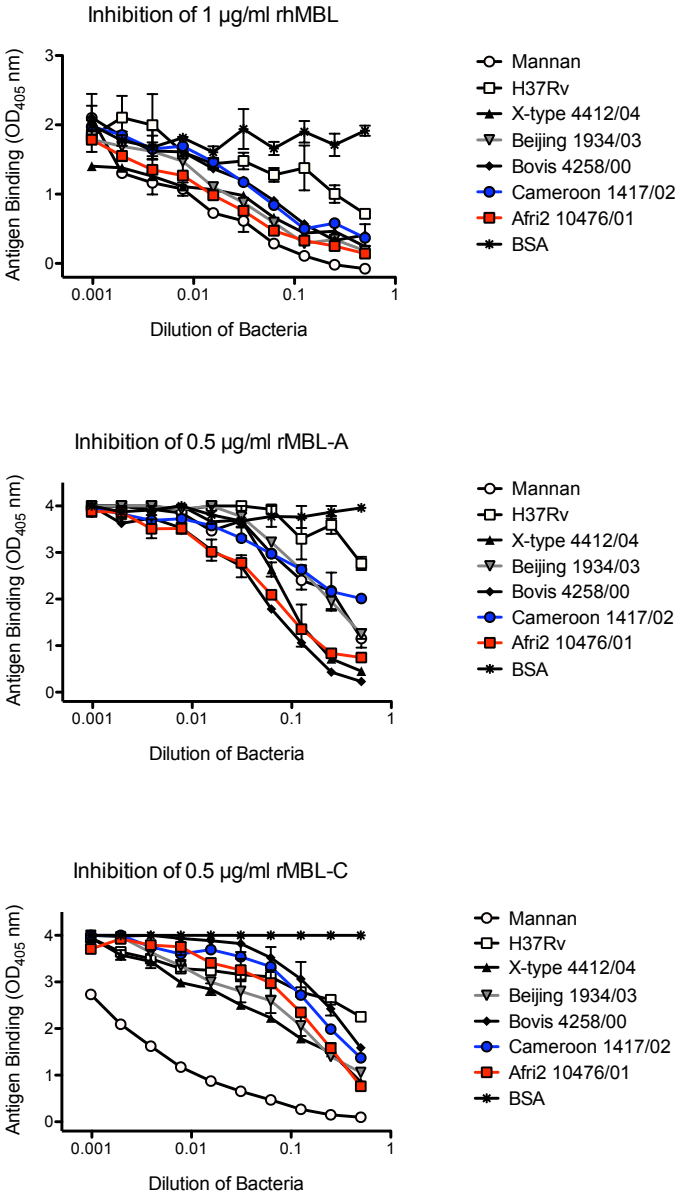

Fig. 39: Inhibition ELISA of various living mycobacteria.
Firstly the optical density of the mycobacteria was determined and the concentration adjusted to an OD_{600} between 1 and 1.28. The living bacteria were titrated 1:2 through ten wells.

Demonstrated are thus differences in the recognition of the various mycobacteria by a given rMBL as well as differences in bacterial interaction between rhMBL, rMBL-A and rMBL-C.

5.3.2. Complement Activation Assay

MBL is able to activate the complement system through a complexed serine protease. To determine the activation of complement factor C4 by the MBL-associated serine protease a complement activation assay was established (Fig. 40).

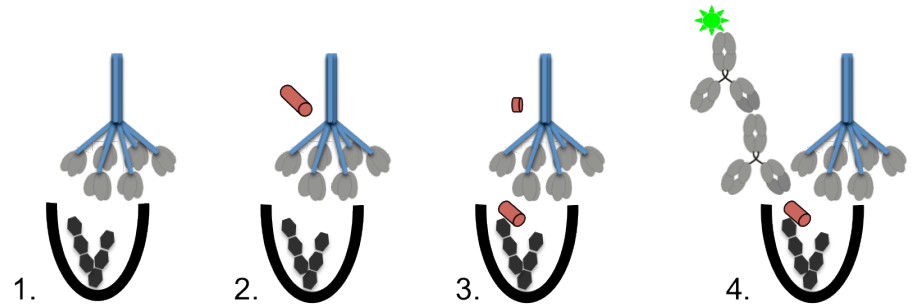

Fig. 40: Complement activation assay.
In the first step the MBL is incubated with the immobilised ligands (1). Secondly the MBL-associated serin protease cleaves complement factor C4 (2). When C4 is activated a reactive thiol ester is exposed and C4b binds covalently to closely amino or hydroxyl groups (3) and can be detected by an anti-C4 antibody (4).

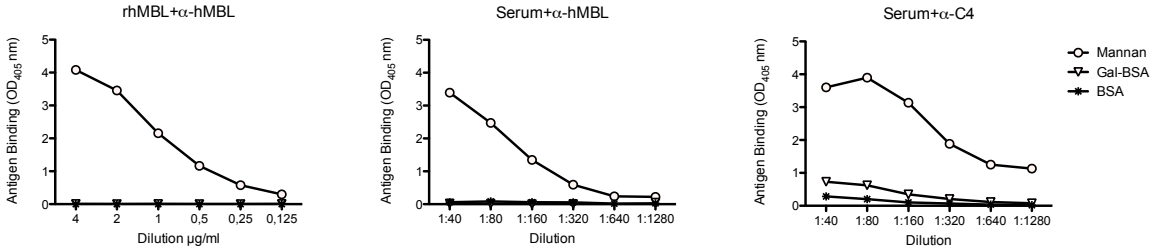

Fig. 41: MBL complement activation ELISA.
The binding of rhMBL and serum MBL was compared. The C4 cleavage was determined by detection with an α-C4 antibody.

After incubation of the serum with the ligands the C4 cleavage was detectable. No binding of hMBL was determined for the Gal-BSA conjugate and the BSA, but a moderate C4 cleavage. To investigate, whether antibodies participating in this activation binding of serum IgG and IgM was determined (Fig. 42).

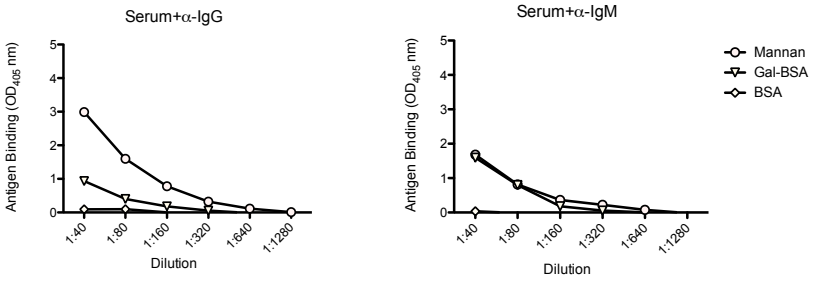

Fig. 42: ELISA for the IgG and IgM detection in human complement serum.
To determine the levels of other complement activating components in the human complement serum, the IgG and IgM presence was detected.

In conclusion, it was possible to show the complent activation via MBL and the MBL-associated serine protease. Also other complement activating components, which share ligands with the MBL, were determined in the serum.

6. Discussion

Carbohydrates as target molecules of the innate and adaptive immune system are currently being intensively investigated [39, 82]. For the immune system, microorganism-associated carbohydrates provide a valid target because of their often conserved and unique structures. In contrast there are the mostly poor immunogenicity of carbohydrates and the low binding affinities of antibodies and lectins to their carbohydrate-binding partners.
Several strategies are being investigated to overcome this poor immunogenicity and to receive long-term protection from carbohydrate antigens [106, 107]. In this context, peptides that mimic carbohydrate antigens are being discussed as alternatives to usually on protein carriers conjugated carbohydrate antigens [48, 108, 109].
In this study, the reaction to a carbohydrate mimicking protein was to be investigated as well as the binding characteristics to bacterial carbohydrates by the "antibodies of the innate immune system", the lectins.

6.1. Isolation of Anti-Anti-Idiotype ScFvs

In initial carbohydrate antigen mimicry experiments mice were immunised with the LPS neutralising mAb WN1 222-5 by Dr L. Brade [63]. From these immunisations the mAb S81-19 was gained and characterised as an anti-idiotype (Ab2β) antibody to the WN1 222-5. The anti-idiotype S81-19 was further used for an immunisation of four rabbits with the aim of inducing LPS neutralising antibodies in these rabbits. A binding activity of antibodies in the rabbit serum against some isolated and well characterised LPS molecules could be shown in dot blot tests. To further characterise the anti-anti-idiotype antibody response, in particular the specific binding properties of the raised antibodies, the mimicry derived binding sites were to be isolated. For this the phage display system was applied, a rapid screening method to identify binding fragments from a random combinatorial library [110].

A scFv of the WN1 222-5 idiotype antibody was constructed. It was cloned into the pComb3XSS phagemid vector, like the scFv rabbit libraries. The binding of the idiotype scFv-phage was tested to verify, whether the binding characteristics of the idiotype antibody

are transferable to the scFv. The binding to the *E. coli* heat killed bacteria, the core-oligosaccharide conjugate and the anti-idiotype antibody S81-19 could be shown. It was used as a positive control for phage binding.

Initially scFv libraries were constructed from the mRNA of four anti-idiotype immunised rabbits. To obtain the RNA of plasma cells containing the highest level of specific antibody mRNA, bone marrow, spleen and peripheral blood lymphocytes were used for the isolation [111]. The main deposits for plasma cells are the bone marrow and spleen, which are commonly used for the isolation of antibody mRNA from immunised individuals. Although the amount of antibody mRNA in the peripheral blood is also considerable, but it decreases rapidly after the last antigen boost and, moreover, about 80% of blood B cells are resting or naïve IgM and IgD cells. The use of peripheral blood lymphocytes is usual for naïve human antibody libraries rather than for immunised libraries [112]. During this study, they were considered as a potential RNA source because of the possibility that the response of some of the various anti-anti-idiotype clones covers the response of the paratopic antibodies. The proportion of the B cells clones to each other could be different and thus is possibly favourable.

As the isolation of RNA from the three different sources was feasible, it was implemented and stored as cDNA at -80°C until different libraries were constructed. Initial libraries were constructed using RNA of bone marrow and spleen separate as well as in mixtures of both, later the RNA repertoire was extended to the peripheral blood lymphocyte RNA. The isolation of RNA and the reverse transcription were realised fluently.

In the first round of PCR rabbit variable region genes were amplified. In total 24 different primer combinations were used. As reviewed by Knight [113] this minor number of primers, compared to mice and humans, is feasible, because rabbit B lymphocytes receive their antibody diversity rather by gene conversion and hypermutation than by gene rearrangement. Only one V_λ chain primer combination was used and nine combinations for the V_κ genes. A few of them resulted in no PCR product at all, whereas others led to abundant amplified DNA. This implies differing occurrence of the gene RNAs, anyway after immunisation and thus differences in the antibody abundance.

The second round of PCR, also named overlap extension PCR, was performed to link the light and heavy chain variable region fragments together to one fragment. Initially the linker

regions, appended in the first round of PCR, congregate to form one fragment out of the two variable region fragments. In a second step this single chain fragment was amplified using one pair of primers, recognising the SfiI restriction site generated during the first round of PCR.

Initial PCR reactions resulted in low amounts of amplified overlap products, but rather many starting material and background bands were visible. Several attempts were made to improve the yield of the overlap product, such as increasing the temperature for primer annealing, using different polymerases and varying the amount of template material. With the hot start Taq polymerase, the relation of overlap product to background site products could be enhanced (Fig. 18, Fig. 19), presumably due to diminished apposition of the primers to rather unintended template sequences.

Furthermore, the ratio of applied light to heavy chain fragments appeared to be highly critical. Indeed reasonable, due to the absence of a binding partner, if one fragment quantitatively prevails over the other and as a consequence is incapable of forming an overlap product. Therefore the amount of the material was determined in a photometer as described for the precise quantification of the DNA templates. In subsequent PCR reactions, the DNA fragments were used in a 1:1 molar ratio, achieving appropriate amounts of overlap extension products. When 10 µg of isolated and concentrated PCR product were received, it was digested with the restriction endonuclease SfiI [114]. The enzyme requires two copies of its recognition sequence for cleavage, plenty of single cleaved vector was observed after one-hour digest at 50°C. Since SfiI has no star activity it was possible to extend the incubation time to 16 hours. This resulted in considerably higher amounts of double cleaved vector. Thus also the PCR product was digested for 16 hours. Subsequent digest, the sliced DNA was straight forward isolated, concentrated, the PCR product was ligated into the pComb3XSS vector and transformed via electroporation into *E. coli* ER2537.

Library ligation was performed applying twice the amount vector to insert into the ligation reaction, to avoid loss of scFvs and consequently library complexity.

An indication of the library complexity is provided subsequent ligation, by determining the number of transformants after library transformation. Although it is not possible to determine the absolute complexity of a library, it is not possible that the complexity is higher than the number of transformants after library ligation. Thus the number of transformants provides a hint and consequently it is necessary that the number of transformants is not sparse.

The number of calculated total transformants per library was around 1 x 10^5. ScFv libraries where a total number of transformants is in a range of 10^8 are possible. Still, the versatility of the library should be sufficient, since it is not a naive library, but from immunised animals. However, the library quality was high. 80-100% of the tested colonies contained an insert of the correct size, except for the rabbit 439 library, where in the first colony test only 40% of the inserts revealed a correct size. Furthermore, in the evaluation of the sequencing results, correct rabbit variable regions were detectable, as well as the ompA leader sequence, the his-tag, the haemagglutinin-tag and the introduced linker. There was no indication of general errors, such as frame shifts or sequence mutations. The sequentially validated scFv libraries were applied for the selection of specific scFvs.

The selection of antigen-binding scFv-phages was performed using different variations of panning procedures. As carbohydrate antigen, the *E. coli* R3 rough mutant oligosaccharide conjugated through glutaraldehyde to BSA was used. The R3 LPS was determined in dot blot binding experiments with the rabbit sera after immunisation against various LPS structures as one of the dominant binding structures. Further binding antibodies to the R3 LPS could be detected in the sera of all four rabbits.
It has been described that the selection of carbohydrate binding fragments by phage display is challenging due to the commonly low affinity to the carbohydrate ligands [7, 80]. Therefore firstly the quality of the constructed libraries was examined by panning with the original protein antigen used for immunisation, the anti-idiotype S81-19, as immobilised ligand. Pannings against the mAb S81-19 were implemented with the rabbit 436 long linker library, the 437 library and the 439 library, while the 436 short linker library and the 437 library were panned against the $F(ab)_2$ S81-19. All phage mixtures revealed clear binding at least after the fourth round of panning.
The successful panning procedures evidently prove the capability of the scFv libraries. Therefore the correct expression and folding of the scFvs was validated. Nevertheless non of the anti-anti-idiotype phages revealed binding to the R3 conjugate or R3 heat killed bacteria, like the antibodies in the rabbit sera after immunisation. Thus, they show anti-anti-idiotype reaction, but not a similar carbohydrate-binding pattern like the idiotype antibody WN1 222-5 with the *E. coli* core-structure epitope.

As a next step the rabbit 437 library constructed from bone marrow and spleen with a long linker was used in panning direct against the R3 conjugate. The phages yielded after five

panning rounds were tested in phage ELISA for their binding to the R3 conjugate. No binding of phages could be detected. The phage titer and the scFv inserts bearing colonies were monitored during the panning rounds (Tab. 4). Although there was no marked loss of phages in the titer control determined, a loss of scFv inserts in the bacterial colonies was observable (Fig. 23).

The loss of functional scFvs could be explained by three phage reamplification steps while panning. It is necessary to produce fresh phages prior to each panning step, in order to exclude damaged scFv fusion proteins due to protease cleavage. On the other hand, frequent amplifications promote the selection of phages with growth, but no affinity advantage [115]. Some of the expressed scFvs even have toxic effects on the bacteria cells and thus cells without a functionally expressed scFv can have growth advantages.

A second panning was implemented for the same 437 scFv library. The R3 conjugate was used as immobilised antigen. There was only one phage reamplification step introduced before the first panning. Subsequent incubation for the phage binding to the conjugate, the removal of the non-binders by washing was decreased. Shortened washing times were expected to select for phages with low binding strength, while strong washing conditions lead to high affinity binders [116].

The phage titer during the panning revealed no significant fluctuations and also the insert control by colony PCR showed retention of scFv genes in the phagemids (Tab. 5). The phage mixtures and several single amplified phages were tested for binding in phage ELISA. There was no binding detectable for the phage mixtures to the R3 conjugate, but a slight binding for two of the single phages, which emerged as an unspecific binding also to the casein control (Fig. 24). A minor binding was also detected for the phage mixtures to the S81-19 anti-idiotype as immobilised antigen. To ensure whether there is a weak binding scFv displayed on the phage or not, the phage mixtures and the two slight binding phages were used to express soluble scFvs. The detection of soluble scFvs is less ambiguous than with the often clotting or in valency varying phages.

With the pComb3XSS phagemid vector it is simply feasible to produce soluble scFvs. Between the HA-tag 3'-end of the inserted scFv sequence and the 5'-end of the *gIII* lies an amber stop codon [117] on the plasmid (Fig. 9). In *E. coli* suppressor strains like the ER2537 or TG1 applied for panning phage amplifications, the amber stop codon of the phagemid genome is suppressed, resulting in a scFv-pIII fusion protein. In the non-suppressor strain *E. coli* Top10F' by contrast the amber stop codon is read as a stop codon and the transcription terminated at the 3'-end of the scFv gene.

ELISAs were performed with the soluble scFvs against the R3 conjugate and anti-idiotype S81-19 as antigens (Fig. 25). In parallel the binding was determined in casein buffer and in skim-milk-powder buffer. With skim-milk-powder as binding control, no binding of scFvs was detected. Slight binding against the anti-idiotype of scFvs mixtures was determined, but no binding of scFvs against the R3 conjugate was determined.
The ligand presentation could play a role for the binding of the scFvs. Since it was not possible to determine binding scFvs and phages against the R3 conjugate, the presentation of the R3 core type oligosaccharides was changed. Instead of the isolated and conjugated oligosaccharides the complete R3 rough-type mutant heat-killed bacteria were applied as immobilised antigens for panning and subsequent binding detection.
Again the rabbit 437 library was introduced for panning. As with the second panning against the R3 conjugate, there was no loss of phages or inserts observed, but also no binding phages were detected subsequent to panning.
With two additional scFv libraries the panning was performed against the R3 heat-killed bacteria. The rabbit 438 peripheral blood lymphocyte-derived library was used to alter the variable region mRNA source. And the 436 short linker bone marrow-derived library was used to increase the valency of the displayed scFv on the phages. Both panning procedures resulted in no detectable binding against the R3 heat-killed bacteria.

Three reasons were assumed for untraceablity of binding scFv phages.
First, the abundance of antibodies against the R3 oligosaccharide subsequent anti-idiotype immunisation is outnumbered compared to the high quantity of different anti-anti-idiotype antibodies. Hence the generation of scFv libraries from immunised rabbits is unsuitable.
Second, the scFvs are not adequately folded or presented on the phage surface.
Third, the affinity of the phage displayed scFvs to the carbohydrate antigen is too low to be detectable or cannot sustain the panning washing conditions sufficient to exceed unspecific phages.
The first option to explain the lack of anti-anti-idiotype scFvs which bind to the R3 conjugate could not be excluded: The minor abundance of R3 LPS binding antibodies in the anti-idiotype immunised rabbit sera resulted from a low number of R3 LPS binding antibody mRNA expressing B-cells. If the amount of mRNA of the desired antibody clone is too low compared to other antibody mRNA the possibility of the isolation of the clone is improbable. The first risk is the loss of low abundance sequences during library construction and the second is the loss while panning washing or phage amplification.

The second reason regarding the correct folding and presentation of scFv could be excluded due to the practicable use of the libraries for anti-anti-idiotype isolation.
The third argumentation concerning the scFv affinity was revised by an increase in scFv valency on the phage surface [80]. Therefore, the hyperphage M13K07ΔpIII system was introduced [79]. The hyperphage M13K07ΔpIII is a helper phage, with the exception that it lacks a functional *gIII*. It is consequently capable of incurring the phage assembly, but does not express pIII, which competes with the scFv-pIII fusion protein for assembly.
The pComb3XSS phagemid vector lacks the N-terminal domain of the pIII. This leads to a simplified superinfection with the helper phages, because no immunity to helper phage infection must be suppressed during phage amplification. The disadvantage, however, is that the pComb3XSS is not suitable in combination with the hyperphage. The hyperphage is incapable of supplying functional pIII during phage assembly necessary for subsequent infection. Hence it is necessary to alter the vector system to a phagemid vector harbouring a complete *gIII*.
The pHen1 vector (Fig. 10) is a phagemid vector very similar to the pComb3XSS, whereas the pHen1 includes the complete *gIII* [78]. Therefore the pHen1 vector is appropriate in combination with the hyperphage to increase the scFv valency.
The rabbit 437 scFv library was cloned from the pComb3XSS vector to the pHen1 vector. The amplified pHen1 phage particles were analysed in western blots for their increased scFv expression compared to the helper phage packed pHen1 phages (Fig. 29). The c-myc tagged scFvs expressed in the pHen1 vector revealed scFv-pIII fusion proteins, whereas the amount of determined scFvs in hyperphage packed particles considerably exceeds the helper phage packed. There was also unspecific detection noticeable in western blot staining also to the helper phage and pComb3XSS controls without c-myc tag. The alkaline phosphatase developing was replaced by fluorescent analysis. The c-myc tag detection with the Alexa680 conjugated second antibody revealed a clear band for the hyperphage packed phage particles without staining of other bands. The blot was destained and detected again with an anti-pIII antibody. The pIII was determined for the three phage preparations, while for the hyperphage packed phages also the scFv-pIII fusion protein above the pIII band was clearly visible (Fig. 29).
Two pannings were performed with the 437 library pHen1 vector. Prior to the first and second panning step the phages were packed with the hyperphage M13K07ΔpIII, while the phages used for the third and fourth rounds were packed by the helper phage M13K07. Since it is

especially suitable to increase the valency during the first panning rounds to minimise the risk of losing the desired clones when they are in low abundance.
The two pannings were performed in parallel with the R3 conjugate and the anti-idiotype S81-19 $F(ab)_2$ fragments as antigens. The phage mixtures were tested after the panning rounds in phage ELISA for binding against the R3 conjugate and the S81-19. The phages panned against the S81-19 $F(ab)_2$ revealed distinct binding to the S81-19 subsequent to the third round of panning (Fig. 31). Presumable to clotting phages the ELISA titration curve fluctuates as often observed for phage ELISAs. Anyhow, the phage binding to the S81-19 is undoubtedly determined. Phages of both panning procedures were determined for binding to the R3 conjugate with no indication of binding phages. The valency increase of the scFvs resulted, like the helper phage packed panning phages, in definite binding of phages subsequent to the third panning round against the anti-idiotype S81-19. Also like for the helper phage packed phages, no R3 conjugate binding phages could be isolated. It is conceivable that the affinity of the scFvs presented on the phage was too low, that it was not possible to overcome it solely by increasing the valency on the phage. Supplementarily, the valency of the antigen could be increased to isolate low affinity binders to carbohydrates [118]. Since the low affinity to carbohydrate antigens is a common problem during specific antibody isolation also with the phage display system [119], it is most likely that it is a major difficulty in this anti-anti-idiotype isolation approach.

6.2. Recognition of Bacterial Carbohydrates by MBL

MBL is a multi-subunit protein that not only recognises mannan, but a wide variety of different carbohydrates. The broad-spectrum recognition enables the defence against various pathogens. Bound to bacteria, MBL activates the complement system or enhances phagocytosis by opsonisation, reviewed by Ip 2009 [8]. It thereby makes an important contribution to first-line immune reactions. However, its role in tuberculosis infection is controversially discussed [120, 121]. The enhanced uptake into the host cells could have adverse effects on the establishment of the infection. It is discussed whether inhibiting the MBL activity in mycobacterial infections may even be beneficial for the host [122].
Mycobacteria appear to be the perfectly suitable interaction partner for MBL. With their highly mannosylated cell-envelope structures like mannose-capped lipoarabinomannan (ManLAM) or phosphatidyl-*myo*-inositol mannosides (PIM), they present one of the preferred

carbohydrate targets of MBL. Furthermore, most of these surface carbohydrates are presented in branched structures, observed to be preferred by many lectins compared to their linear counterparts [2, 123].

The molecular composition and organisation of the mycobacterial cell-wall are currently under investigation [124], while the surface-exposed lipoarabinomannans are discussed as being the most important structure for immunopathogenesis [123, 125, 126]. Systematic studies concerning the variations in cell-wall composition, comparing the wide variety of different pathogenic mycobacteria, have not yet been conducted. Strain-specific variations could be a major cause of increased or modified phagocytosis and consequently altered infectivity.

It was shown that genetic variations among clinical isolates of mycobacteria influence their pathogenicity [127]. Several clinical isolates were applied to investigate differences in the interaction with MBL.

Since differences in monosaccharide binding specificity were determined for the hMBL and the two MBL variants existing in mice [87], their preference for pathogenic mycobacteria as well as for some selected *E. coli* strains was investigated.

Initially the inhibition of rMBL binding to immobilised ligand by three different bacteria was determined (Fig. 32). Applied were the *E. coli* R3 rough-type mutant, the enterotoxigenic *E. coli* serotype O8 and the mycobacterial reference strain *M. tuberculosis* H37Rv ATCC. The binding of rhMBL, rMBL-A and rMBL-C was markedly different. The rhMBL binding to the *M. tuberculosis* H37Rv was considerably high, while no inhibition occurred either with *E. coli* rough type or with the smooth type. The rMBL-A, by contrast, binds with no mentionable differences to the three heat-killed bacteria. While the other murine MBL, rMBL-C, revealed no clear binding to the bacteria, but a slight binding to the *M. tuberculosis* H37Rv.

In a second inhibition ELISA, two more mycobacteria and two more *E. coli* were determined for their inhibition potential (Fig. 33). Again, the rhMBL revealed binding to the mycobacteria, but no clear interaction with *E. coli* was observed. The rMBL-A binds noticeably increased to the *E. coli* strains than to the mycobacteria. The rMBL-C showed only slight binding to the *M. tuberculosis* EAI.

The binding of the rMBL-A to the different *E. coli* serotypes was comprehensible. The O111 with the 3,6-dideoxysugar colitose in its O-polysaccharide repeating unit was likely to bind decreased to MBL in comparison to the O4 with Glc, Rha, FucNAc and GlcNAc. Still, the better binding of these two *E. coli* strains is remarkable compared to the highly mannosylated

mycobacteria. Expected was rather a picture as for rhMBL with a clear binding to the mycobacteria, a minor binding to the *E. coli* O4 and no detectable binding to the O111. The rMBL-A must therefore have a preference for either the carbohydrate composition of the *E. coli* strains or the exposure of them. The rhMBL by contrast seems obviously to prefer the exposure form of the mycobacterial carbohydrates, as there was no binding to the *E. coli* O8 detectable, which also bears Man as O-polysaccharide repeating unit components.

Although lectins prefer binding to long and branched structures, they are able to distinguish between single carbohydrate variations in short oligosaccharide molecules. As depicted in Fig. 34 they differentiate not only in single carbohydrate variations, but also in their means of presentation. Only rMBL-A revealed distinct binding to the rough mutant *E. coli* strains, with the exception of the binding to the R2 core type of rhMBL. But the binding varied from the heat-killed bacteria to the isolated oligosaccharides, confirming the presentation form as crucial.

In Fig. 32 and Fig. 33 mycobacteria turned out to bind, as expected for mannose rich cell envelopes, to rhMBL. Based on that, several mycobacterial strains were tested for binding. The inhibition ELISA with heat-killed bacteria was applied. Although quite different strains were applied, they revealed a similar binding pattern.
Since it came with the heat-killed mycobacteria repeatedly to quantification difficulties due to poor solubility and stacking of the bacterial particles on tube surfaces, a direct binding ELISA was introduced. The bottom of a hydrophobic plastic plate was to be completely coated with hydrophobic cell-wall particles of mycobacteria and the rMBL binding was detected. The rhMBL and rMBL-C bound to an extremely low extent to the immobilised heat-killed bacteria, while the rMBL-A revealed increased binding. The rMBL-A clearly distinguishes between the various heat-killed mycobacteria, whereby the quantification of the indeed immobilised material could not be clarified.
In order to understand the discrepancy between the outcomes of the inhibition and the direct ELISA with heat-killed mycobacteria, the coating of the plates should be verified as well as the display of the cell-wall components. Therefore the direct ELISA was performed with living mycobacteria. Three different bacteria were immobilised on a hydrophobic flat bottom plate and detected with rMBL-A. The rMBL-A binding was detected to a different extent for the bacteria strains. However, in a subsequent syto24 staining of the bacteria, it was shown that the immobilisation of the bacteria on the surface of the wells was irregular. For this

reason it cannot be excluded that the detected binding variations are due to differences in immobilisation.

The inhibition ELISA is therefore still the method of choice for the determination of binding interactions. Not solely because both binding partners can interact in solution, but another benefit is also for carbohydrate binding studies, that through the determined binding to mannan it is confirmed that only the binding of the MBL carbohydrate recognition domain (CRD) participates in binding.

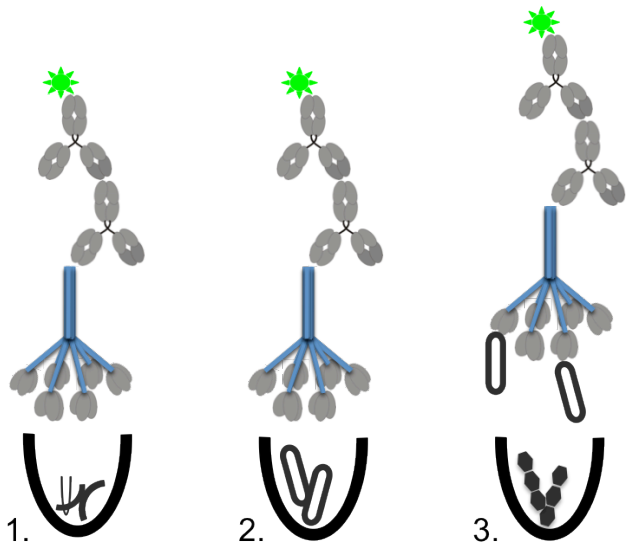

Fig. 43: Different ELISA were compared for MBL binding studies.
The initially introduced direct binding ELISA with heat-killed bacteria as immobilised ligand (1). The ELISA with immobilised living bacteria as ligand (2). The mannan as immobilised ligand, while MBL-bacterial interaction was determined by the inhibition of MBL binding (3).

Not been clarified yet was the question why the rhMBL in inhibition ELISA with several different heat-killed mycobacteria revealed only minor binding differences. It was investigated whether the cell lysis of the bacteria during heat killing and the subsequent ultrasonification alter the ligand display in an rMBL recognition relevant manner. Consequently, the inhibition ELISA was performed using living mycobacteria. The concentration of the bacterial strains was determined by OD_{600} measurements of the resuspensions and subsequent equalisation. Differences in the binding of rhMBL were detectable, not exhibited with the heat-killed mycobacteria. The reference strain *M. tuberculosis* H37 revealed a markedly decreased binding to rhMBL compared to the other strains, while the *M. africanum* Afri2 showed the best binding.

Summarising the findings of these studies, the inhibition ELISA with living mycobacteria was shown to be most promising examination method for the interaction of rMBLs with bacteria. It has the advantages over the other ELISA variations, that the cell-wall is presented intact

and the binding interaction takes place in solution. A destroyed cell-wall could support binding to molecule parts which are otherwise hidden in the intact cell and consequently would not participate in binding. The avoidance of the immobilisation of the bacteria to solid surfaces circumvents possible immobilisation differences of the bacteria.
Furthermore, it was shown that rhMBL and the murine rMBL-A and –C differ markedly in their interaction with different bacteria. The binding to various *E. coli* strains and mycobacteria was compared, resulting in the general outcome that rMBL-A binds enhanced to *E. coli*, while rhMBL and rMBL-C revealed better binding to mycobacteria. This observation correlates with the findings that the sequence of hMBL is closer related to the sequence of MBL-C than of MBL-A [86]. All three rMBLs have the ability to discriminate between different mycobacterial strains. This could be used in further studies regarding the recognition of various mycobacteria by the immune system.
Furthermore, it could be investigated whether the discrimination in binding plays a role in subsequent events of the immune system. The complement activation assay was successfully introduced and could valuably enrich further studies.

7. Abstract

Carbohydrate-protein interactions play a crucial role in the immunological recognition of microorganisms. Bacterial carbohydrates as major cell-wall components are therefore of special interest. In general carbohydrate-protein interactions are described as rather weak compared to protein-protein interactions. The focus in this thesis was on antibodies and mannose-binding lectin (MBL) as protein-binding partners. Both take advantage of the same strategy, an increase in valency, to overcome the weak interaction with carbohydrates and achieve a significant immune reaction. Antibodies that are often involved in carbohydrate recognition are the pentameric IgMs, while lectins form oligomers ranging from dimers to hexamers composed of their trimeric units.

In this study the phage display method was applied to isolate anti-anti-idiotype antibodies. The peculiarity of these antibodies is that they recognise besides the protein (anti-idiotype), which was used for immunisation to circumvent carbohydrate immunisation, also the original antigen of the idiotypic cascade. The original antigen was the *E. coli* LPS core region, thus a carbohydrate structure. The induction of an antibody response with similar binding characteristics as the LPS-neutralising and cross-reactive idiotype antibody WN1 222-5 would be a desirable vaccination strategy.

For the isolation of carbohydrate binding scFvs (single chain variable region fragments), the valency is contemplated to play an important role in enabling the detection and separation of scFv-phages from abundant clones. In varying experimental approaches, anti-anti-idiotype scFvs could be exhibited, but no recognition of the original antigen, the *E. coli* LPS core-structures, could be confirmed.

In a second approach the recognition of bacterial carbohydrates was investigated by MBLs, also referred as the antibodies of the innate immune system. It activates the complement system independently of antibodies and is involved in enhancing phagocytosis by opsonisation. Despite the determined monosaccharide preferences of MBLs, it is not possible to predict the binding to bacterial surface structures. This leads to the assumption that the exposition of the target structures is crucial, precisely because branched structures seem to be preferred to linear ones. Various ELISA were introduced to examine the binding of MBLs to different pathogenic and non-pathogenic *E. coli* and mycobacteria. Moreover, considerable differences between human MBL and the two murine MBLs were detected. The rhMBL

revealed increased binding to mycobacteria compared to *E. coli*, while the mouse rMBL-A showed opposite binding preferences.

Furthermore, an MBL complement activation assay was introduced successfully.

8. Zusammenfassung

Die Wechselwirkung von Kohlenhydraten mit Proteinen spielt bei der Erkennung von Mikroorganismen durch das Immunsystem eine entscheidende Rolle. Kohlenhydrate gehören zu den Hauptbestandteilen der bakteriellen Zellwand und sind daher in diesem Zusammenhang von besonderem Interesse. Generell werden Kohlenhydrat-Protein-Wechselwirkungen im Gegensatz zu Protein-Protein-Wechselwirkungen als eher schwach beschrieben. Der Fokus dieser Arbeit lag auf Antikörpern und Mannose-bindendem Lektin (MBL) als jenen Proteinen, die an der Kohlenhydrat-Protein Wechselwirkung beteiligt sind. Beide nutzen die gleiche Strategie, eine hohe Valenz, um trotz der häufig schwachen Affinität einzelner Bindungsstellen zu Kohlenhydraten, maßgeblich an der Erkennung durch das Immunsystem beteiligt zu sein. Antikörper, die Kohlenhydrate binden, gehören meist dem pentameren IgM Isotyp an, und MBLs formen aus ihren Triplett-Untereinheiten Oligomere, die von Dimeren bis zu Hexameren reichen.
Als ein Ziel dieser Studie sollten Anti-Anti-Idiotyp-Antikörper mit Hilfe der „Phage Display“ Methode isoliert werden. Die Besonderheit dieser Antikörper ist, dass sie neben dem Protein (Anti-Idiotyp), das für ihre Induzierung verwendet wurde, um eine Kohlenhydrat-Immunisierung zu umgehen, auch das originale Antigen einer idiotypischen Kaskade erkennen. Das Antigen war in diesem Fall die *E. coli* LPS-Kernregion und folglich eine Kohlenhydratstruktur. Die Induzierung einer Antikörperantwort, welche die Bindungseigenschaften des Idiotyp Antikörpers WN1 222-5 aufweist, wie Kreuzreaktivität gegenüber verschiedenen Bakterien und LPS-Neutralisation könnte eine Impfstrategie darstellen.
Bei der Isolierung eines Kohlenhydrat-bindenden ScFvs (Single chain variable region fragments) durch „Phage Display“ spielt die Valenz eine wichtige Rolle. Sie ist entscheidend sowohl bei der Detektion als auch bei der Anreicherung von ScFv-Phagen aus einer großen Anzahl verschiedener Klone. In unterschiedlichen experimentellen Ansätzen konnten in dieser Studie Anti-Anti-Idiotypen bestimmt werden, aber es wurde keine Bindung zum ursprünglichen Kohlenhydrat-Antigen nachgewiesen.

In einem zweiten Ansatz wurde die Erkennung von bakteriellen Kohlenhydraten durch MBL untersucht, welches auch als Antikörper des angeborenen Immunsystems beschrieben wird. Es aktiviert das Komplementsystem unabhängig von Antikörpern und ist außerdem als

Opsonin an Phagozytoseprozessen beteiligt. Obwohl die Monosaccharidspezifitäten des MBL beschrieben sind, ist es nicht möglich, aus ihnen Vorhersagen über eine bevorzugte Bindung an verschiedene bakterielle Oberflächen zu treffen. Dies führt zu der Annahme, dass die Präsentation der jeweiligen Strukturen entscheidend ist.

Es wurden verschiedene ELISA entwickelt, um die Bindung von MBL an pathogene und nicht-pathogene *E. coli* und Mykobakterien Stämme zu untersuchen. Dabei wurden u.a. erhebliche Unterschiede in der Bindung von humanem und den zwei murinen MBLs festgestellt. Das rhMBL zeigte eine bessere Bindung an die getesteten Mykobakterien als an die *E. coli*, das rMBL-A hingegen bindet bevorzugt an *E. coli*. Sowohl das hMBL als auch die beiden murinen Formen unterschieden in ihrer Bindung zwischen verschiedenen Mykobakterien Stämmen.

Es konnte außerdem ein MBL Komplement-Aktivierungs-Test erfolgreich eingeführt werden.

9. Literature

1. Jimenez-Barbero, J. & al., e. Hevein Domains: An Attractive Model to Study Carbohydrate-Protein Interactions at Atomic Resolution, in *Advances in Carbohydrate Chemistry and Biochemistry*. (ed. D. Horton)2006).
2. Wu, A.M., Lisowska, E., Duk, M. & Yang, Z. Lectins as tools in glycoconjugate research. *Glycoconj J* **26**, 899-913 (2009).
3. Beck, A., Wurch, T., Bailly, C. & Corvaia, N. Strategies and challenges for the next generation of therapeutic antibodies. *Nat Rev Immunol* **10**, 345-352 (2010).
4. Reichert, J.M. Antibodies to watch in 2010. *MAbs* **2**, 84-100 (2010).
5. Dimitrov, A.S. *Therapeutic Antibodies*. (Humana Press, 2009).
6. Dübel, S. *Handbook of Therapeutic Antibodies*. (Wiley-VCH, 2007).
7. Astrom, E. & Ohlson, S. Detection of weakly interacting anti-carbohydrate scFv phages using surface plasmon resonance. *J Mol Recognit* **19**, 282-286 (2006).
8. Ip, W.K., Takahashi, K., Ezekowitz, R.A. & Stuart, L.M. Mannose-binding lectin and innate immunity. *Immunol Rev* **230**, 9-21 (2009).
9. Gupta, K., Gupta, R.K. & Hajela, K. Disease associations of mannose-binding lectin & potential of replacement therapy. *Indian J Med Res* **127**, 431-440 (2008).
10. Nikaido, H. Molecular basis of bacterial outer membrane permeability revisited. *Microbiol Mol Biol Rev* **67**, 593-656 (2003).
11. Rietschel, E.T. & Brade, H. Bacterial endotoxins. *Sci Am* **267**, 54-61 (1992).
12. Galanos, C. *et al.* Synthetic and natural *Escherichia coli* free lipid A express identical endotoxic activities. *Eur J Biochem* **148**, 1-5 (1985).
13. Seydel, U., Brandenburg, K. & Rietschel, E.T. A case for an endotoxic conformation. *Prog Clin Biol Res* **388**, 17-30 (1994).
14. Rietschel, E.T. *et al.* Bacterial endotoxin: molecular relationships between structure and activity. *Infect Dis Clin North Am* **5**, 753-779 (1991).
15. www.casper.organ.su.se/ECODAB/list.php (2010/06/04).
16. Stenutz, R., Weintraub, A. & Widmalm, G. The structures of *Escherichia coli* O-polysaccharide antigens. *FEMS Microbiol Rev* **30**, 382-403 (2006).
17. Jann, B., Shashkov, A.S., Kochanowski, H. & Jann, K. Structural comparison of the O4-specific polysaccharides from *E. coli* O4:K6 and *E. coli* O4:K52. *Carbohydr Res* **248**, 241-250 (1993).
18. Aucken, H.M. & Pitt, T.L. Serological relationships of the O antigens of *Klebsiella pneumoniae* O5, *Escherichia coli* O8 and a new O serotype of *Serratia marcescens*. *FEMS Microbiol Lett* **64**, 93-97 (1991).
19. Edstrom, R.D. & Heath, E.C. The biosynthesis of cell wall lipopolysaccharide in *Escherichia coli*. VII. Studies on the structure of the O-antigenic polysaccharide. *J Biol Chem* **242**, 4125-4133 (1967).
20. Vinogradov, E.V. *et al.* The structures of the carbohydrate backbones of the lipopolysaccharides from *Escherichia coli* rough mutants F470 (R1 core type) and F576 (R2 core type). *Eur J Biochem* **261**, 629-639 (1999).
21. Holst, O. & Müller-Loennies, S. Microbial Polysaccharide Structures, in *Comprehensive Glycoscience: from chemistry to systems biology*, Vol. 1. (eds. J.P. Kamerling *et al.*) 123-179 (Elsevier, Amsterdam; 2007).
22. Alexander, C. & Rietschel, E.T. Bacterial lipopolysaccharides and innate immunity. *J Endotoxin Res* **7**, 167-202 (2001).
23. Beutler, B. & Rietschel, E.T. Innate immune sensing and its roots: the story of endotoxin. *Nat Rev Immunol* **3**, 169-176 (2003).

24. Bone, R.C. *et al.* Sepsis syndrome: a valid clinical entity. Methylprednisolone Severe Sepsis Study Group. *Crit Care Med* **17**, 389-393 (1989).
25. Cohen, J. Non-antibiotic strategies for sepsis. *Clin Microbiol Infect* **15**, 302-307 (2009).
26. http://www.sepsis-gesellschaft.de/ (2010/12/12).
27. Kumar, A. *et al.* Duration of hypotension before initiation of effective antimicrobial therapy is the critical determinant of survival in human septic shock. *Crit Care Med* **34**, 1589-1596 (2006).
28. Jackson, J.J., Kropp, H. & Hurley, J.C. Influence of antibiotic class and concentration on the percentage of release of lipopolysaccharide from *Escherichia coli*. *J Infect Dis* **169**, 471-473 (1994).
29. Lepper, P.M. *et al.* Clinical implications of antibiotic-induced endotoxin release in septic shock. *Intensive Care Med* **28**, 824-833 (2002).
30. Cohen, J. The immunopathogenesis of sepsis. *Nature* **420**, 885-891 (2002).
31. Di Padova, F.E. *et al.* A broadly cross-protective monoclonal antibody binding to *Escherichia coli* and *Salmonella* lipopolysaccharides. *Infect Immun* **61**, 3863-3872 (1993).
32. Fink, M.P. Adoptive immunotherapy of gram-negative sepsis: use of monoclonal antibodies to lipopolysaccharide. *Crit Care Med* **21**, S32-39 (1993).
33. Warren, H.S., Novitsky, T.J., Bucklin, A., Kania, S.A. & Siber, G.R. Endotoxin neutralization with rabbit antisera to *Escherichia coli* J5 and other gram-negative bacteria. *Infect Immun* **55**, 1668-1673 (1987).
34. Reichert, J.M. & Dewitz, M.C. Anti-infective monoclonal antibodies: perils and promise of development. *Nat Rev Drug Discov* **5**, 191-195 (2006).
35. Müller-Loennies, S., Holst, O. & Brade, H. Chemical structure of the core region of *Escherichia coli* J-5 lipopolysaccharide. *Eur J Biochem* **224**, 751-760 (1994).
36. Gregory, S.H. *et al.* Detoxified endotoxin vaccine (J5dLPS/OMP) protects mice against lethal respiratory challenge with *Francisella tularensis* SchuS4. *Vaccine* **28**, 2908-2915 (2010).
37. Opal, S.M. *et al.* Active immunization with a detoxified endotoxin vaccine protects against lethal polymicrobial sepsis: its use with CpG adjuvant and potential mechanisms. *J Infect Dis* **192**, 2074-2080 (2005).
38. Cross, A.S., Opal, S., Cook, P., Drabick, J. & Bhattacharjee, A. Development of an anti-core lipopolysaccharide vaccine for the prevention and treatment of sepsis. *Vaccine* **22**, 812-817 (2004).
39. Astronomo, R.D. & Burton, D.R. Carbohydrate vaccines: developing sweet solutions to sticky situations? *Nat Rev Drug Discov* **9**, 308-324 (2010).
40. Jerne, N.K. Towards a network theory of the immune system. *Ann Immunol (Paris)* **125C**, 373-389 (1974).
41. Nisonoff, A. & Lamoyi, E. Implications of the presence of an internal image of the antigen in anti-idiotypic antibodies: possible application to vaccine production. *Clin Immunol Immunopathol* **21**, 397-406 (1981).
42. Fischer, P. & M., U.-F. Emerging Therapeutic Concepts IV: Anti-idiotypic Antibodies, in *Handbook of Therapeutic Antibodies*. (ed. S. Dübel) (Wiley-vch, 2007).
43. Köhler, H. *et al.* Idiotypic networks and nature of molecular mimicry: an overview. *Methods Enzymol* **178**, 3-35 (1989).
44. Fields, B.A., Goldbaum, F.A., Ysern, X., Poljak, R.J. & Mariuzza, R.A. Molecular basis of antigen mimicry by an anti-idiotope. *Nature* **374**, 739-742 (1995).
45. McNamara, M.K., Ward, R.E. & Köhler, H. Monoclonal idiotope vaccine against *Streptococcus pneumoniae* infection. *Science* **226**, 1325-1326 (1984).

46. Fung, M.S. *et al.* Monoclonal anti-idiotypic antibody mimicking the principal neutralization site in HIV-1 GP120 induces HIV-1 neutralizing antibodies in rabbits. *J Immunol* **145**, 2199-2206 (1990).
47. Westerink, M.A., Giardina, P.C., Apicella, M.A. & Kieber-Emmons, T. Peptide mimicry of the meningococcal group C capsular polysaccharide. *Proc Natl Acad Sci U S A* **92**, 4021-4025 (1995).
48. Lesinski, G.B. & Westerink, M.A. Vaccines against polysaccharide antigens. *Curr Drug Targets Infect Disord* **1**, 325-334 (2001).
49. Westerink, M.A. & Apicella, M.A. Anti-idiotypic antibodies as vaccines against carbohydrate antigens. *Springer Semin Immunopathol* **15**, 227-234 (1993).
50. Cunto-Amesty, G., Luo, P., Monzavi-Karbassi, B. & Kieber-Emmons, T. Exploiting molecular mimicry: defining rules of the game. *Int Rev Immunol* **20**, 157-180 (2001).
51. Behn, U. Idiotypic networks: toward a renaissance? *Immunol Rev* **216**, 142-152 (2007).
52. Grothaus, M.C. *et al.* Selection of an immunogenic peptide mimic of the capsular polysaccharide of *Neisseria meningitidis* serogroup A using a peptide display library. *Vaccine* **18**, 1253-1263 (2000).
53. Pashov, A., Perry, M., Dyar, M., Chow, M. & Kieber-Emmons, T. Defining carbohydrate antigens as HIV vaccine candidates. *Curr Pharm Des* **13**, 185-201 (2007).
54. Schreiber, J.R., Nixon, K.L., Tosi, M.F., Pier, G.B. & Patawaran, M.B. Anti-idiotype-induced, lipopolysaccharide-specific antibody response to *Pseudomonas aeruginosa*. II. Isotype and functional activity of the anti-idiotype-induced antibodies. *J Immunol* **146**, 188-193 (1991).
55. Müller-Loennies, S., Brade, L. & Brade, H. Neutralizing and cross-reactive antibodies against enterobacterial lipopolysaccharide. *Int J Med Microbiol* **297**, 321-340 (2007).
56. Müller-Loennies, S., Brade, L., MacKenzie, C.R., Di Padova, F.E. & Brade, H. Identification of a cross-reactive epitope widely present in lipopolysaccharide from enterobacteria and recognized by the cross-protective monoclonal antibody WN1 222-5. *J Biol Chem* **278**, 25618-25627 (2003).
57. Di Padova, F.E. *et al.* Anti-lipopolysaccharide core antibodies. *Prog Clin Biol Res* **388**, 85-94 (1994).
58. Iwagaki, A., Porro, M. & Pollack, M. Influence of synthetic antiendotoxin peptides on lipopolysaccharide (LPS) recognition and LPS-induced proinflammatory cytokine responses by cells expressing membrane-bound CD14. *Infect Immun* **68**, 1655-1663 (2000).
59. Bailat, S. *et al.* Similarities and disparities between core-specific and O-side-chain-specific antilipopolysaccharide monoclonal antibodies in models of endotoxemia and bacteremia in mice. *Infect Immun* **65**, 811-814 (1997).
60. Bahrami, S. *et al.* Monoclonal antibody to endotoxin attenuates hemorrhage-induced lung injury and mortality in rats. *Crit Care Med* **25**, 1030-1036 (1997).
61. http://www.glycosciences.de/modeling/sweet2/doc/index.php (2008/10/02).
62. http://www.yasara.org/ (2008/10/02).
63. Brade, L. *et al.* Immunization with an anti-idioypic antibody against the broadly lipopolysaccharide-reactive antibody WN1 222-5 induces *Escherichia coli* R3-core-type specific antibodies in rabbits. *Innate Immunity*, 1-15 (2011).
64. Krishnaswamy, S., Kabir, M.E., Miyamoto, M., Furuichi, Y. & Komiyama, T. Different buffer effects in selecting HM-1 killer toxin single-chain fragment variable anti-idiotypic antibodies. *J Biochem* **147**, 723-733 (2010).

65. Kabir, M.E., Krishnaswamy, S., Miyamoto, M., Furuichi, Y. & Komiyama, T. An improved phage-display panning method to produce an HM-1 killer toxin anti-idiotypic antibody. *BMC Biotechnol* **9**, 99 (2009).
66. Hoogenboom, H.R. Selecting and screening recombinant antibody libraries. *Nat Biotechnol* **23**, 1105-1116 (2005).
67. Smith, G.P. Filamentous fusion phage: novel expression vectors that display cloned antigens on the virion surface. *Science* **228**, 1315-1317 (1985).
68. Parmley, S.F. & Smith, G.P. Antibody-selectable filamentous fd phage vectors: affinity purification of target genes. *Gene* **73**, 305-318 (1988).
69. Dennis, M.S. & Lowman, H.B. Phage Selection Strategies for Improved Affinity and Specificity of Proteins and Peptides, in *Phage Display: a practical approach*. (eds. T. Clackson & H.B. Lowman) (Oxford University Press, 2004).
70. Model, P. & Russel, M. *Filamentous bacteriophage*, Vol. 2. (Plenum Press, New York and London, 1988).
71. Hust, M. & Dübel, S. Phage Display Vectors for the In Vitro Generation of Human Antibody Fragments, in *Immunochemical Protocols*, Vol. 295, Edn. third. (ed. R. Burns) (Human Press Inc., 2005).
72. Dolezal, O. *et al.* ScFv multimers of the anti-neuraminidase antibody NC10: shortening of the linker in single-chain Fv fragment assembled in V(L) to V(H) orientation drives the formation of dimers, trimers, tetramers and higher molecular mass multimers. *Protein Eng* **13**, 565-574 (2000).
73. Kirsch, M., Zaman, M., Meier, D., Dübel, S. & Hust, M. Parameters affecting the display of antibodies on phage. *J Immunol Methods* **301**, 173-185 (2005).
74. Barbas, C.F., 3rd, Kang, A.S., Lerner, R.A. & Benkovic, S.J. Assembly of combinatorial antibody libraries on phage surfaces: the gene III site. *Proc Natl Acad Sci U S A* **88**, 7978-7982 (1991).
75. http://www.scripps.edu/mb/barbas/ (2011/02/12)
76. Barbas III, C.F., Burton, D.R., Scott, J.K. & Silverman, G.J. *Phage Display: A Laboratory Manual*. (Cold Spring Harbor Laboratory Press, 2001).
77. Arbabi-Ghahroudi, M., Tanha, J. & MacKenzie, R. Prokaryotic expression of antibodies. *Cancer Metastasis Rev* **24**, 501-519 (2005).
78. Hoogenboom, H.R. *et al.* Multi-subunit proteins on the surface of filamentous phage: methodologies for displaying antibody (Fab) heavy and light chains. *Nucleic Acids Res* **19**, 4133-4137 (1991).
79. Rondot, S., Koch, J., Breitling, F. & Dübel, S. A helper phage to improve single-chain antibody presentation in phage display. *Nat Biotechnol* **19**, 75-78 (2001).
80. MacKenzie, R. & To, R. The role of valency in the selection of anti-carbohydrate single-chain Fvs from phage display libraries. *J Immunol Methods* **220**, 39-49 (1998).
81. Drickamer, K., Dordal, M.S. & Reynolds, L. Mannose-binding proteins isolated from rat liver contain carbohydrate-recognition domains linked to collagenous tails. Complete primary structures and homology with pulmonary surfactant apoprotein. *J Biol Chem* **261**, 6878-6887 (1986).
82. Palaniyar, N. Antibody equivalent molecules of the innate immune system: parallels between innate and adaptive immune proteins. *Innate Immun* **16**, 131-137 (2010).
83. Weis, W.I., Drickamer, K. & Hendrickson, W.A. Structure of a C-type mannose-binding protein complexed with an oligosaccharide. *Nature* **360**, 127-134 (1992).
84. Hansen, S. & Holmskov, U. Structural aspects of collectins and receptors for collectins. *Immunobiology* **199**, 165-189 (1998).
85. Jayaraman, N. Multivalent ligand presentation as a central concept to study intricate carbohydrate-protein interactions. *Chem Soc Rev* **38**, 3463-3483 (2009).

86. Sastry, R. *et al.* Characterization of murine mannose-binding protein genes Mbl1 and Mbl2 reveals features common to other collectin genes. *Mamm Genome* **6**, 103-110 (1995).
87. Hansen, S., Thiel, S., Willis, A., Holmskov, U. & Jensenius, J.C. Purification and characterization of two mannan-binding lectins from mouse serum. *J Immunol* **164**, 2610-2618 (2000).
88. Devyatyarova-Johnson, M. *et al.* The lipopolysaccharide structures of *Salmonella enterica* serovar Typhimurium and *Neisseria gonorrhoeae* determine the attachment of human mannose-binding lectin to intact organisms. *Infect Immun* **68**, 3894-3899 (2000).
89. Sheriff, S., Chang, C.Y. & Ezekowitz, R.A. Human mannose-binding protein carbohydrate recognition domain trimerizes through a triple alpha-helical coiled-coil. *Nat Struct Biol* **1**, 789-794 (1994).
90. Möller, M., de Wit, E. & Hoal, E.G. Past, present and future directions in human genetic susceptibility to tuberculosis. *FEMS Immunol Med Microbiol* **58**, 3-26.
91. Varki, A. *et al. Essentials of Glycobiology, a genomic view of glycobiology*, Edn. 2. (2009).
92. Summerfield, J.A., Sumiya, M., Levin, M. & Turner, M.W. Association of mutations in mannose binding protein gene with childhood infection in consecutive hospital series. *BMJ* **314**, 1229-1232 (1997).
93. Takahashi, K., Ip, W.E., Michelow, I.C. & Ezekowitz, R.A. The mannose-binding lectin: a prototypic pattern recognition molecule. *Curr Opin Immunol* **18**, 16-23 (2006).
94. Selvaraj, P., Narayanan, P.R. & Reetha, A.M. Association of functional mutant homozygotes of the mannose binding protein gene with susceptibility to pulmonary tuberculosis in India. *Tuber Lung Dis* **79**, 221-227 (1999).
95. Brennan, P.J. & Nikaido, H. The envelope of mycobacteria. *Annu Rev Biochem* **64**, 29-63 (1995).
96. Schlesinger, L.S. Entry of *Mycobacterium tuberculosis* into mononuclear phagocytes. *Curr Top Microbiol Immunol* **215**, 71-96 (1996).
97. Kang, B.K. & Schlesinger, L.S. Characterization of mannose receptor-dependent phagocytosis mediated by *Mycobacterium tuberculosis* lipoarabinomannan. *Infect Immun* **66**, 2769-2777 (1998).
98. Venisse, A., Berjeaud, J.M., Chaurand, P., Gilleron, M. & Puzo, G. Structural features of lipoarabinomannan from *Mycobacterium bovis* BCG. Determination of molecular mass by laser desorption mass spectrometry. *J Biol Chem* **268**, 12401-12411 (1993).
99. Chatterjee, D., Lowell, K., Rivoire, B., McNeil, M.R. & Brennan, P.J. Lipoarabinomannan of *Mycobacterium tuberculosis*. Capping with mannosyl residues in some strains. *J Biol Chem* **267**, 6234-6239 (1992).
100. van der Spuy, G.D. *et al.* Changing *Mycobacterium tuberculosis* population highlights clade-specific pathogenic characteristics. *Tuberculosis (Edinb)* **89**, 120-125 (2009).
101. Vieira, J. & Messing, J. Production of single-stranded plasmid DNA. *Methods Enzymol* **153**, 3-11 (1987).
102. Sambrook, J., Fritsch, E.F. & Maniatis, T. Molecular Cloning: A Laboratory Manual. 2nd Edition. *Cold Spring Harbor Laboratory Press* (1989).
103. Saiki, R.K. *et al.* Primer-directed enzymatic amplification of DNA with a thermostable DNA polymerase. *Science* **239**, 487-491 (1988).
104. Lefranc, M.P. [Antibody databases: IMGT, a French platform of world-wide interest]. *Med Sci (Paris)* **25**, 1020-1023 (2009).

105. Tesar, M. *et al.* Monoclonal antibody against pIII of filamentous phage: an immunological tool to study pIII fusion protein expression in phage display systems. *Immunotechnology* **1**, 53-64 (1995).
106. Snapper, C.M. & Mond, J.J. A model for induction of T cell-independent humoral immunity in response to polysaccharide antigens. *J Immunol* **157**, 2229-2233 (1996).
107. Mond, J.J., Lees, A. & Snapper, C.M. T cell-independent antigens type 2. *Annu Rev Immunol* **13**, 655-692 (1995).
108. Clement, M.J. *et al.* Toward a better understanding of the basis of the molecular mimicry of polysaccharide antigens by peptides: the example of *Shigella flexneri* 5a. *J Biol Chem* **281**, 2317-2332 (2006).
109. Jiang, X.T., Liu, B.Y., Zhu, P. & Fu, N. Production and characterization of a cross-reactive monoclonal antibody to lipopolysaccharide. *Hybridoma (Larchmt)* **28**, 93-99 (2009).
110. Huse, W.D. *et al.* Generation of a large combinatorial library of the immunoglobulin repertoire in phage lambda. *Science* **246**, 1275-1281 (1989).
111. Hawlisch, H., Meyer zu Vilsendorf, A., Bautsch, W., Klos, A. & Kohl, J. Guinea pig C3 specific rabbit single chain Fv antibodies from bone marrow, spleen and blood derived phage libraries. *J Immunol Methods* **236**, 117-131 (2000).
112. Burton, D.R. & Barbas, C.F., 3rd Human antibodies from combinatorial libraries. *Adv Immunol* **57**, 191-280 (1994).
113. Knight, K.L. & Winstead, C.R. Generation of antibody diversity in rabbits. *Curr Opin Immunol* **9**, 228-232 (1997).
114. Wentzell, L.M., Nobbs, T.J. & Halford, S.E. The SfiI restriction endonuclease makes a four-strand DNA break at two copies of its recognition sequence. *J Mol Biol* **248**, 581-595 (1995).
115. Hoogenboom, H.R. *et al.* Antibody phage display technology and its applications. *Immunotechnology* **4**, 1-20 (1998).
116. Guo, X. & Chen, R.R. An improved phage display procedure for identification of lipopolysaccharide-binding peptides. *Biotechnol Prog* **22**, 601-604 (2006).
117. Epstein, R.H. *et al.* Physiological studies of conditional lethal mutants of bacteriophage T4D. *Cold Spring Harbor Symp. Quant. Biol. 28:*, 375-394. (1963).
118. Bertozzi, C.R. & Kiessling, L.L. Chemical glycobiology. *Science* **291**, 2357-2364 (2001).
119. Schoonbroodt, S. *et al.* Engineering antibody heavy chain CDR3 to create a phage display Fab library rich in antibodies that bind charged carbohydrates. *J Immunol* **181**, 6213-6221 (2008).
120. Denholm, J.T., McBryde, E.S. & Eisen, D.P. Mannose-binding lectin and susceptibility to tuberculosis: a meta-analysis. *Clin Exp Immunol* **162**, 84-90 (2010).
121. Cosar, H. *et al.* Low levels of mannose-binding lectin confers protection against tuberculosis in Turkish children. *Eur J Clin Microbiol Infect Dis* **27**, 1165-1169 (2008).
122. Torrelles, J.B., Azad, A.K., Henning, L.N., Carlson, T.K. & Schlesinger, L.S. Role of C-type lectins in mycobacterial infections. *Curr Drug Targets* **9**, 102-112 (2008).
123. Daffe, M. & Draper, P. The envelope layers of mycobacteria with reference to their pathogenicity. *Adv Microb Physiol* **39**, 131-203 (1998).
124. Pitarque, S. *et al.* The immunomodulatory lipoglycans, lipoarabinomannan and lipomannan, are exposed at the mycobacterial cell surface. *Tuberculosis (Edinb)* **88**, 560-565 (2008).
125. Khoo, K.H., Tang, J.B. & Chatterjee, D. Variation in mannose-capped terminal arabinan motifs of lipoarabinomannans from clinical isolates of *Mycobacterium tuberculosis* and *Mycobacterium avium* complex. *J Biol Chem* **276**, 3863-3871 (2001).

126. Barenholz, A. *et al.* A peptide mimetic of the mycobacterial mannosylated lipoarabinomannan: characterization and potential applications. *J Med Microbiol* **56**, 579-586 (2007).
127. Homolka, S., Niemann, S., Russell, D.G. & Rohde, K.H. Functional genetic diversity among *Mycobacterium tuberculosis* complex clinical isolates: delineation of conserved core and lineage-specific transcriptomes during intracellular survival. *PLoS Pathog* **6**, e1000988 (2010).

Acknowledgement

I would like to express my great gratitude to my supervisor PD Dr. Sven Müller-Loennies for guiding me through this work, for sharing his wide knowledge with me, for his helpful scientific instructions, support and fruitful discussions.
I thank Prof. Dr. Helmut Brade for giving me the opportunity to complete this thesis in his group and for pioneering scientific discussions as well as Dr. Lore Brade for the useful consulting in all antibody issues.
I am very grateful for PD Dr. Buko Lindner for his kind support and advice from the initial to the final phase of this thesis.
I would like to thank Kolja Schaale for the help in many situations, constructive discussions and his every day sunny mood.
Prof. Dr. Satish Raina and Prof. Dr. Graciana Klein I would like to thank for their enthusiasm in discussing scientific issues and for the great time we had together.
Prof. Dr. Ulrich Schaible I would like to thank for his financial support and his warm way of leading the department.
For his kind providing of the mycobacteria strains I would like to thank PD Dr. Stefan Niemann.
I would like to thank Nadine Harmel for introducing me in many methods and being an enjoyable lab companion.
Max Koistinen and John Constable I would like to thank for helping me with the English orthography.
I thank Veronika Susott, Irina von Cube and Brigitte Kunz for their excellent technical assistance.
Christine Steinhäuser and PD Dr. Norbert Reiling I would like to thank for their mycobacterial support and many constructive conversations.
Yani Kaconis, Nicole Zehethofer, Julius Brandenburg, Susanne Keese and Daniel Kähler
I would like to thank for sharing many moments of frustration and fun with me during this work.
I would like to thank my parents, grandmothers and friends. Without their encouragement and understanding it would have been impossible for me to finish this work.
Finally, I offer my regards to all of those who supported me in any respect during the completion of this thesis.

Erklärung

Hiermit versichere ich, dass ich die vorliegende Arbeit selbständig angefertigt habe und keine weiteren als die angegebenen Quellen und Hilfsmittel verwendet wurden.

Diese Arbeit wurde in der jetzigen oder ähnlichen Form noch bei keiner anderen Hochschule eingereicht und hat darüber hinaus noch keinen Prüfungszwecken gedient.

Lena Heinbockel

Hamburg, 2011